Evaluation and modelling of data from a magnetic survey of the Majuagaa kimberlite occurrence in West Greenland

Report prepared for Icefire A/S

T. M. Rasmussen

GEOLOGICAL SURVEY OF DENMARK AND GREENLAND
MINISTRY OF CLIMATE AND ENERGY

GEUS

Evaluation and modelling of data from a magnetic survey of the Majuagaa kimberlite occurrence in West Greenland

Report prepared for Icefire A/S

T. M. Rasmussen

Released 01.01.2014

G E U S

Contents

1. Summary and conclusions

Magnetic profile data are reported from an area of the Majuagaa kimberlite dike system. The survey area contains a sub-circular lake, which has the potential of being an expression of a kimberlite pipe. In total 25 profiles were measured above and adjacent to the lake, with the purpose of investigating the possibility of a kimberlite pipe.

The evaluation of the measured data is done by comparing the data to synthetic responses obtained from some simple structures and responses due to topography.

The magnetic data have no indication of a (large) kimberlite pipe immediately below the lake surface, but the data are not conclusive with respect to any presence of kimberlite at larger depth (>50 m below lake bottom). A weak positive anomaly exists above the lake. This anomaly may be associated with the presence of kimberlite intrusion. However, in-situ magnetic susceptibility observations of gneisses in the area indicate that the cause of this anomaly also may be attributed to gneiss.

Some of the measured profiles adjacent to the lake contain high amplitude short wave-length anomalies. The data indicates a fairly inhomogeneous occurrence of kimberlite in the measurement area. The size of the kimberlite bodies associated with these narrow anomalies is interpreted to be of the order of a few metres in size horizontally.

2. Introduction

The Majuagaa kimberlite dike system (Jensen et al., 2004a, Jensen et al. 2004b) can be traced for a distance of about 17 km from the west coast of Greenland and inland. The orientation of the dykes is approximately N80E and thickness of the dykes reach a maximum of about two metres. Magnetic profiles covering an area associated with intense brecciation was performed in September 2010 with the purpose of evaluating a possible existence of a kimberlite pipe or a larger volume of kimberlite rocks. Adjacent to the breccia is a sub-circular lake with a diameter of about 40 m. Kimberlite rocks are exposed, but most of the area is covered by quaternary material.

In total 25 profiles were measured as outlined on the map in Figure 1. Additional in-situ measurements of the magnetic susceptibility were measured on rock exposures and boulders.

The terrain in the measurement area is characterised as a gently undulating surface between profiles 1 and 7, whereas profiles 17, 18 and 19 are located on a steep eastward facing slope. Profile 7 is on a topographic high with a mean elevation of approximately 4 m above the lake surface. Profiles 24 and 25 cross a boulder field, which is oriented along strike of the Majuagaa dyke system. No kimberlite boulders were, however, observed in the vicinity of these two profiles.

The maximum depth of the lake was measured to approximately 6 m. The lake bottom has steep slopes approximately 1-2 m from the lake shore. An exception to this is along the southern shore, where the steep part is further away (approximately 5 m) from the shore line.

3. Measuring procedure

The magnetic profiling was done by using a Geometrics G858 caesium-vapour magnetic gradiometer and with a Geometrics G836 proton magnetometer as base station. A configuration with measurements of the vertical magnetic gradient was used by recording magnetic data with two sensors at a vertical separation of 76 cm. The sensors are placed on a non-magnetic metal rod, which is moved along the profiles; either by walking along ground profiles or dragged over the lake surface while placed in a rubber boat. On average the bottom sensor is about 75 cm above ground, when walking with the instrument, but the distance vary by approximately +/- 50 cm in rough terrain. Recordings are done at a constant rate of 10 samples per second, which on average corresponds to a sampling for every 20 cm. The magnetic sensor orientations must be kept within a certain angle from the main magnetic field direction in order to provide useful data. Therefore, some samples of the magnetic field are lost, when performing measurements in rough terrain.

Before measuring, geographic coordinates are determined by GPS for a number of pre-selected positions along each profile. The marked locations are used to geo-reference the recordings, which are time-stamped at each profile mark. Geo-referencing between marks is done by assuming a constant speed between marks, when traversing the profiles. Figure 2 shows a map with all marked positions with GPS waypoint numbers and profile numbers. Some marks were measured more than one time and these data provide an estimate of the absolute error of about 2 m for the GPS measurements. Tables 1 and 2 in Appendix A include coordinates for all GPS readings.

Each profile was measured at least twice by traversing the profile in opposite directions. Some profiles were measured more than twice because of difficulties of obtaining useful data, when walking in rough terrain. One profile was split into two separate sections (profile 17 & 18) due to difficult terrain. The repeated profile measurements ensure that reliable data are obtained for the entire length of the profiles and provide an estimate of data repeatability and thereby reliability.
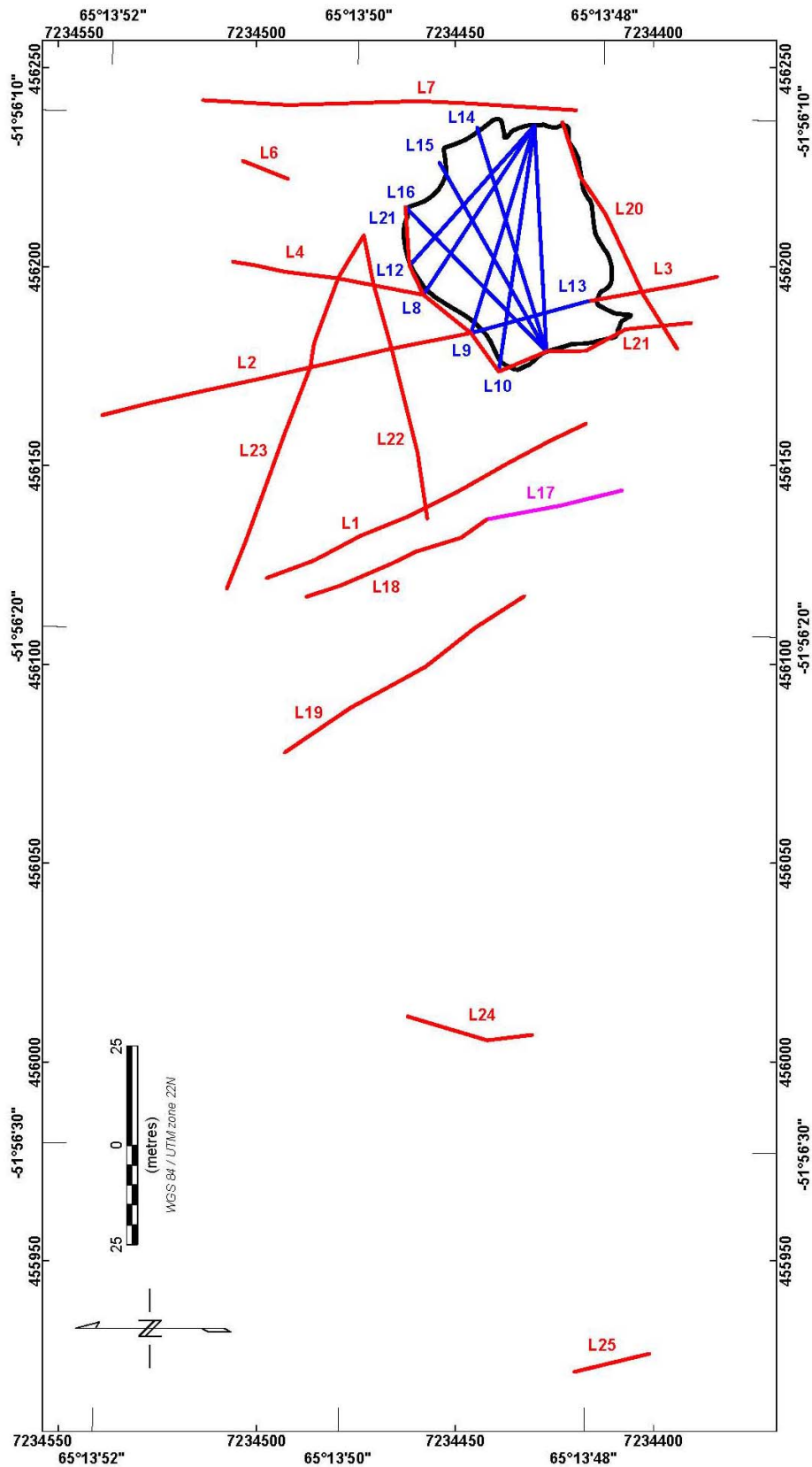
Figure 1. *Location of all measured profiles marked with lines in red, cyan and blue colours. Numbers refer to profile numbering. The lake shore is marked by polygon in black colour.*

4. Data processing

Three basic processing steps are required before data evaluation and modelling. These are
1. Geo-referencing
2. Removal of diurnal variations by subtraction of the base station data
3. De-spiking

For marks measured with GPS more than one time, only the firstly obtained coordinates were used. This ensures that the geo-referenced profile data are consistent with respect to any crossing of profiles. The uncertainty involved in the GPS data are not of any significant relevance for the evaluation of the data with respect to kimberlite volume, but is clearly of importance for absolute position determination. Figure 2 shows marked locations and corresponding waypoint numbers covering the lake area and adjacent terrain (Profiles L1-L23).

Total magnetic field anomalies are obtained by subtraction of magnetic base station recordings from the profile measurements using time as the link. Vertical magnetic gradient data are calculated by subtracting data recorded by the top-sensor from the data recorded by the bottom-sensor and dividing by the fixed distance between top and bottom sensor.

Some of the profile data contained several spikes and these were removed by manual inspection of the data. The spikes are mainly linked to profiles in rough terrain. The profile data are shown on the maps in Figures 3 and 4 and included as separate plots in Appendix B. Only profiles above and adjacent to the lake are shown in Figure 3 and 4.

The profile density is not suitable for gridding into a reliable surface representation of the magnetic field variations in the survey area. Only in the case of profiles crossing the lake, a reliable grid presentation is possible. The grids provide an easy overview of the magnetic field variations as recorded by the top and bottom sensors (Figures 5-8) but profile data are better suited for the final modelling and evaluation of the data. The grids shown in Figures 5 and 6 are based on data in one of the profile traverse directions, whereas the grids in Figures 7 and 8 are based on profiles recorded in the opposite direction. In cases where only one traverse gave useful data, the data from the other traverse direction is included in these Figures. Colour coded circles are used along profiles outside the gridded region. The same colour scale is used for all grids and profile presentations in order to facilitate comparison between them. The results are discussed in succeeding sections.

The two data sets obtained from traversing the profiles in opposite directions are in good agreement. Some deviations can be noticed, which primarily are attributed to small variations in sensor altitude, when traversing in opposite directions. Deviations may also be introduced as a result of imperfect geo-referencing, which is based on an assumption of a constant traverse speed between profile marks.
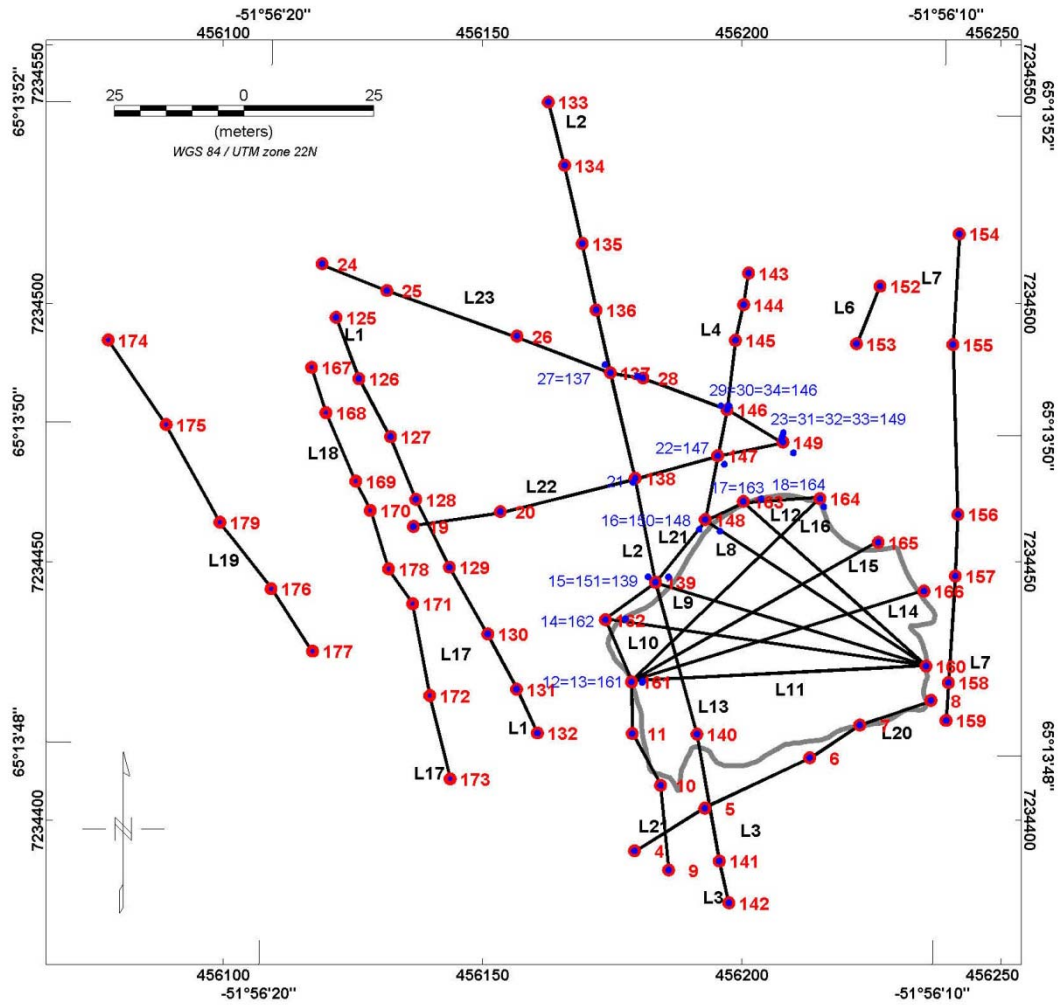
Figure 2. *Marked locations used for profile definition and corresponding waypoint and profile numbers for profiles L1-L23. Profiles are marked by black lines and profile number in black colour. Waypoints marked by large red circles that surround a filled blue circle are used for geo-referencing of profiles. Waypoints marked by blue circles represent repeated measuring of a location. For locations with more than one GPS measurement (filled blue circle and number in blue colour), coordinates from the first reading (number in red colour) is used.*
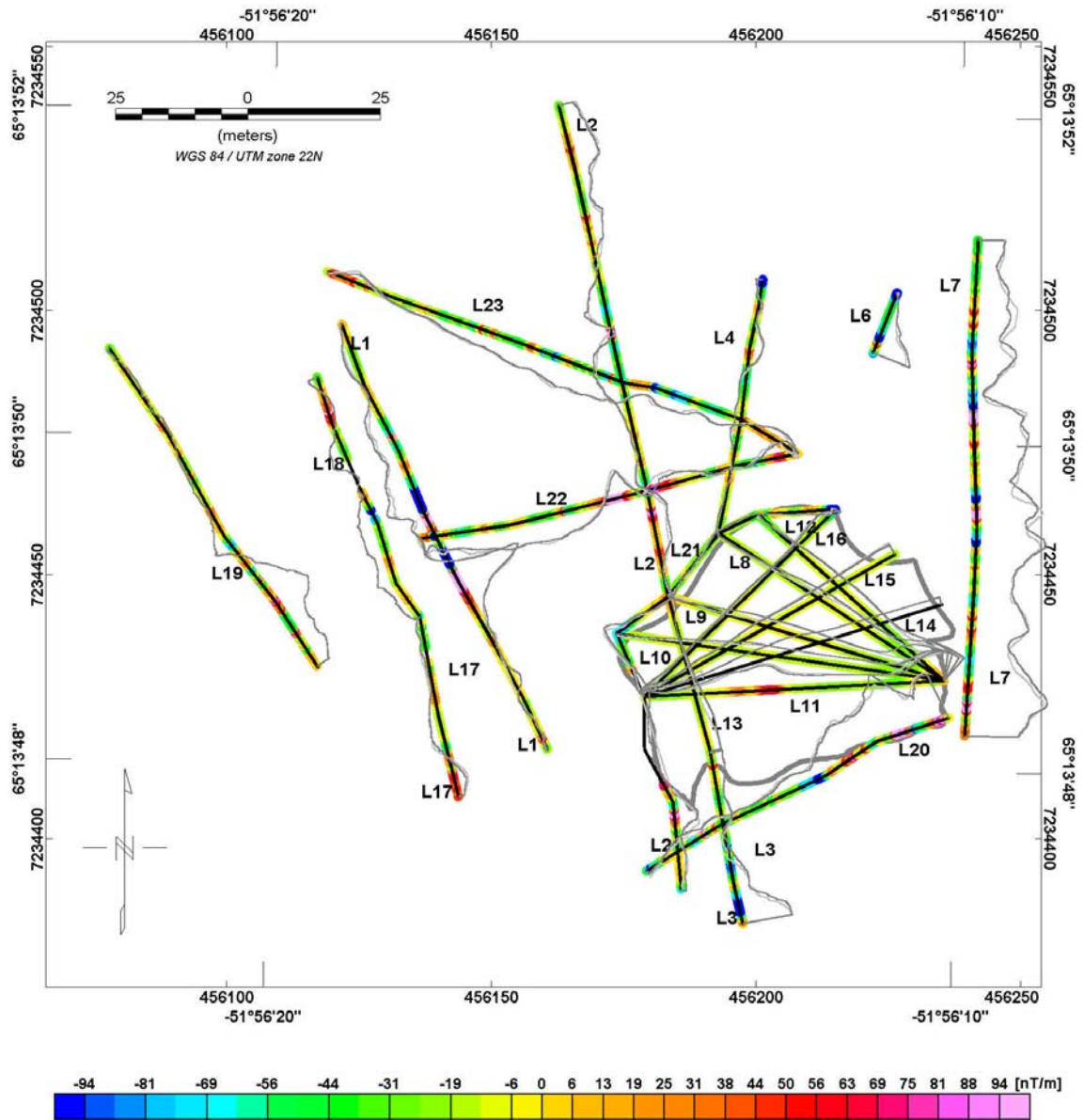
Figure 3. *Magnetic field recorded by top sensor and shown by profiles in dark and light grey colours for the two traverses of profiles (opposite directions if useful data were obtained for both traverses). The colour filled symbols show the calculated vertical gradient. The thick grey line marks the location of the lake.*
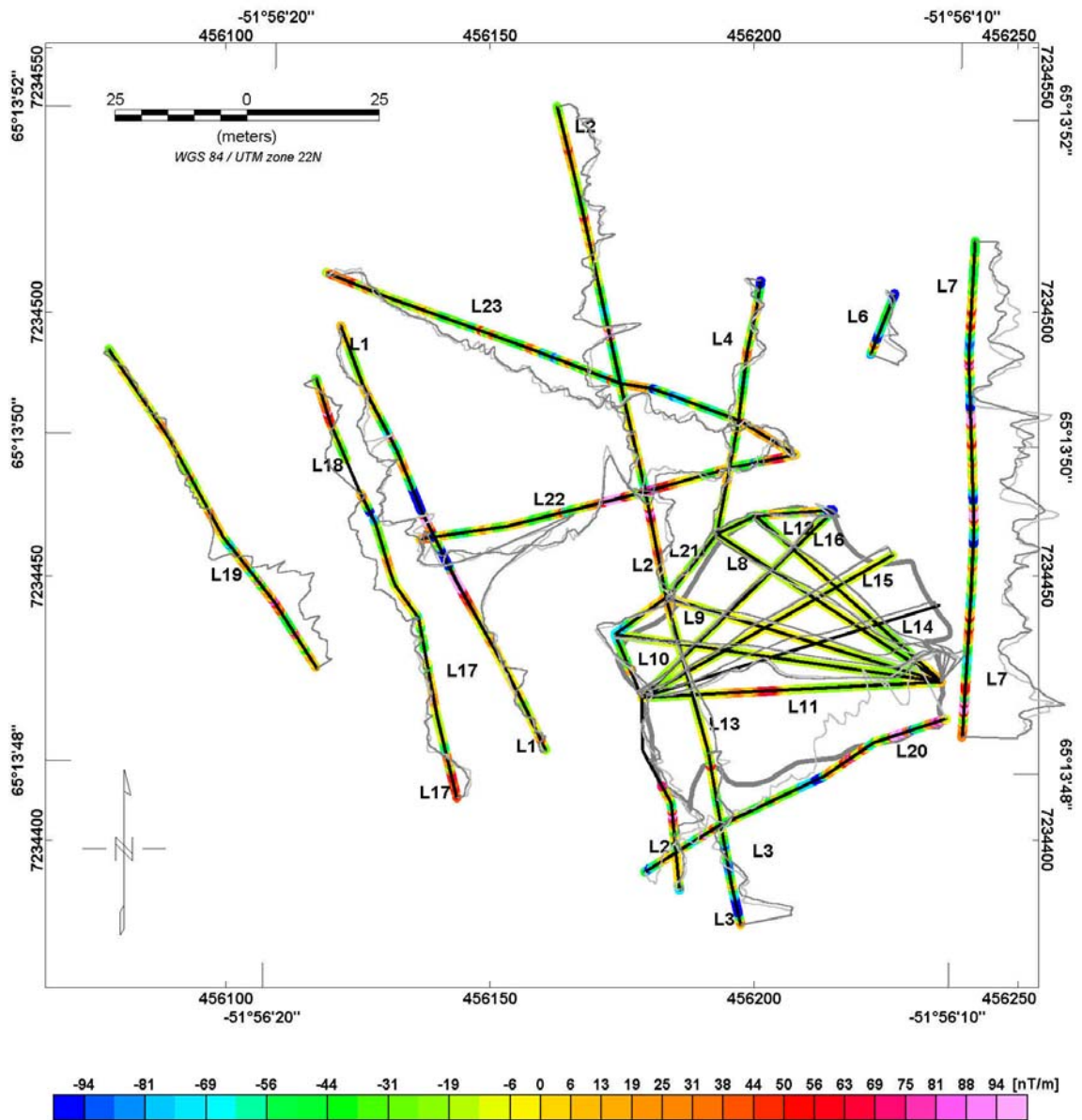
Figure 4. *Magnetic field recorded by bottom sensor and shown by profiles in dark and light grey colours for the two traverses of profiles (opposite directions if useful data were obtained for both traverses). The colour filled symbols show the calculated vertical gradient. The thick grey line marks the location of the lake.*
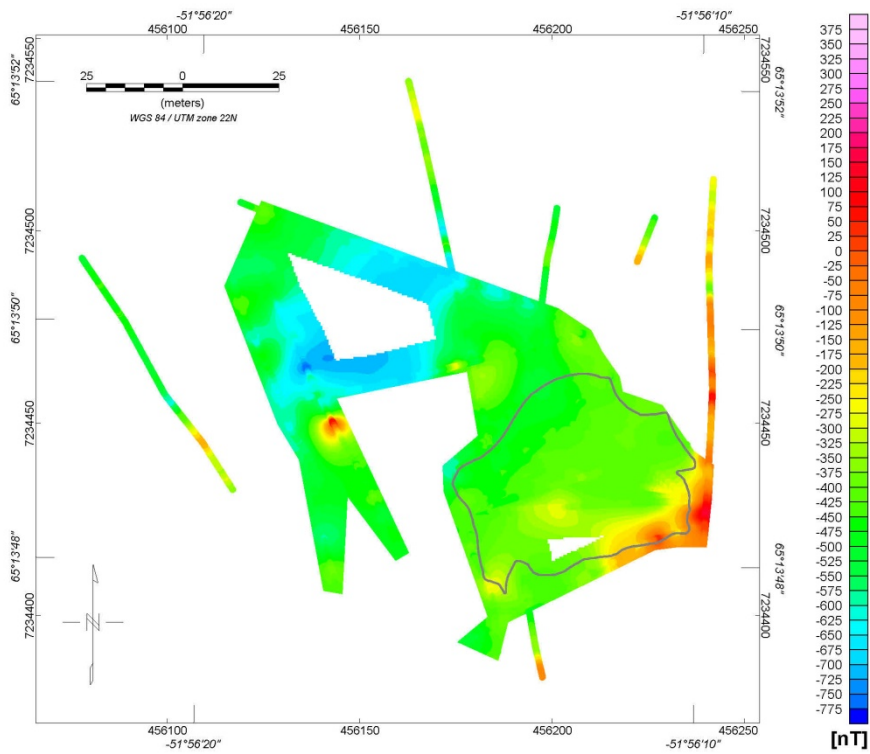
Figure 5. *Grid of magnetic data recorded by the top sensor and obtained from the first traverse of profiles. Colour filled symbols are superimposed on the map.*
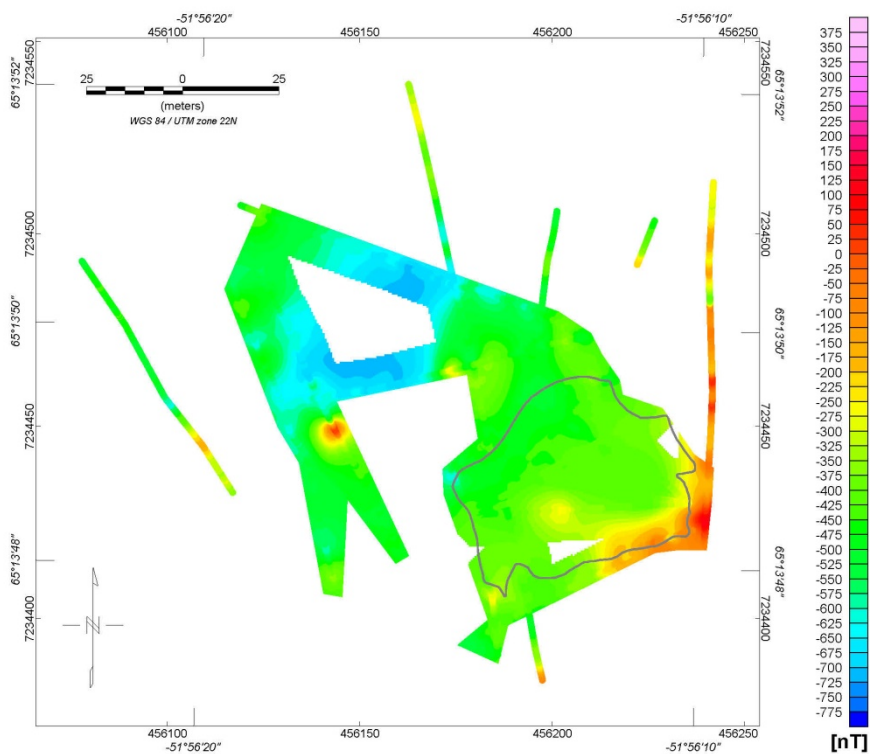
Figure 6. *Grid of magnetic data recorded by the top sensor and obtained from the second traverse of profiles. Colour filled symbols are superimposed on the map.*
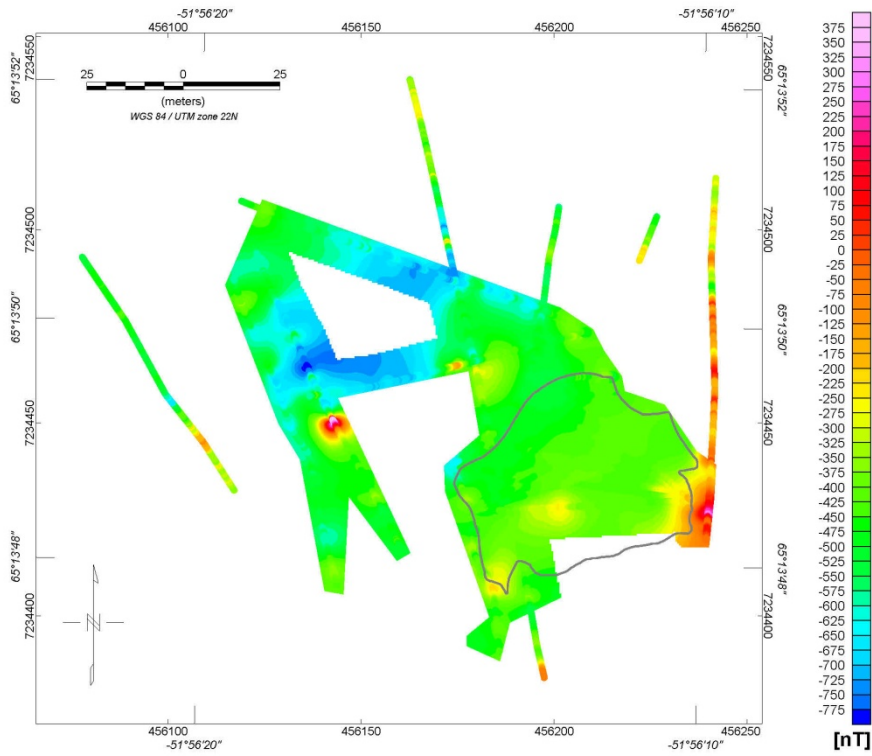
Figure 7. *Grid of magnetic data recorded by the bottom sensor and obtained from the first traverse of profiles. Colour filled symbols are superimposed on the map.*
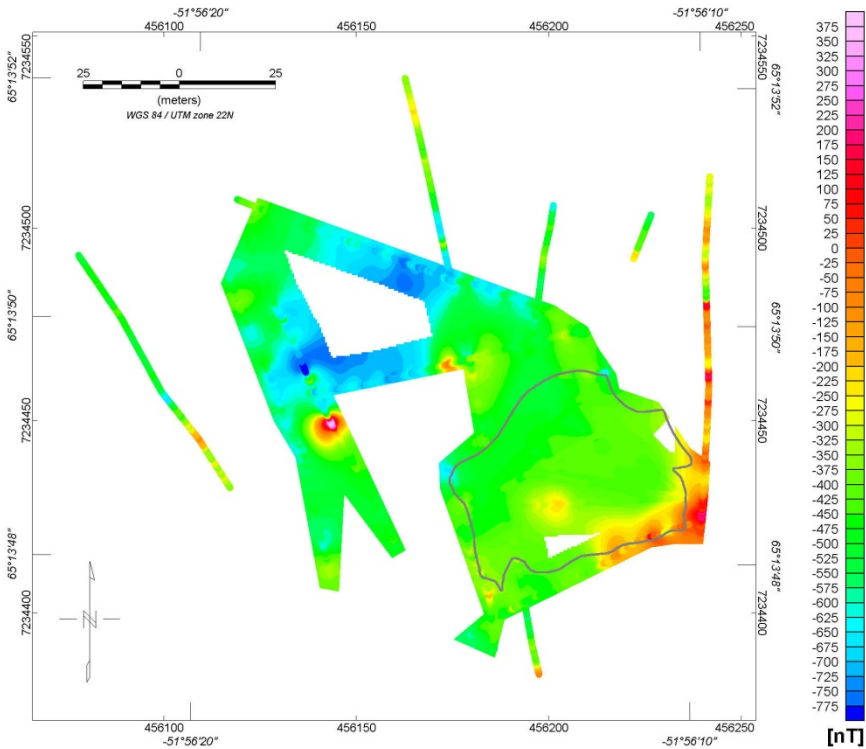
Figure 8. *Grid of magnetic data recorded by the bottom sensor and obtained from the second traverse of profiles. Colour filled symbols are superimposed on the map.*
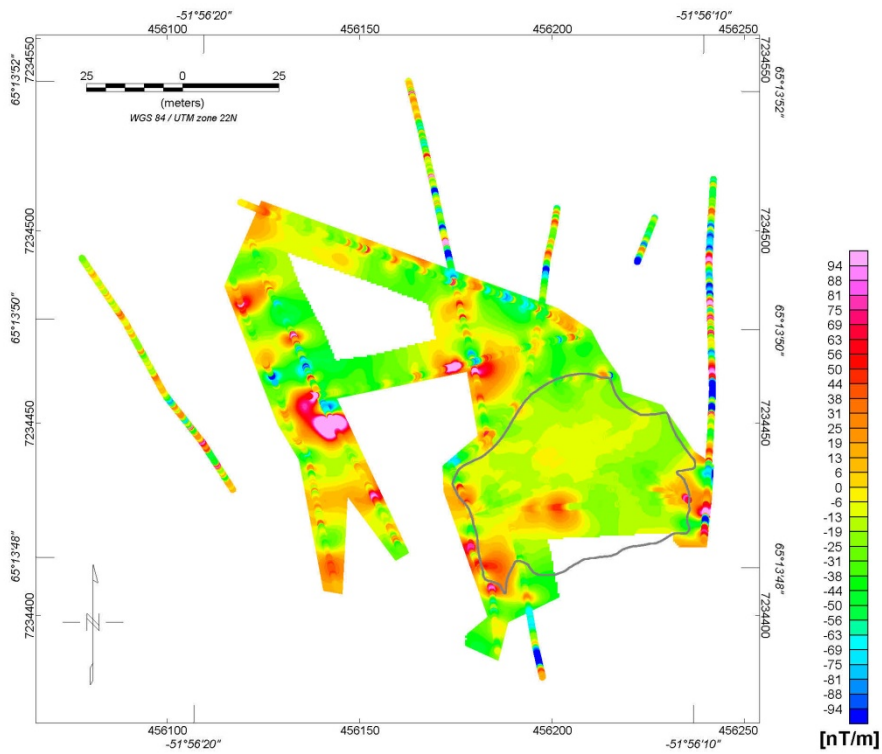
Figure 9. *Grid of magnetic gradient data obtained from the first traverse of profiles. Colour filled symbols are superimposed on the map.*
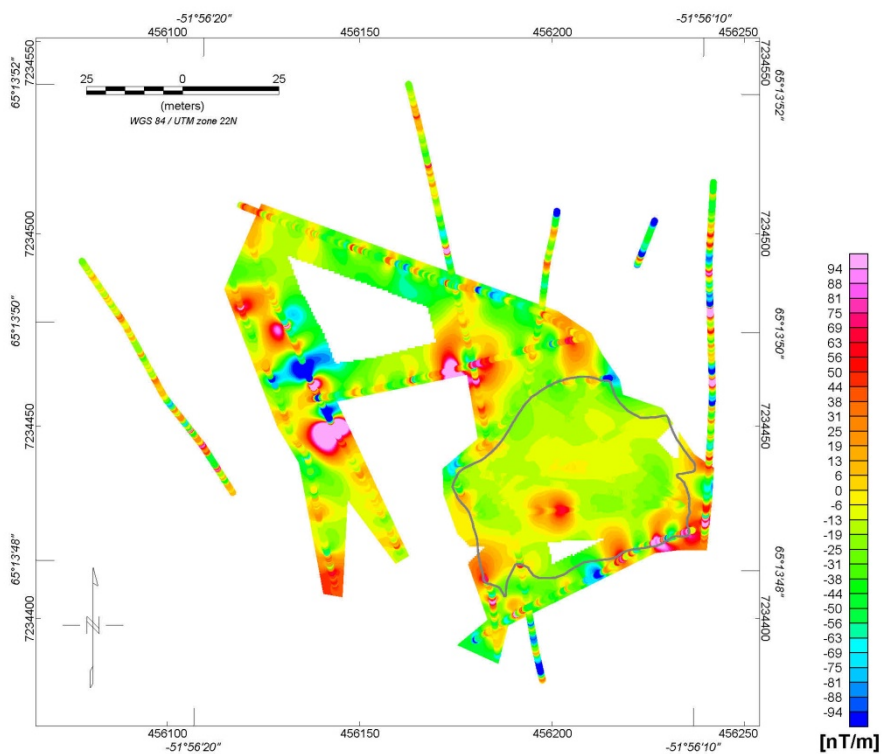
Figure 10. *Grid of magnetic gradient data obtained from the second traverse of profiles. Colour filled symbols are superimposed on the map.*

5. Magnetic susceptibility measurement

Table 2 (Appendix A) contains susceptibility values and corresponding rock descriptions obtained along some of the profiles. A general feature is that the gneiss affected by brecciation have low magnetic susceptibility, whereas the rocks that appear less or not at all affected by brecciation, have higher values. Maximum values for gneiss are in the order of 5-23*10^{-3} SI units. The highest susceptibilities are observed for the kimberlite exposures, which in some cases are about an order of magnitude higher that the values obtained for the gneisses. Exceptions to this general pattern exist. For example, susceptibilities obtained for kimberlite boulders between waypoints 136 and 137 are in the same range as observed for the gneisses with high magnetisation.

6. General features of the magnetic anomalies

A general observation is evident from the data in Figures 3-8 and from the profile plots (Appendix B): the bottom sensor data are more smooth (contain less short wavelength features) than the data from the top sensor. This is to be expected and is only a result of the strong decay of short wavelength features with distance to the sources. A highly magnetic boulder may have a strong short wavelength response at the bottom sensor, whereas the top sensor data are less influenced by minor occurrences of strong magnetic material located close to the ground surface. The top sensor data may therefore provide a more unbiased representation of sub-surface structures. The attenuation of anomalies with distance to the source is also reflected in the smooth magnetic variations recorded for the profiles crossing the lake.

Outside the lake, the profiles contain numerous short wavelength anomalies superimposed on anomalies of longer wavelength. The long wavelength features are viewed easily in the grids of the magnetic field (Figures 5-8) where the lowest magnetic field values are found in the triangle confined by profiles 1, 22 and 23. Mean values of the magnetic field above the lake is about 300 nT higher than the value for the long wavelength minimum.

Maximum values for the magnetic field are found east of the lake along profile 7 and at a location close to waypoint 129 on profile 1. The high values east of the lake correlates with the observation of intermediate to high magnetic susceptibility values, but topographic effects may contribute to these high values. The width of the anomaly on profile 1 is a few metres and indicates a structure of small size (<2 m) in width. The amplitude of this anomaly is about 1000 nT for the top sensor and about 500 nT for the bottom sensor. The large deviation between top and bottom sensor data indicates a structure close to ground level.

The magnetic field obtained above the lake has a local maximum of about 150-200 nT (defined as deviation from background level) along profile 11. With the exception of profile 13, the other profiles crossing the lake have a local weakly positive anomaly. The figures in Appendix B are most suitable for viewing this feature. The presence of this weak positive anomaly (approximately 50-100 nT) may partly be linked to the presence of a negative side-lope caused by topographic effect at the eastern and southern part of the lake. An important observation for the lake data is that the vertical gradient is negative except for the location mentioned above with a positive magnetic anomaly on profile 11. A weak local gradient maximum (relative to values close to the lake boundary; values of -10 nT/m compared to a background of -20 nT/m) is coincident with the weak magnetic field anomaly over the lake.

7. Catalogue of responses from some simple structures

This chapter contains synthetic responses from some simple structures of relevance for the understanding of the measured data. The main purpose is to provide a reference with respect to anomaly amplitude and shape that can be used in a comparison with the measured data. The following general properties of magnetic anomalies should be kept in mind, when interpreting magnetic responses:

- A magnetic response has both positive and negative values, which add to zero when integration is performed over the entire (to infinity) anomaly.
- For local structures in areas where the magnetisation direction is close to vertical, the following is valid:
    - The positive part of the anomaly is usually of shorter wavelength than the part with negative values.
    - The positive part of the anomaly is mainly linked to the top of the structure and the negative part is linked to the bottom of the structure.
    - The anomaly maximum is found close to the top of the structure
    - If the bottom is very deep compared to the top, the negative side lopes are characterised by very long wavelength and low amplitude, numerically. In some cases the magnitude of the negative part will be below the detection limit for actual measurements.
- A flat structure of infinite extension has zero response.
- A thin flat structure of finite extent has anomalies associated with the edges, and the maximum and minimum are numerically within the same order of magnitude.

The susceptibility data presented previously indicated that the kimberlite rocks in general are more magnetic than the gneisses, and that rocks affected by brecciation are low in magnetic susceptibility. For the modelling presented here, a susceptibility of 0.08 SI is used for kimberlite and 0.01 SI is used for the host rocks; i.e. a contrast in susceptibility of 0.07 SI. The anomaly amplitude depends linearly on the contrast in susceptibility, whereas the absolute values have no influence on responses. The anomaly shape is fully determined by the geometry of the structures; i.e. multiplication of a constant scaling factor to all susceptibilities will not affect the shape, except for the simple linear scaling.

Evaluation of topographic effects is difficult. Firstly, no detailed terrain model exists for the area. Secondly, calculations of synthetic responses are often subject to approximation due to computational difficulties. A first order approximation for models with both structure and topography is to use a superposition of two separate responses. for which one part is based on a flat earth response and the other part is solely due to topography. This approach is used in the evaluation for this report. The model response calculations are done by using the commercial software Model Vision Pro v10.2.

7.1   Responses for dykes

Magnetic responses are calculated for dykes with thickness of 1 m, 2 m and 4 m for sensor locations 0.5 m, 1.5 m, 5 m and 10 m above the top of the dyke. The vertical extent is 200 m. A magnetic susceptibility of 0.070 SI is used for the causative body and the inducing magnetic field is 55500 nT with an inclination of 80 degree and declination of -30 degree. Profiles orthogonal to strike are presented for a north-south strike and east-west strike of the dyke. Figures 11 and 12 show the responses. The following observations are made:

- For distances of 5 and 10 m to the top, the response amplitude is almost linearly related to the thickness of the dykes.
- For distances of 0.5 m and 1.5 m to the top, the shape of the anomalies show clear dependency on width of the dyke and the peak amplitude is not approximated by a linear relationship to dyke width.
- For distances of 0.5 m and 1.5 the maximum values is in the order of 1000 nT.

A comparison with the measured responses shows that these are similar with respect to both amplitude and shape obtained for the synthetic models.
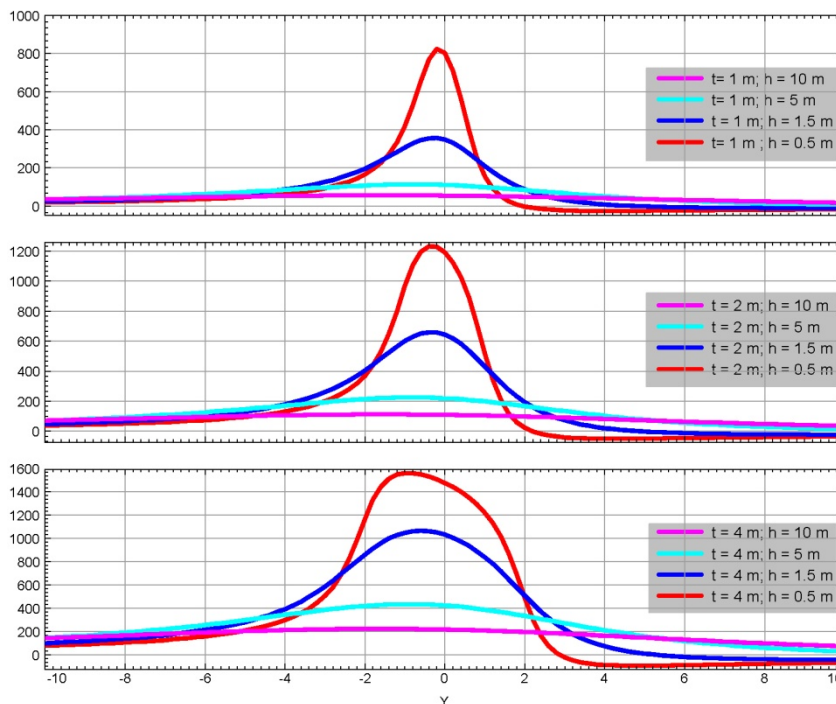
Figure 11.   *Magnetic response for dykes with widths of t=1 m, 2 m and 4 m and distances to top of dykes of h = 0.5m, 1.5 m, 5 m and 10. The dykes are oriented NS and the profile cross the centre of dyke at coordinate Y= 0 m. Units of responses in nT.*
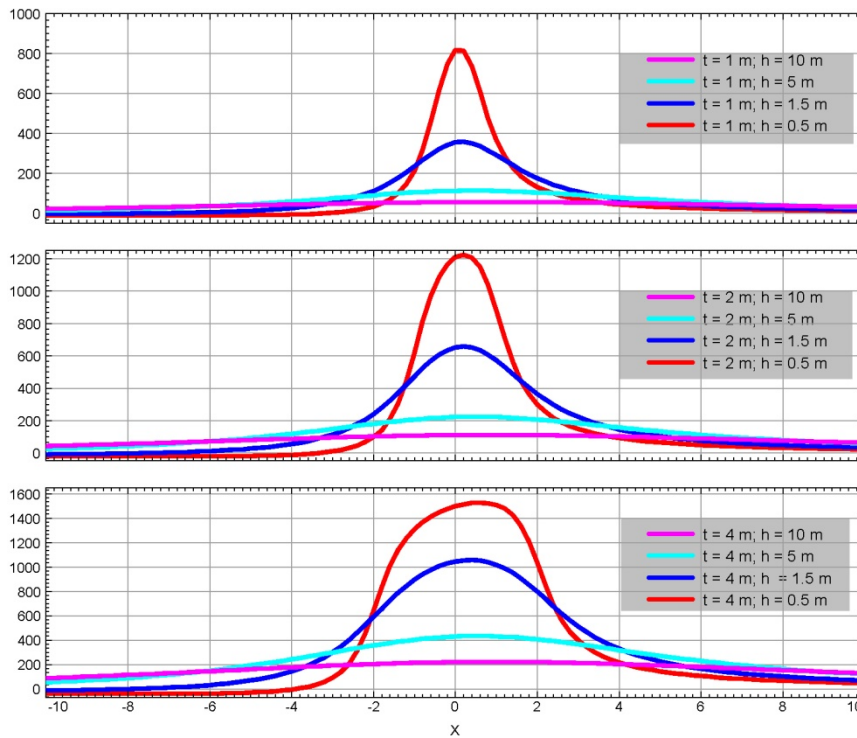
Figure 12. *Magnetic response for dykes with widths of t=1 m, 2 m and 4 m and distances to top of dykes of h = 0.5m, 1.5 m, 5 m and 10. The dykes are oriented EW and the profile cross the centre of dyke at coordinate X= 0 m. Units of responses in nT.*

7.2 Responses for pipes

Magnetic responses are presented for a pipe-like structure (vertical cylinder) with a magnetic susceptibility of 0.07 SI. The inducing field is 80 degree and declination is -30 degree. Examples with radius 5 m and 10 m are presented. The depth to the top of the structure is 6.5 m (corresponds to depth of lake) and responses are presented at altitudes of 0.5 m, 1.5 m, 50 m and 120 m above ground. Alternatively, the responses at altitudes of 50 m and 120 m represent the responses from cylinders at depth of 48.5 m and 118.5 m below the lake bottom, respectively, for measurement performed with the top sensor 1.5 m above ground or lake surface. The vertical extent of the cylinder is 200 m.

Figures 13 and 14 show images centred at the pipe location and Figures 15 and 16 show magnetic responses along east-west and north-south oriented profiles crossing the centre of the pipe. The following is noted for the responses:

- Width of anomalies measured at 0.5 m and 1.5 m above ground is slightly less than 20 m for a cylinder with radius of 5 m.
- Width of anomalies measured at 0.5 m and 1.5 m above ground is slightly larger than 20 m for a cylinder with radius of 10 m.
- Peak values are approximately 4000 nT for the cylinder with radius 5 m and approximately 9000 nT for the cylinder with radius 10 m for measurements at altitudes of 0.5 m and 1.5 m above ground.
- Width of anomalies measured at distance 50+6.5 m to a cylinder with radius of 5 m is approximately 80 m. For a distance of 120 m the width is approximately 175 m.

- Width of anomalies measured at distance 50+6.5 m to a cylinder with radius of 10 m is approximately 90 m. For a distance of 120 m the half-width is approximately 180 m.
- Peak value is approximately 83 nT and 14 nT respectively for the cylinder with radius 5 m and distances to cylinder of 50+6.5 m and 120+6.5 m
- Peak value is approximately 330 nT and 60 nT respectively for the cylinder with radius 10 m and distances to cylinder of 50m and 120 m.
- The lack of rotational symmetry for the responses is caused by the deviations from 90 degree of the magnetic inclination. The peak response is however located inside the perimeter of the cylinder.
- The vertical gradient is positive above the cylinder.

A comparison with the measured responses shows that the synthetic responses for a pipe structure close to the lake bottom have amplitudes about an order of magnitude larger than those observed. A pipe located at larger depth (> 50 m) may have amplitudes of the same order as those observed.

(a)

(b)

(c)
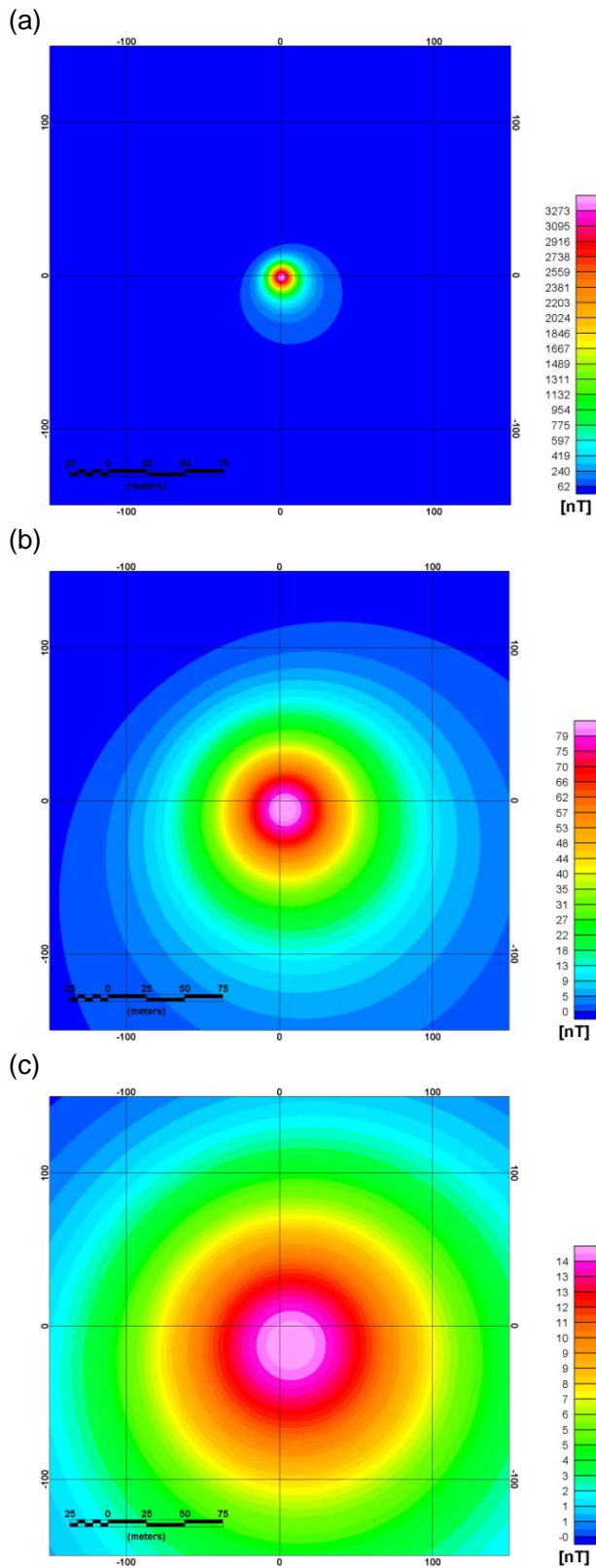
Figure 13. *Magnetic responses at altitudes of (a) 1.5.m, (b) 50 m and (c) 120 m above ground from a vertical cylinder with upper surface 6.5 m below ground surface and radius 5 m. The centre of the cylinder is at coordinate (0,0). The inducing magnetic field has an inclination of 80 degree and declination -30 degree. Note different scales for the magnetic field.*

(a)

(b)

(c)
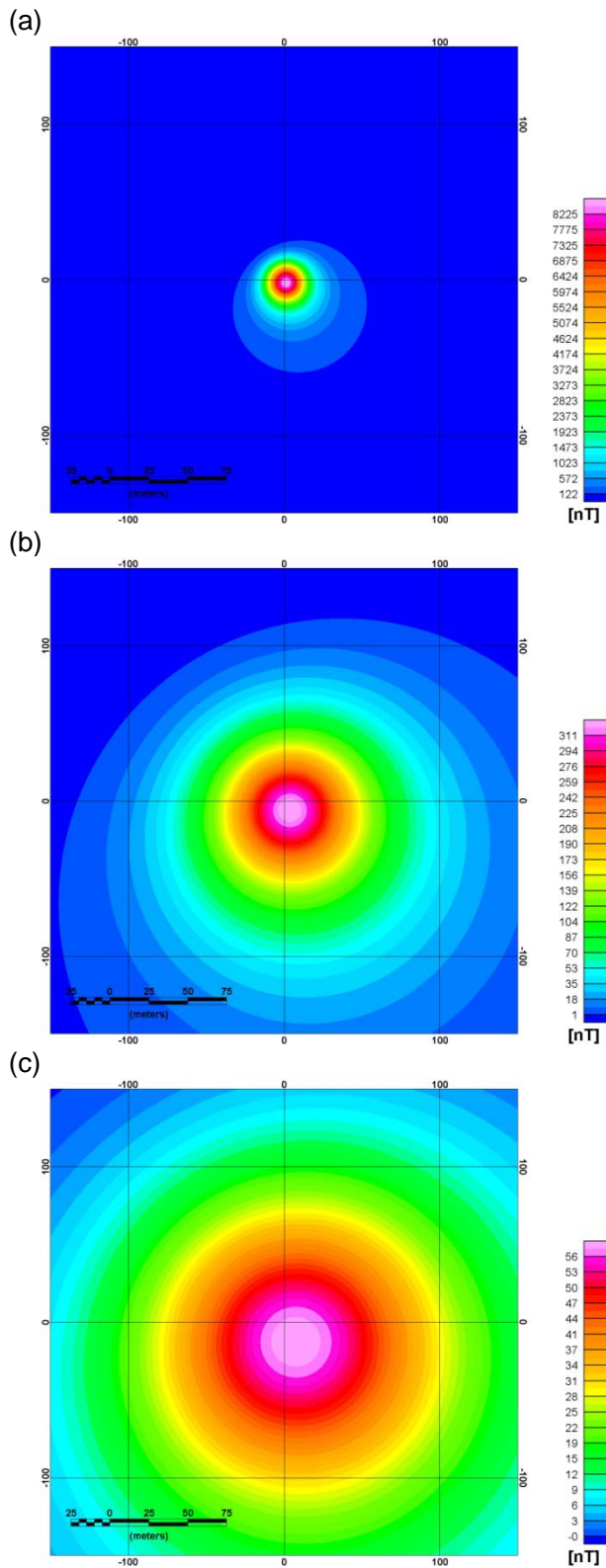
Figure 14. *Magnetic responses at altitudes of (a) 1.5.m, (b) 50 m and (c) 120 m above ground from a vertical cylinder with upper surface 6.5 m below ground surface and radius 10 m. The centre of the cylinder is at coordinate (0,0). The inducing magnetic field has an inclination of 80 degree and declination -30 degree.*

(a)

(b)
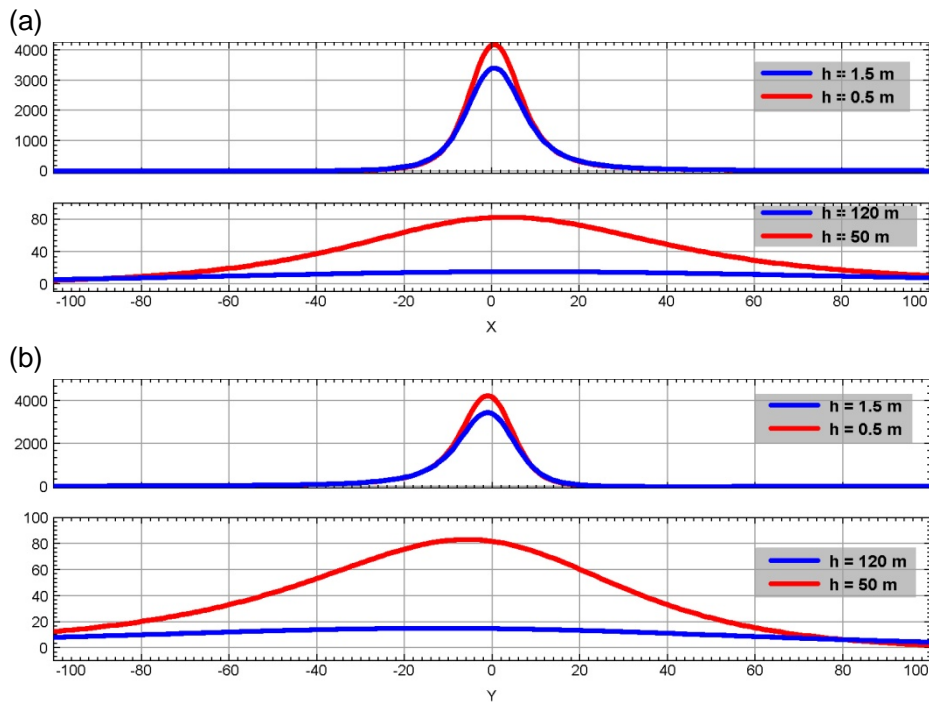
Figure 15. *Magnetic responses at altitudes h=0.5 m, 1.5 m, 50 m and 120 m above ground from a vertical cylinder with upper surface 6.5 m below ground surface and radius 5 m. The centre of the cylinder is at coordinate (0,0). The inducing magnetic field has an inclination of 80 degree and declination -30 degree. The responses are shown for (a) an east-west profile and (b) north-south profile. Units in nT.*

(a)

(b)
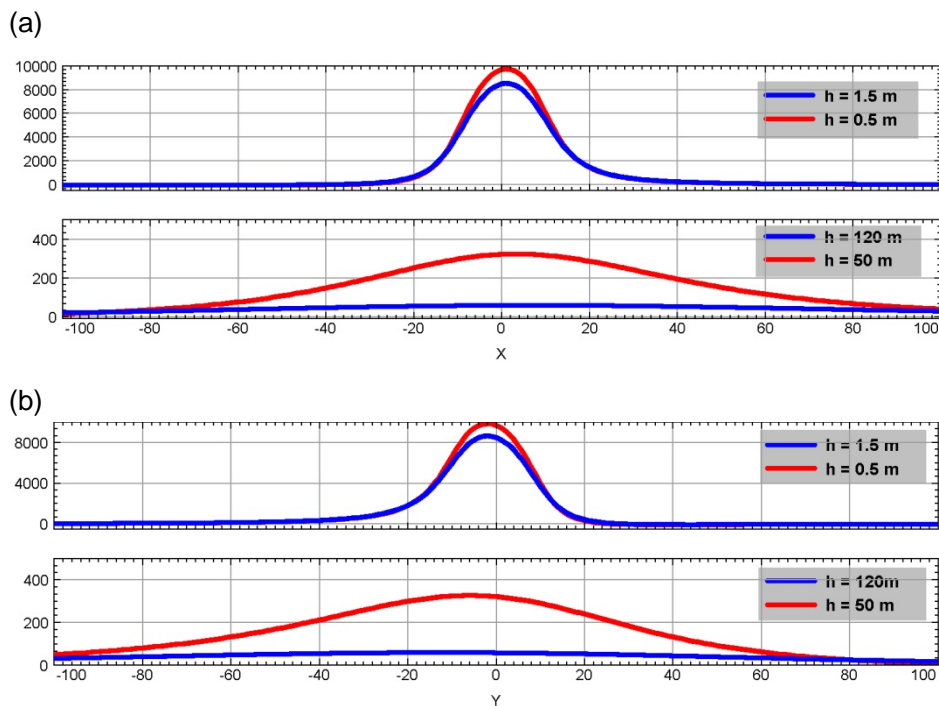
Figure 16. *Magnetic responses at altitudes h=0.5 m, 1.5 m, 50 m and 120 m above ground from a vertical cylinder with upper surface 6.5 m below ground surface and radius 10 m. The centre of the cylinder is at coordinate (0,0). The inducing magnetic field has an inclination of 80 degree and declination -30 degree. The responses are shown for (a) an east-west profile and (b) north-south profile. Units in nT.*

7.3 Response caused by topography

Two models are presented, which illustrate the significance of topography on the measured responses. The first is a simple sloping interface with two superimposed depressions, and the second is based on a combination of hyperspektral Aster data and the height information from the actual GPS measurements.

7.4 Synthetic sloping interface model

A simple synthetic topographic model of the measurement area is constructed, which is considered a reasonable approximation for the actual topography in the measurement area in relation to an evaluation of topographic effects. A perspective view of the model is shown in Figure 17. The model is composed of a sloping plane and two circular symmetric depressions superimposed onto each other. The slope has a dip towards south-east. An outer depression (northern half-circle only) with a radius of r_1=150 m is used to simulate the valley or depression in which the circular lake is found in the south-western-most part. The shape of the valley is defined to have a circular symmetric morphology, but only the northern half of this is used. The shape along the radial direction is defined as a weighted average of a horizontal plane and the intersected sloping plane, where the weight factors w_1 and w_2 are given by $w_1 = 0.5 - 0.5\cos(\pi\,r_1/150m)$ and w_2=1-w_1 The lake is simulated by an ellipsoid with a circular shaped horizontal cross-section of diameter 30 m that represents the lake surface. The depth of the lake is 6.5 m at the centre. Responses are calculated 1.5 m above ground/lake surface on a grid representation of the topography with grid node spacing of 1 m. The model is discretizised into a large number of triangular shaped blocks that approximates the topography (Figure 18). The response from topography is calculated by superposition of responses from the individual blocks. The discretization mesh is an approximation to the smooth surface described above. Some short-wavelength artefacts can be found in the final response, which mainly is attributed to deviations from the 1.5 m in altitude above ground requested for the modelling. Some long wavelength artefact is also present due to the final horizontal extent of the model. A susceptibility of 0.01 SI is used and the inducing field has a strength of 55500 nT, an inclination of 80 degree and a declination of -30 degree, which is similar to real values for the survey area.

The magnetic response from topography is shown in Figure 19 for a 380x380 m^2 area centred at the lake, and in Figures 20 and 21 for 4 profiles with locations marked in Figure 19. The following can be noted after removal of the regional response:

- The response over the lake has a well defined minimum with an amplitude of -120 nT and positive "shoulders" are located around the perimeter of the lake
- The valley is associated with a long wave-length minimum with amplitude of about -60 nT.
- The vertical gradient is negative (-10nT/m) above the lake centre at the surface of the lake (field increases upwards).

The most important conclusion from this modelling of the topography is that amplitudes numerically are an order of magnitude lower than those noticed for the synthetic models

with the pipe-like structures with a top close to the lake bottom as presented in the previous section. Thus, a response from a kimberlite pipe will **not** be masked by an oppositely directed response from topography, provided that the pipe has an upper surface at the lake bottom. Note that the conclusion is not straightforward for a pipe located at a larger depth. In this case, the responses are of similar amplitude and with opposite sign. The wavelength content of these anomalies is, however, different and the two contributions will therefore not cancel to zero level. The response due to the lake will be easy to identify. The response from the deep kimberlite may be more difficult to identify due to the long-wavelength character, which is likely to have similarities with responses possible from inhomogeneously magnetised gneisses.
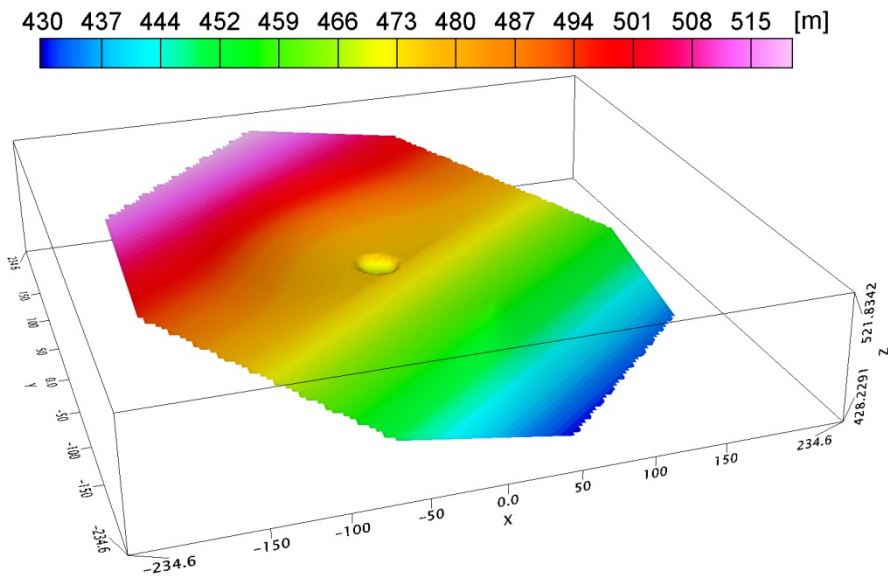
Figure 17. *Perspective view of topographic relief used in simulation of magnetic response due to topographic variation. The model has a southeast ward sloping plane with two superimposed depressions. View from west-southwest.*
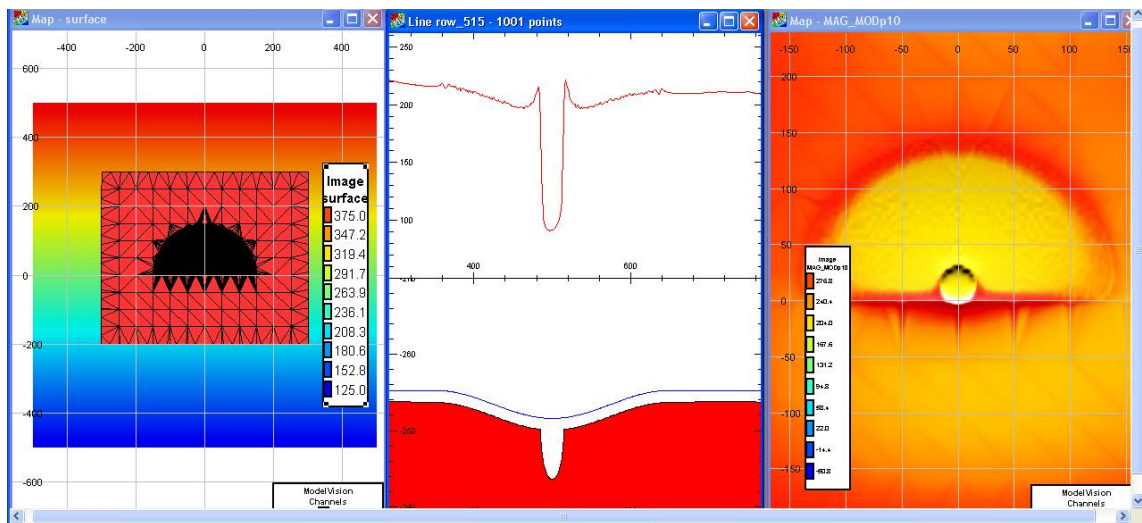
Figure 18. *Screen-dump from the ModelVision PRO software used for generating the synthetic response from topography. Three images are shown. The leftmost image shows the discretization of the topography, where each black line represent a block boundary within the mesh approximating the topography. The image in the middle is a vertical cross section through the model (red colour) along an east-west profile crossing the lake. The blue curve above and adjacent to the model is the measuring location. The magnetic field in units of nT is shown by the red curve in the upper panel. The rightmost image is the calculated magnetic field. Coordinates and data values in this figure are relative, and the images are rotated into a coordinate system with y-axis along strike of topography.*
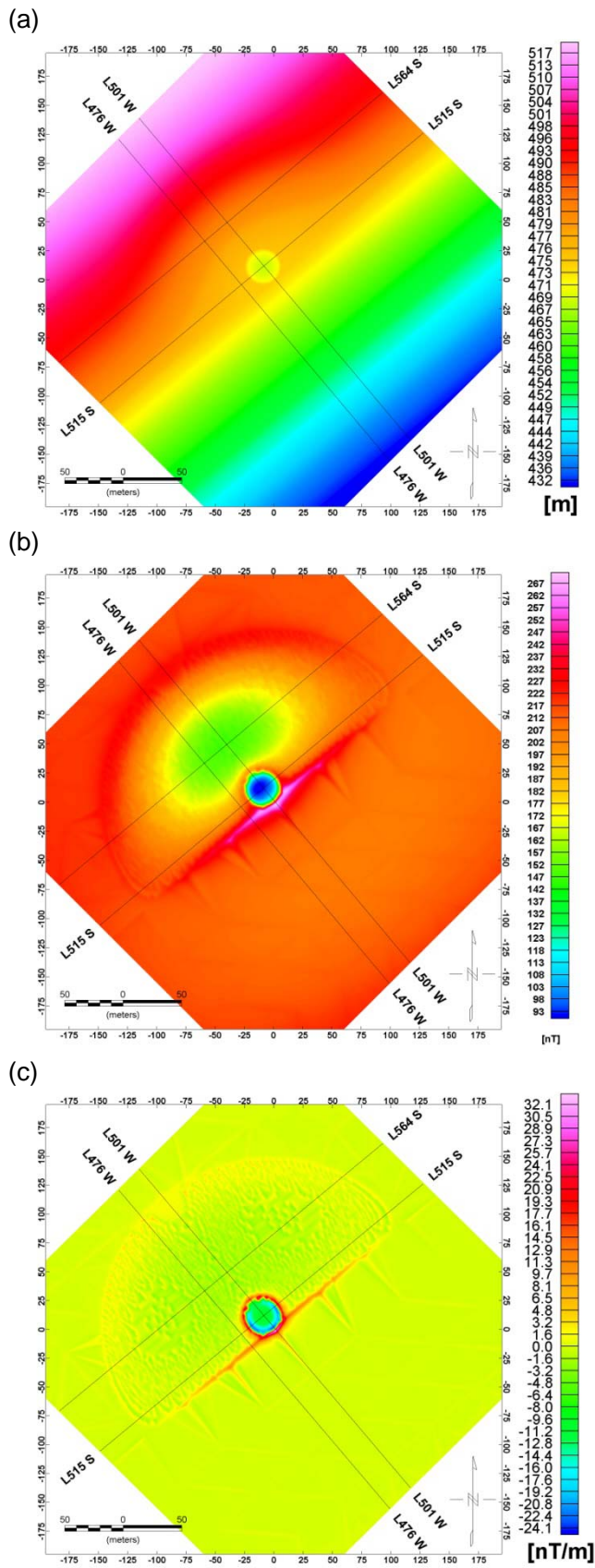
Figure 19. *(a) Subsection of the ground morphology with position of 4 profiles selected for display in separate Figures and (b) corresponding magnetic response and (c) vertical gradient.*

(a)

(b)
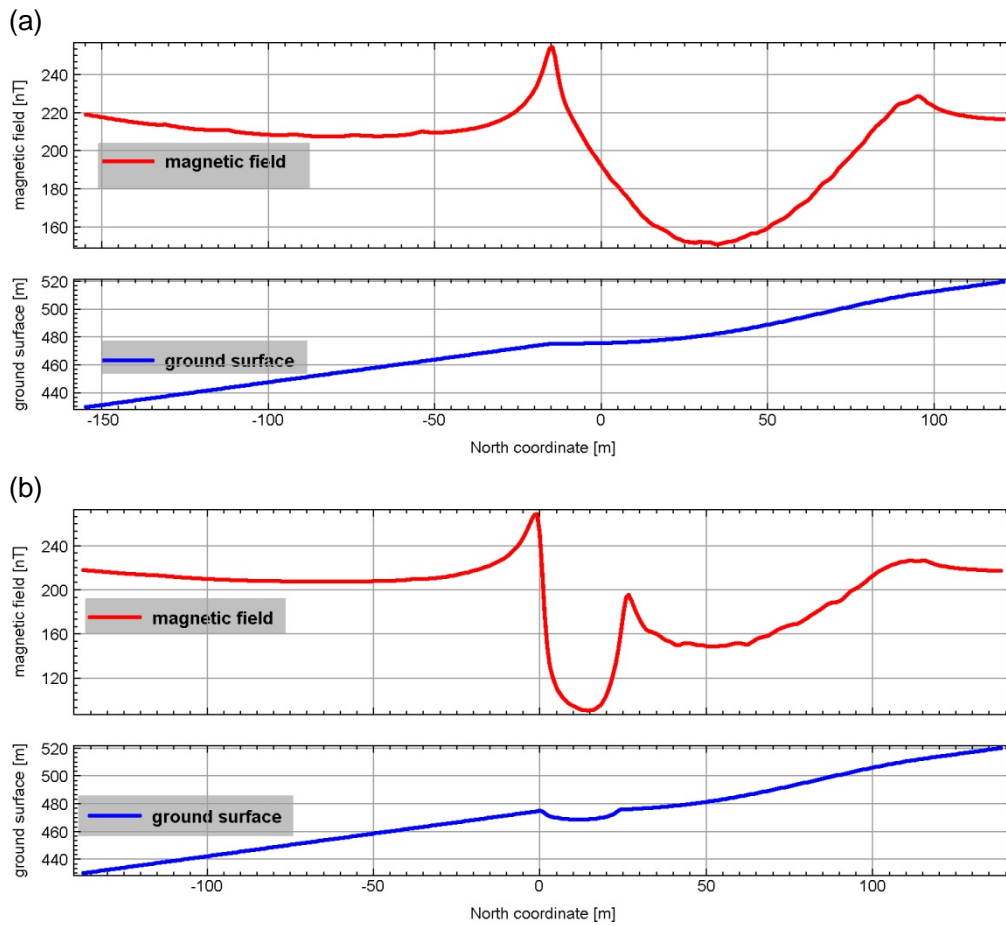
Figure 20. *Magnetic response (red curve) along two SE-NW oriented profiles (see location in Figure 19; (a):Line L476 W, (b):Line 501 W, and the corresponding topography (blue curve).*
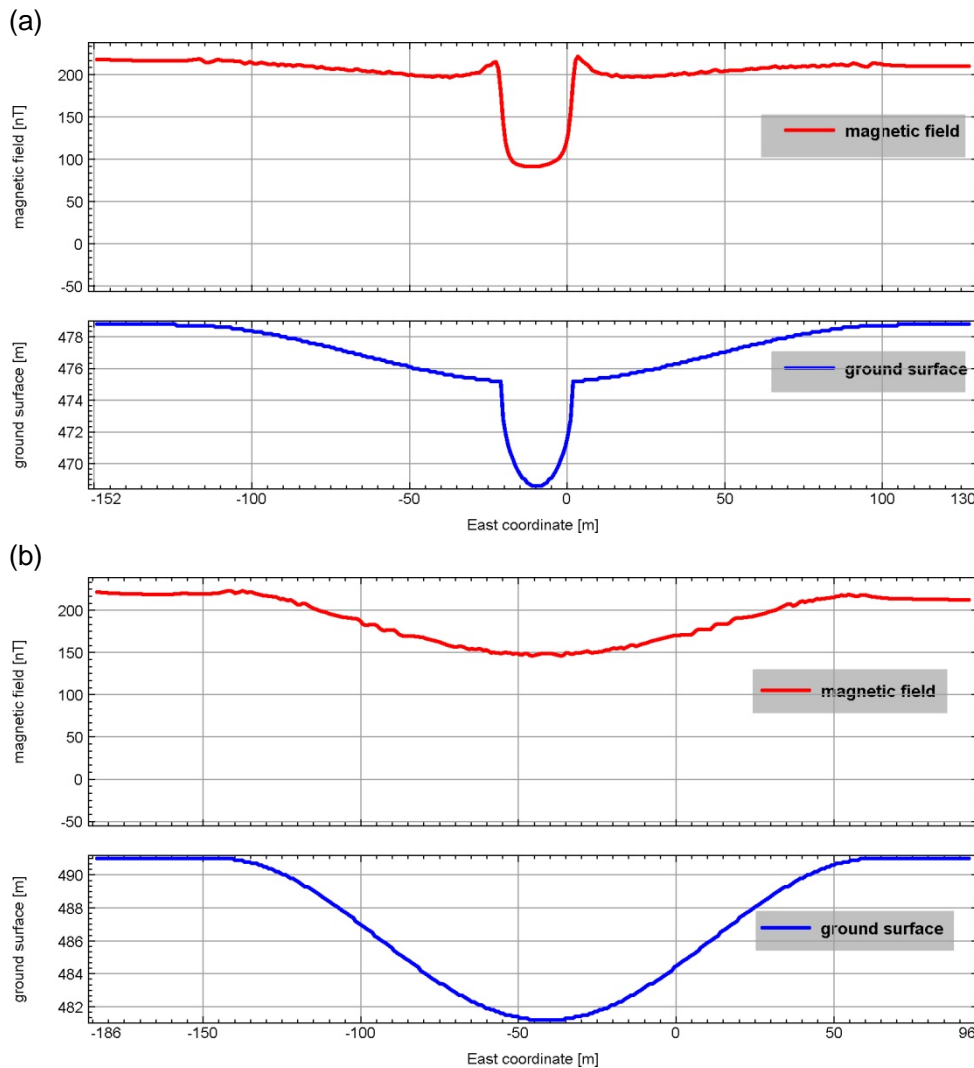
Figure 21. *Magnetic response (red curve) along three SW-NE oriented profiles (see location in Figure 19; (a):Line 515 S, (b):Line 564 S, and the corresponding topography (blue curve).*

7.5 Topographic model from Aster data and GPS-measurements

The most detailed digital elevations model available from the area is derived from hyper-spectral Aster data. This model has a 30 m horizontal resolution and is therefore very coarse in relation to the scale of the actual magnetic survey. The digital terrain model was supplemented by the GPS measurements along the magnetic profiles in order to improve the resolution of the terrain model. A model of the lake bottom was constructed using the same procedure as outlined in the previous section. A diameter of 35 m was used for the lake and maximum depth of the lake is 7 m. Figure 22 shows the final terrain model. It must be emphasized that the digital terrain model also after the inclusion of GPS data really is too coarse for a detailed study of terrain effects on the measured data.

Calculation of terrain effects is done by using the same magnetic properties as in the previous section. The response is shown in Figure 23 which also includes an grid image of the

actual measured data for comparison. Measured and model responses are extracted along a profile crossing the lake and they displayed in Figure 24 together with the topography and the magnetic sensor location. The measured data corresponds to the gridded data in Figure 23b. The location of the profile is marked in Figure 23a. The vertical gradient of the magnetic field above the lake is approximately -8 nT/m (not shown in Figures).

The following can be noted after removal of the regional response:

- The model response over the lake has a well-defined minimum with an amplitude of -200 nT and positive "shoulders" are located around the perimeter of the lake.
- Most of the triangular area confined by profiles 1, 22 and 23 has <u>modelled</u> magnetic field values larger than those above the lake, but a few local minima exist.
- High values of the magnetic field are found east and south of the lake.
- The vertical gradient is negative (- 8 nT/m) above the centre of and at the surface of the lake (field increases upwards).
- The measured and model responses along the extracted profile in Figure 24 show similarity in terms of both shape and amplitude above the lake if a longer wavelength tilt correction is applied to the measured response data. The longer wavelength correction is linked the <u>measured </u>magnetic minimum in the triangular area confined by profiles 1, 22 and 23.

(a)

(b)
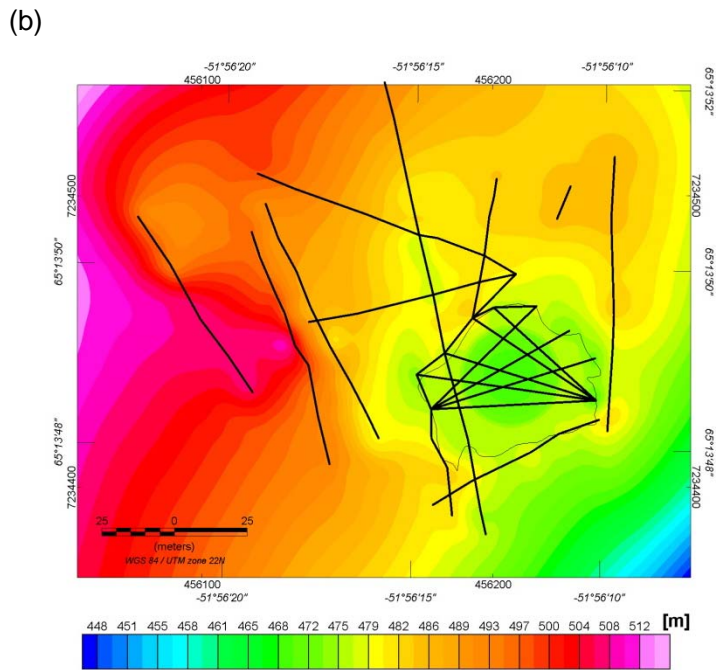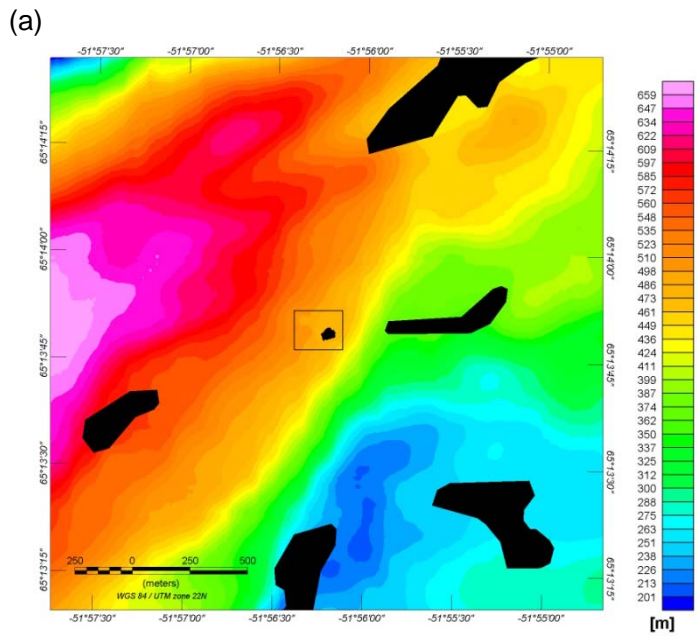
Figure 22. *(a) Digital terrain model derived from Aster data with lakes marked by filled polygons in black colour. The rectangle in black colour marks the location of (b) a digital terrain model from merged Aster data and GPS measurements along measuring profiles .The actual lake perimeter is outlined by the dark grey polygon and measurement profiles are shown by black lines.*

(a)
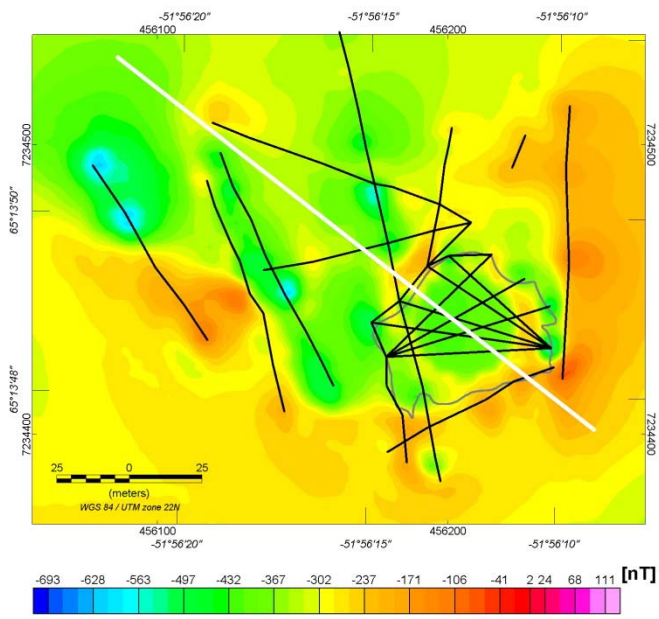
(b)
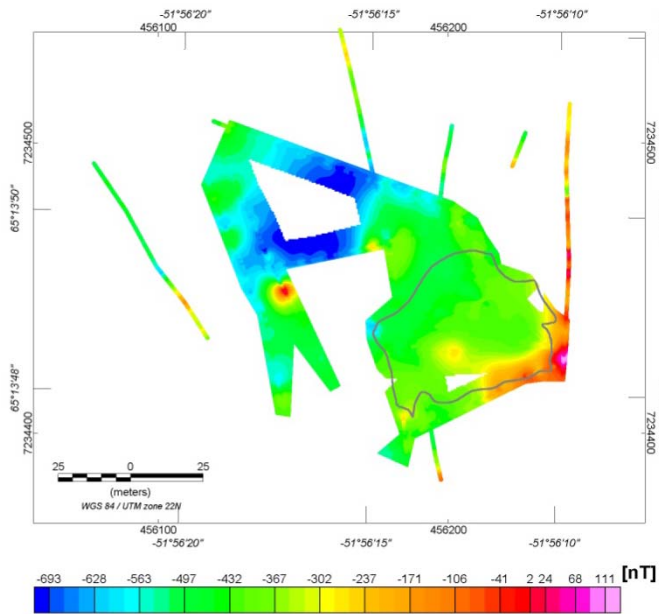
Figure 23. *(a) Calculated response from topography with measured profiles shown by lines in black colour and an extracted profile (Figure 24) marked by the line in white colour, and (b) measured responses from the survey (similar to data in Figure 8). The colour scales used for calculated and measured responses are similar.*
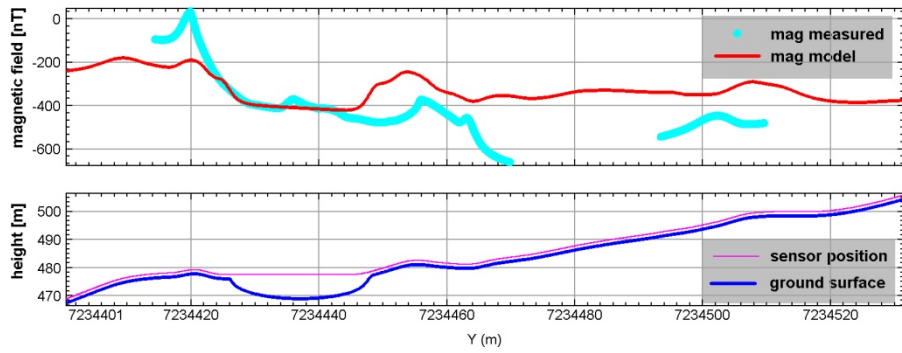
Figure 24. *Upper panel shows measured (filled blue circles) and modelled (red curve) magnetic response extracted along the profile marked in Figure 23. Measured data refer to the grid of the measured profile data. The lower panel shows the ground surface in units of m (blue colour) and location of sensor position (cyan colour) which is 1.5 m above ground/lake surface. Abscissa is UTM north coordinate.*

8. Interpretation of measured data

A comparison between measured responses and model responses from the two pipe models with top surface close to the lake bottom show synthetic responses an order of magnitude larger than those measured. The widths of the synthetic responses are furthermore much wider than measured on any of the profiles. A reduction of the susceptibility from 0.07 SI to 0.007 SI or lower is required to reduce the amplitude to values similar to the maximum observed, but the width of the synthetic responses will remain unchanged. **Therefore, the two pipe models with top surface close to the ground level are <u>not</u> consistent with the measured anomalies.**

Model responses from pipes with top surface at depth of 50 m and 120 m are in the same order of magnitude of the observed anomalies. The widths of the anomalies for these deep structures are furthermore very large. The dominating wavelengths are in the same range as observed for the responses possible from topography. These similarities imply that it is **not possible to exclude the existence of deep pipe structures**. The magnetic data are not conclusive for these cases. It should be noted that the pipe models have diameters of only 10 m and 20 m respectively. An increase of the diameter by a factor of α will increase the amplitude approximately by α^2. An interpretation with the existence of a pipe with larger diameters might still be difficult to exclude based on an evaluation of the measured data. In particular, the uncertainties related to the choice of magnetic susceptibilities imply that the existence of a pipe like structure cannot be excluded.

A weak magnetic maximum was noted for profiles 8, 9, 10, 11, 12 and 14 above the lake. Profiles 15 and 16 have two weak local maxima. This contrasts the response from topography that showed a clear minimum above the lake. The contribution to the response from the ground below the lake bottom is therefore expected to be slightly higher than indicated in profile data. The measured vertical gradient data over the lake are consistent with the values obtained for the synthetic responses from topography. The vertical gradient is negative with mean values of -10 nT/m. The weak maximum in magnetic field may be caused by kimberlite rocks below the lake, but an interpretation with high susceptibilities for gneisses is also possible. A volume estimation of the causative body cannot be done with any confidence.

The largest anomaly observed is on profile 1 close to waypoint 129 and is likely caused by kimberlite. **The anomaly is narrow and indicates a horizontal extent of a few square meters and most likely a small volume.** The data are not conclusive with respect to geometry and continuation of this kimberlite body to locations on other profiles with high magnetic field values. Although the measured response is similar to those obtained for the synthetic dyke models in chapter 7, it should be noted that a simple dyke structure is not valid. The double peak anomaly on profile 22 around waypoint 138 indicates a fairly inhomogeneous occurrence of kimberlite close to this location. The low magnetic field values within the triangular area confined by lines 1, 22 and 23 may partly be linked to the negative side lopes associated with the above mentioned maxima on lines 1 and 22. Low susceptibilities due to brecciation may contribute to these low values.

9. References

Jensen, S.M., Secher K. & Rasmussen, T.M. 2004a: Diamond content of three kimberltic occurrences in southern West Greenland. Diamond identification results, field description and magnetic profiling. Danmarks og Grønlands Geologiske Undersøgelse Rapport 2004/19 , 41 pp.

Jensen, S.M., Secher, K., Rasmussen, T.M. & Schjøth, F. 2004b: Diamond exploration data from West Greenland: 2004 update and revision. Danmarks og Grønlands Geologiske Undersøgelse Rapport 2004/117 , 90 pp. + 1 DVD.

10. Appendix A - GPS waypoints, rock observations and in-situ susceptibilities

Table 1 contains a complete list of GPS waypoints measured together with a few comments. Comments on rock types and in-situ susceptibilities measurements are found in Table 2. GPS coordinates used for geo-referencing the profiles with magnetic data are found in Table 3. Some locations have two or more GPS-measurements and thereby also waypoint numbers. The GPS-measurement done first is used for these cases.

Table 1. *All GPS-locations*

Waypoint	Easting	Northing	Elevation	comment	Date	Description
125	456121.7	7234497	491.1		01/09/2010 20:26	
126	456126.1	7234485	489.0		01/09/2010 20:28	
127	456132.2	7234474	488.7		01/09/2010 20:29	
128	456137.1	7234462	485.3		01/09/2010 20:31	
129	456143.6	7234449	481.5		01/09/2010 20:33	
130	456151	7234436	484.1		01/09/2010 20:35	
131	456156.5	7234425	479.8		01/09/2010 20:36	
132	456160.5	7234417	479.1		01/09/2010 20:38	
133	456162.7	7234539	491.4		01/09/2010 20:46	
134	456165.8	7234527	489.4		01/09/2010 20:48	
135	456169.2	7234512	484.1		01/09/2010 20:50	
136	456171.9	7234499	480.3		01/09/2010 20:52	
137	456174.6	7234487	477.2		01/09/2010 20:53	
138	456179.4	7234466	474.1		01/09/2010 20:57	
139	456183.3	7234446	473.3		01/09/2010 20:59	
140	456191.3	7234417	472.6		01/09/2010 21:08	
141	456195.6	7234392	474.5		01/09/2010 21:10	
142	456197.5	7234384	477.2		01/09/2010 21:12	
143	456201.3	7234506	484.4		02/09/2010 13:43	
144	456200.3	7234500	482.9		02/09/2010 13:45	
145	456198.7	7234493	482.9		02/09/2010 13:47	
146	456197.1	7234479	481.3		02/09/2010 13:49	
147	456195.3	7234471	481.7		02/09/2010 13:50	

Table 1 continued

Way-point	Easting	Northing	Eleva-tion	com-ment	Date	Description
148	456192.9	7234458	483.9		02/09/2010 13:52	
149	456207.9	7234473	480.8		02/09/2010 13:57	
150	456191.7	7234456	480.3		02/09/2010 13:58	
151	456181.9	7234447	479.6		02/09/2010 14:00	
152	456226.6	7234503	485.1		02/09/2010 14:04	
153	456222.1	7234492	485.3		02/09/2010 14:06	
154	456241.9	7234513	486.3		02/09/2010 14:09	
155	456240.7	7234492	485.1		02/09/2010 14:13	
156	456241.6	7234459	483.4		02/09/2010 14:14	
157	456241.1	7234447	478.9		02/09/2010 14:16	
158	456239.8	7234427	481.5		02/09/2010 14:18	
159	456239.4	7234419	480.1		02/09/2010 14:19	
160	456235.5	7234430	471.2	Lake	02/09/2010 16:35	
161	456178.7	7234427	473.8	Lake	02/09/2010 17:30	
162	456173.6	7234439	474.3	Lake	02/09/2010 17:30	
163	456200.2	7234462	474.8	Lake	02/09/2010 17:49	
164	456215	7234462	476.5	Lake	02/09/2010 18:41	
165	456226.3	7234454	473.1	Lake	02/09/2010 18:44	
166	456235.1	7234444	472.6	Lake	02/09/2010 18:46	
167	456117	7234488	496.6		03/09/2010 12:55	
168	456119.8	7234479	494.5		03/09/2010 12:58	
169	456125.5	7234466	498.1		03/09/2010 13:00	
170	456128.3	7234460	496.2		03/09/2010 13:02	Stand still between 170 and 178
171	456136.5	7234442	498.6		03/09/2010 13:04	On top of kimberlite ?
172	456139.8	7234424	493.0		03/09/2010 13:05	
173	456143.7	7234408	493.0		03/09/2010 13:07	
174	456077.8	7234493	493.0		03/09/2010 13:15	
175	456089	7234477	493.0		03/09/2010 13:28	
176	456109.2	7234445	507.5		03/09/2010 13:30	
177	456117.2	7234433	507.5		03/09/2010 13:31	
178	456131.9	7234449	507.5		03/09/2010 13:48	
179	456099.3	7234458	507.5		03/09/2010 14:18	Kimberlite in situ 3m E of wp.

Table 1 continued

Waypoint	Easting	Northing	Elevation	comment	Date	Description
1	456186.2	7234478	481.7	test	03/09/2010 12:06	
2	456162.5	7234465	482.2	test	03/09/2010 12:07	
3	456162.7	7234465	483.2	test	03/09/2010 12:07	
4	456179.3	7234394	481.3		03/09/2010 12:25	
5	456192.8	7234402	479.6		03/09/2010 12:26	
6	456213	7234412	478.4		03/09/2010 12:27	
7	456222.7	7234418	481.0		03/09/2010 12:28	
8	456236.4	7234423	480.3		03/09/2010 12:29	
9	456185.8	7234390	481.7		03/09/2010 12:31	
10	456184.3	7234407	482.9		03/09/2010 12:32	
11	456178.8	7234417	479.3		03/09/2010 12:32	
12	456180.8	7234427	477.4		03/09/2010 12:33	
13	456180.8	7234427	478.4		03/09/2010 12:33	
14	456177.5	7234439	478.4		03/09/2010 12:34	
15	456185.8	7234447	477.9		03/09/2010 12:34	
16	456195.8	7234456	477.7		03/09/2010 12:35	
17	456203.7	7234462	477.9		03/09/2010 12:35	
18	456215.8	7234461	479.1		03/09/2010 12:36	
19	456136.6	7234457	490.2		03/09/2010 12:39	
20	456153.4	7234460	485.6		03/09/2010 12:40	
21	456179	7234465	480.3		03/09/2010 12:40	
22	456196.6	7234469	480.1		03/09/2010 12:41	
23	456209.9	7234471	479.1		03/09/2010 12:41	
24	456119	7234508	499.3		03/09/2010 13:22	
25	456131.5	7234503	494.7		03/09/2010 13:23	
26	456156.6	7234494	486.5		03/09/2010 13:23	
27	456173.6	7234488	482.5		03/09/2010 13:24	
28	456180.9	7234486	481.7		03/09/2010 13:24	
29	456197.4	7234480	481.5		03/09/2010 13:24	
30	456197.5	7234480	481.5		03/09/2010 13:24	
31	456208	7234475	480.5		03/09/2010 13:25	
32	456207.6	7234474	480.5		03/09/2010 13:27	
33	456207.8	7234474	479.3		03/09/2010 13:27	
34	456195.9	7234480	481.0		03/09/2010 13:28	
35	456179.9	7234486	481.0		03/09/2010 13:28	
36	456006.8	7234431	528.6		03/09/2010 14:18	
37	456005.4	7234442	526.4		03/09/2010 14:19	
38	456011.4	7234462	525.0		03/09/2010 14:19	
39	455926.6	7234401	542.8		03/09/2010 14:35	
40	455922.1	7234420	545.4		03/09/2010 14:36	

Table 2. *Measured susceptibilities, rock types and corresponding waypoint.*

Waypoint	Value 1	Value 2	Value 3	Value 4	Value 5	Value 6	Value 7	Remarks
125	3.81	1.73	1.18					
126								No in situ outcrop only boulders
127								No in situ outcrop only boulders
Between 127 and 128	111.00	76.70	112.00	86.00	86.00			Kimberlite
	13.60							Breccia
	-0.66							Red stained gneiss
	0.00							Breccia matrix
128	0.91							In situ gneiss
129	21.30	44.80	30.20	52.80	7.32			Kimberlite
Between 129 and 130	1.40	2.36	1.82					Gneiss boulder in breccia
130								Boulder field
131								Boulder field
132	-0.78	4.07						Reddish gneiss
	4.29	1.94	12.20	9.27	4.28			Coarse-grained granite
	7.22	10.80	10.10	9.46				Grey gneiss south of lake
141	5.72	3.91	6.37	11.70	9.50			Red gneiss 3 m north of 141
	10.20	14.40	6.20	2.00				Grey gniess
142	6.19	10.90	10.70	12.80				Light pink gneiss
133	4.98	9.28	4.09	3.39	3.95			Grey-pink gneiss
135	3.12	5.15	6.27	2.43	5.94			Grey-pink gneiss
Between 136 and 137	11.40	13.20	6.84	27.50	14.60	13.50	14.20	Kimberlite boulders
	8.95	12.70	3.29	0.75				Gneiss outcrop
143	10.90	11.90	6.80	14.60	5.12			Grey gneiss
145	5.82	6.41	3.54	11.80	7.79	7.67		Pegmatitic granite
164	2.20	5.02	4.52	7.68	3.64			Red gneiss wall E of lake
152	17.90	13.40	13.70	3.08	8.53			Redish gneiss
153	19.00	12.50	6.85	17.00	15.50			Grey gneiss
154	4.05	6.25	2.88	10.10	22.70	4.30		Grey gneiss
155	11.20	12.30	12.00	23.50				Grey gneiss
156	3.93	5.33	10.30	9.89	12.40			Grey gneiss
157	2.07	8.07	4.24	4.73	6.00			Grey gneiss
158	7.47	16.10	19.80	6.55	9.54			Grey gneiss

Table 3. *Waypoints and profile numbering*

Profile	X_UTM22N	Y_UTM22N	Waypoint No.
1	456122	7234497	125
1	456126	7234485	126
1	456132	7234474	127
1	456137	7234462	128
1	456144	7234449	129
1	456151	7234436	130
1	456157	7234425	131
1	456161	7234417	132
2	456163	7234539	133
2	456166	7234527	134
2	456169	7234512	135
2	456172	7234499	136
2	456175	7234487	137
2	456179	7234466	138
2	456183	7234446	139
3	456191	7234417	140
3	456196	7234392	141
3	456197	7234384	142
4	456201	7234506	143
4	456200	7234500	144
4	456199	7234493	145
4	456197	7234479	146
4	456195	7234471	147
4	456193	7234458	148
5	456208	7234473	149
5	456193	7234458	148
5	456183	7234446	139
6	456227	7234503	152
6	456222	7234492	153

Table 3 – continued

Profile	X_UTM22N	Y_UTM22N	Waypoint No.
7	456242	7234513	154
7	456241	7234492	155
7	456242	7234459	156
7	456241	7234447	157
7	456240	7234427	158
7	456239	7234419	159
8	456235	7234430	160
8	456193	7234458	148
9	456235	7234430	160
9	456183	7234446	139
10	456235	7234430	160
10	456174	7234439	162
11	456235	7234430	160
11	456179	7234427	161
12	456235	7234430	160
12	456200	7234462	163
13	456183	7234446	139
13	456191	7234417	140
14	456179	7234427	161
14	456235	7234444	166
15	456179	7234427	161
15	456226	7234454	165
16	456179	7234427	161
16	456215	7234462	164
17	456136	7234442	171
17	456140	7234424	172
17	456144	7234408	173

Table 3 – continued

Profile	X_UTM22N	Y_UTM22N	Waypoint No.
18	456117	7234488	167
18	456120	7234479	168
18	456126	7234466	169
18	456128	7234460	170
18	456132	7234449	178
18	456136	7234442	171
19	456078	7234493	174
19	456089	7234477	175
19	456099	7234458	179
19	456109	7234445	176
19	456117	7234433	177
20	456236	7234423	8
20	456223	7234418	7
20	456213	7234412	6
20	456193	7234402	5
20	456179	7234394	4
21	456215	7234462	164
21	456200	7234462	163
21	456193	7234458	148
21	456183	7234446	139
21	456174	7234439	162
21	456179	7234427	161
21	456179	7234417	11
21	456184	7234407	10
21	456186	7234390	9
22	456208	7234473	149
22	456195	7234471	147
22	456179	7234466	138
22	456153	7234460	20
22	456137	7234457	19

Table 3 – continued

Line	X_UTM22N	Y_UTM22N	Waypoint No.
23	456208	7234473	149
23	456197	7234479	146
23	456181	7234486	28
23	456175	7234487	137
23	456157	7234494	26
23	456132	7234503	25
23	456119	7234508	24
24	456011	7234462	38
24	456005	7234442	37
24	456007	7234431	36
25	455922	7234420	40
25	455927	7234401	39

11. Appendix B – profile data

Magnetic profile data corrected for diurnal variation and after removal of spikes are displayed in this appendix. All profiles were measured by moving the magnetometers along the profiles simultaneously with a sampling of the sensor data 10 times per second. The profiles were measured twice or more by moving along the profile in opposite directions. Useful data were obtained for both directions in most cases but some profiles have data from only one measuring direction.
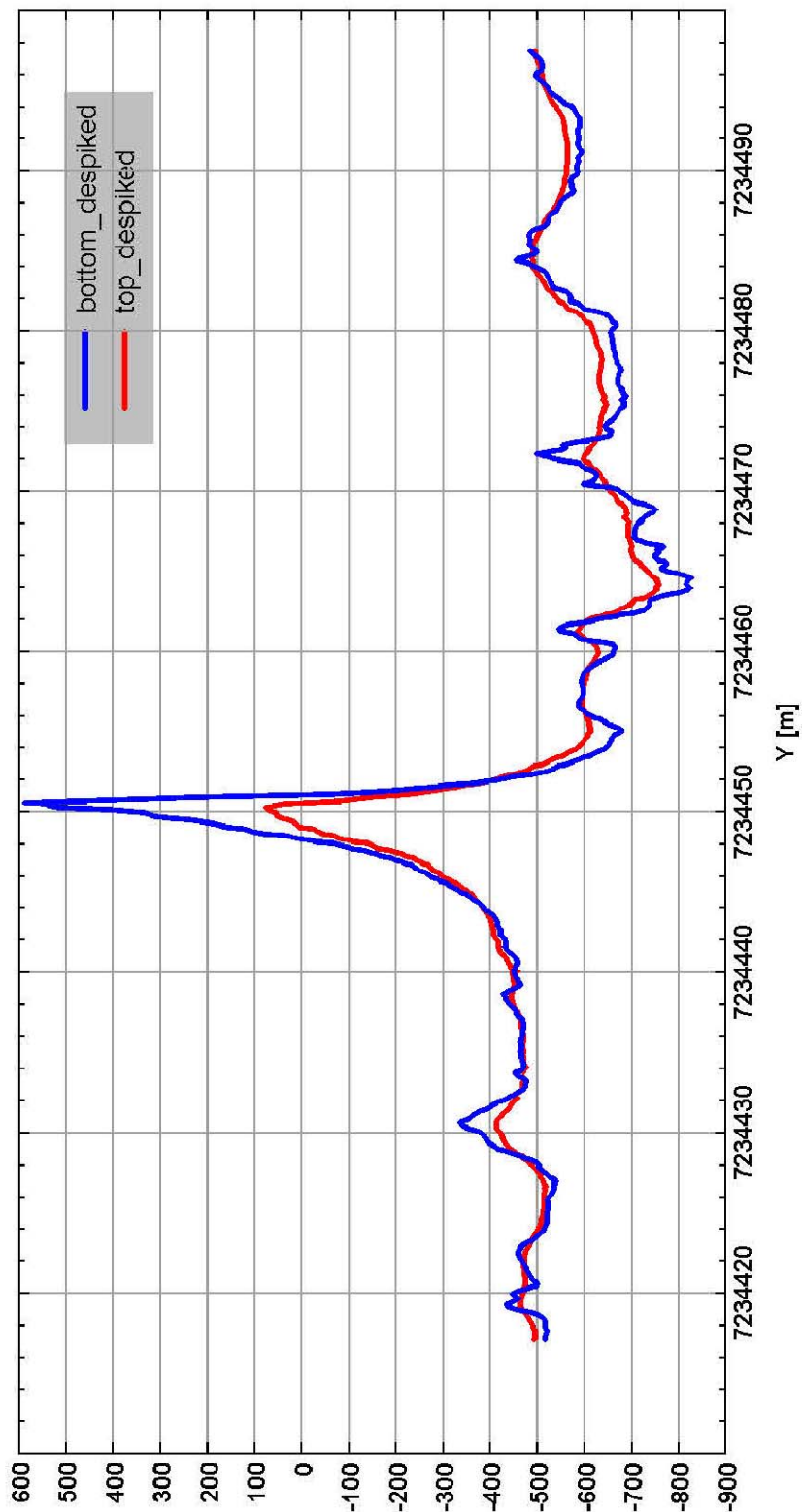
Figure 25. *Magnetic data along profile 1 measured while moving with the magnetometer in North direction. The blue curve shows data measured by the bottom sensor and the red curve shows data measured by the top sensor. The unit of the magnetic field is in nT and abscissa Y is UTM22N North coordinate.*
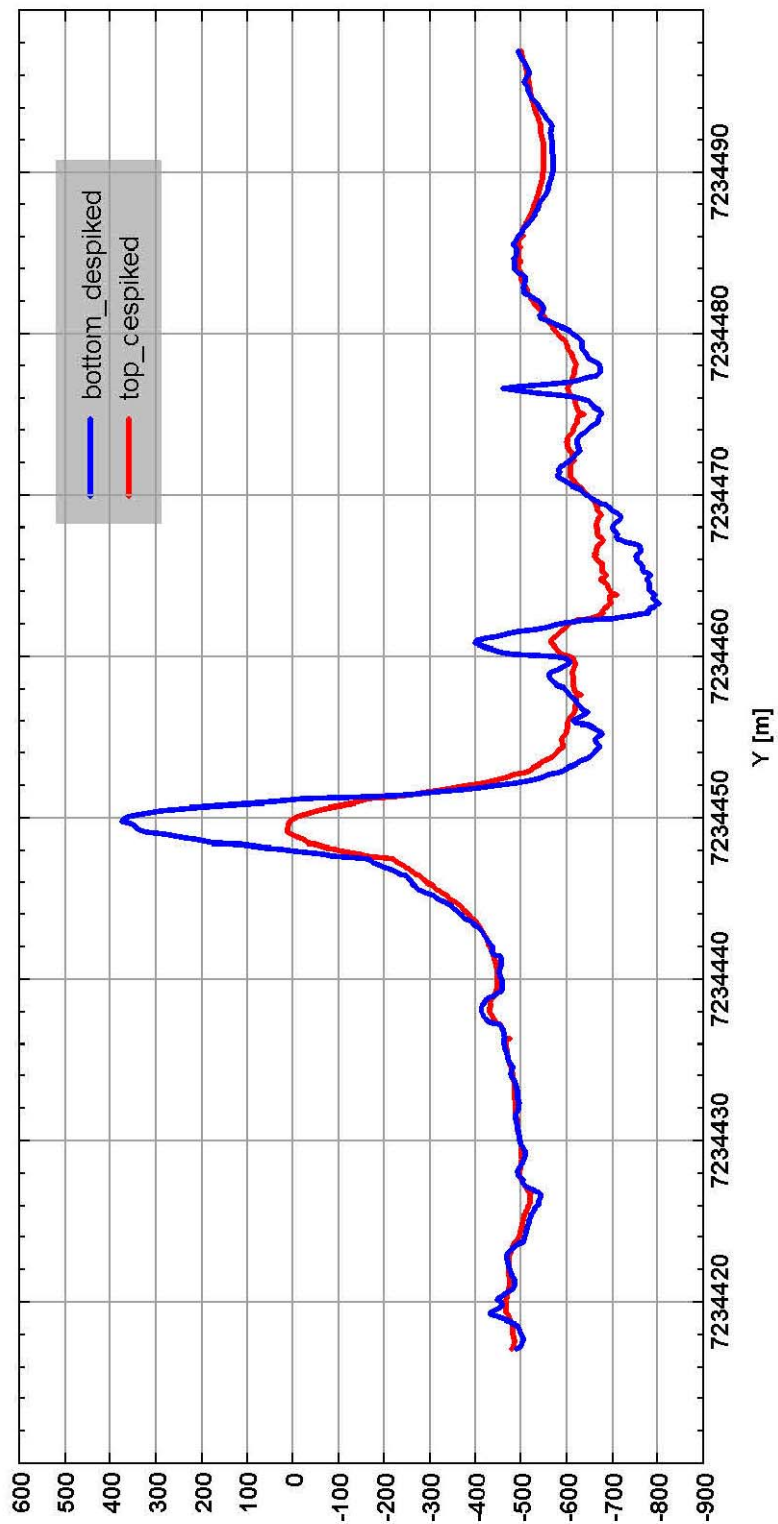
Figure 26. *Magnetic data along profile 1 measured while moving with the magnetometer in South direction. The blue curve shows data measured by the bottom sensor and the red curve shows data measured by the top sensor. The unit of the magnetic field is in nT and abscissa Y is UTM22N North coordinate.*
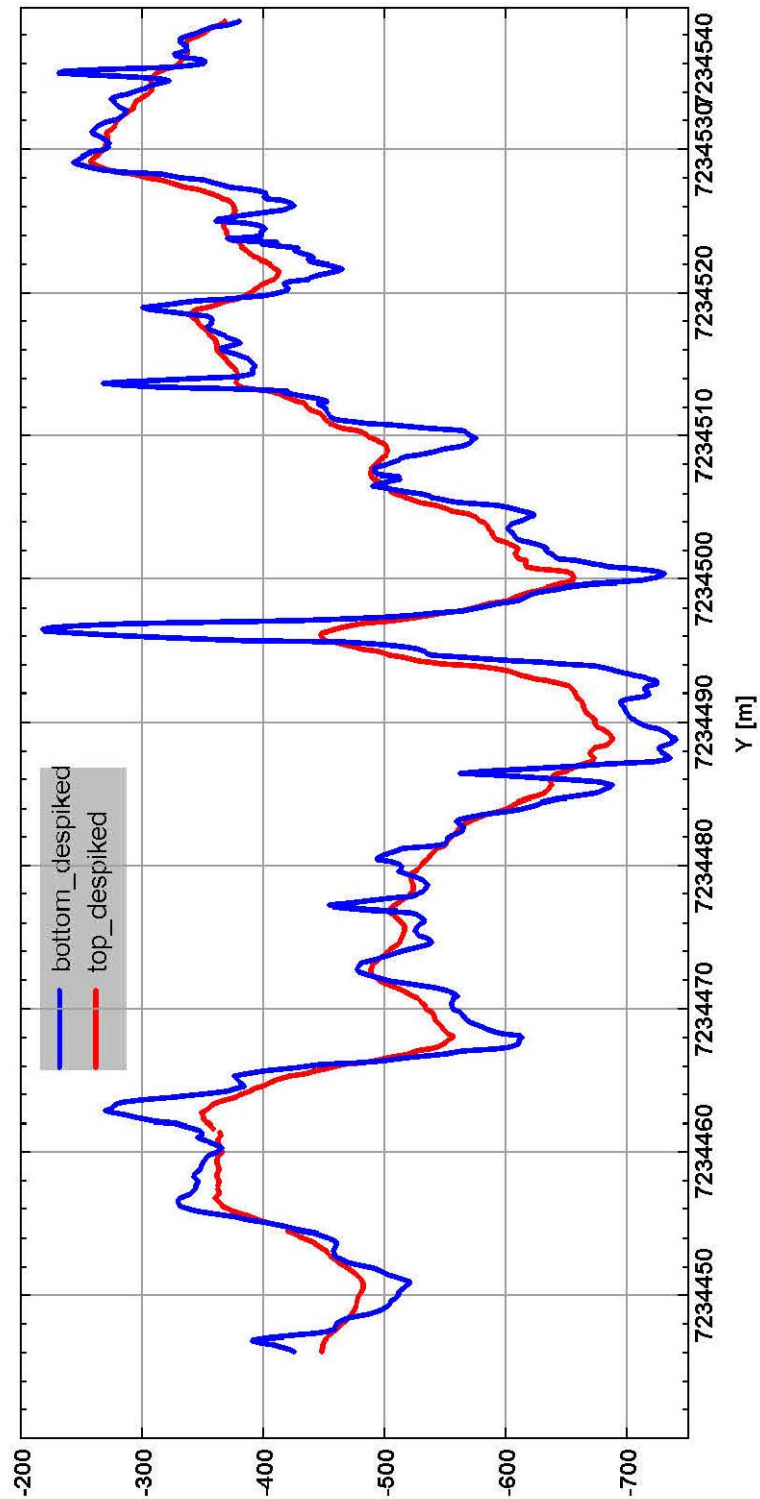
Figure 27. *Magnetic data along profile 2 measured while moving with the magnetometer in North direction. The blue curve shows data measured by the bottom sensor and the red curve shows data measured by the top sensor. The unit of the magnetic field is in nT and abscissa Y is UTM22N North coordinate.*
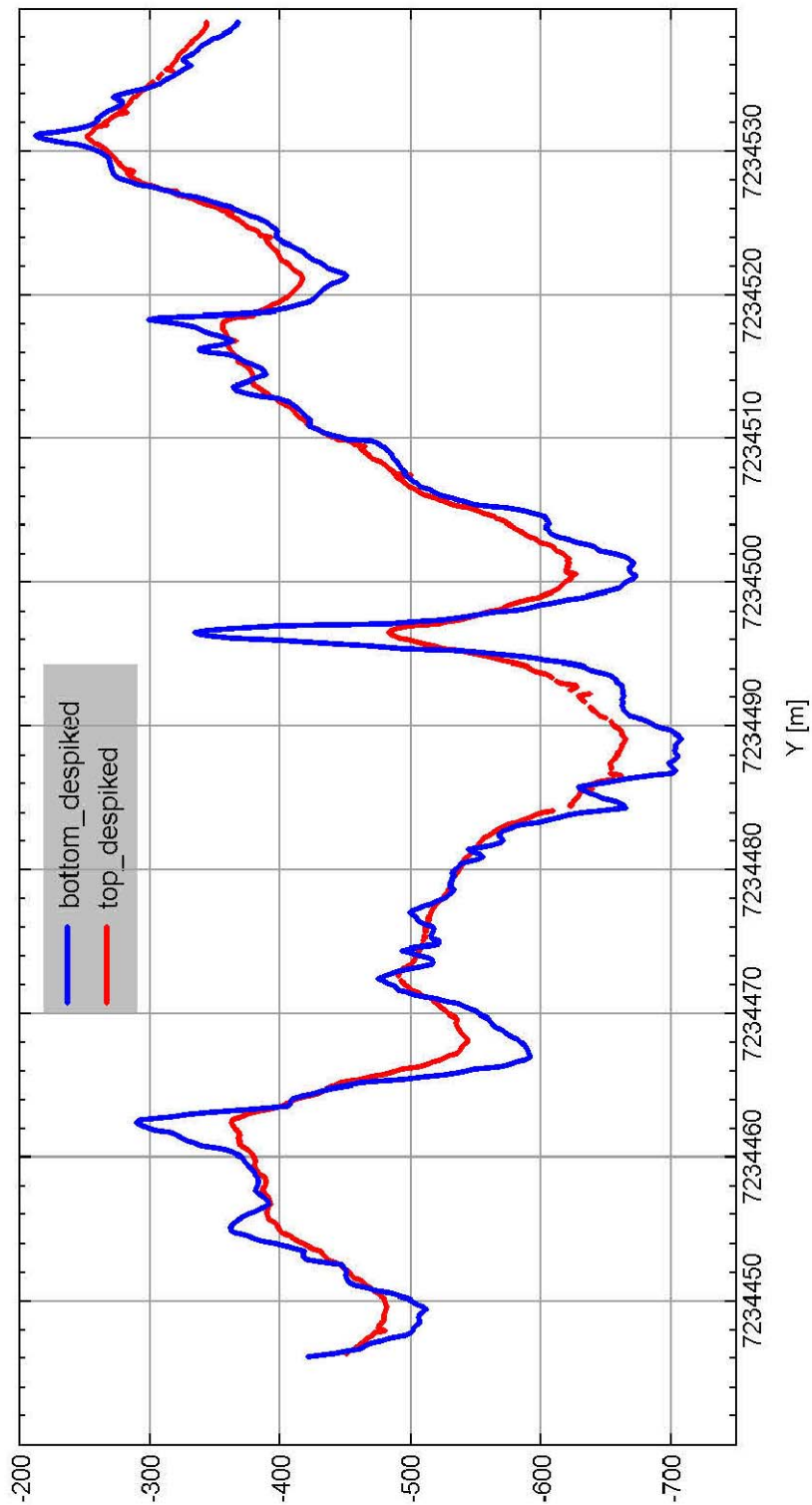
Figure 28. *Magnetic data along profile 2 measured while moving with the magnetometer in South direction. The blue curve shows data measured by the bottom sensor and the red curve shows data measured by the top sensor. The unit of the magnetic field is in nT and abscissa Y is UTM22N North coordinate.*
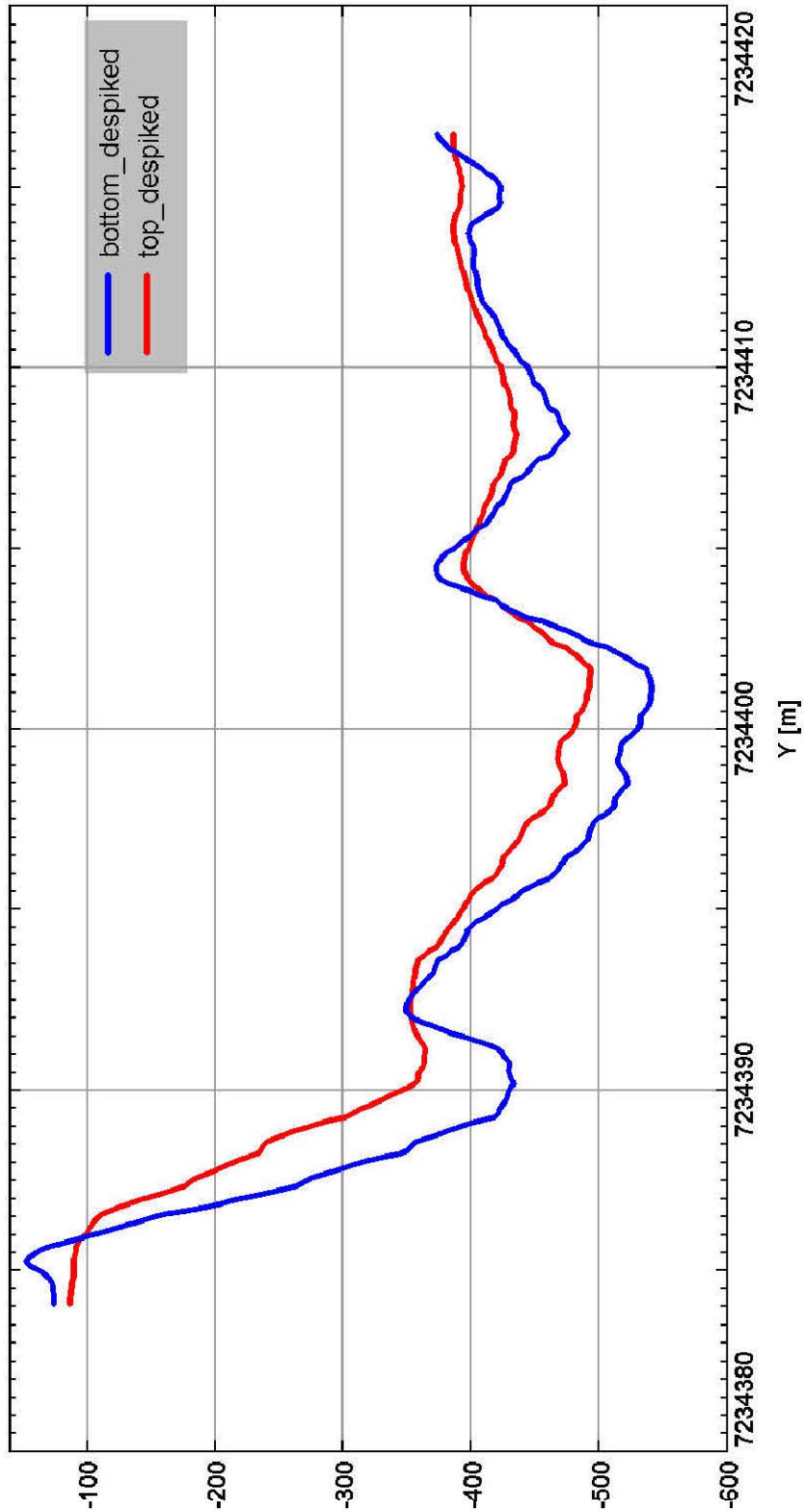
Figure 29. *Magnetic data along profile 3 measured while moving with the magnetometer in North direction. The blue curve shows data measured by the bottom sensor and the red curve shows data measured by the top sensor. The unit of the magnetic field is in nT and abscissa Y is UTM22N North coordinate.*
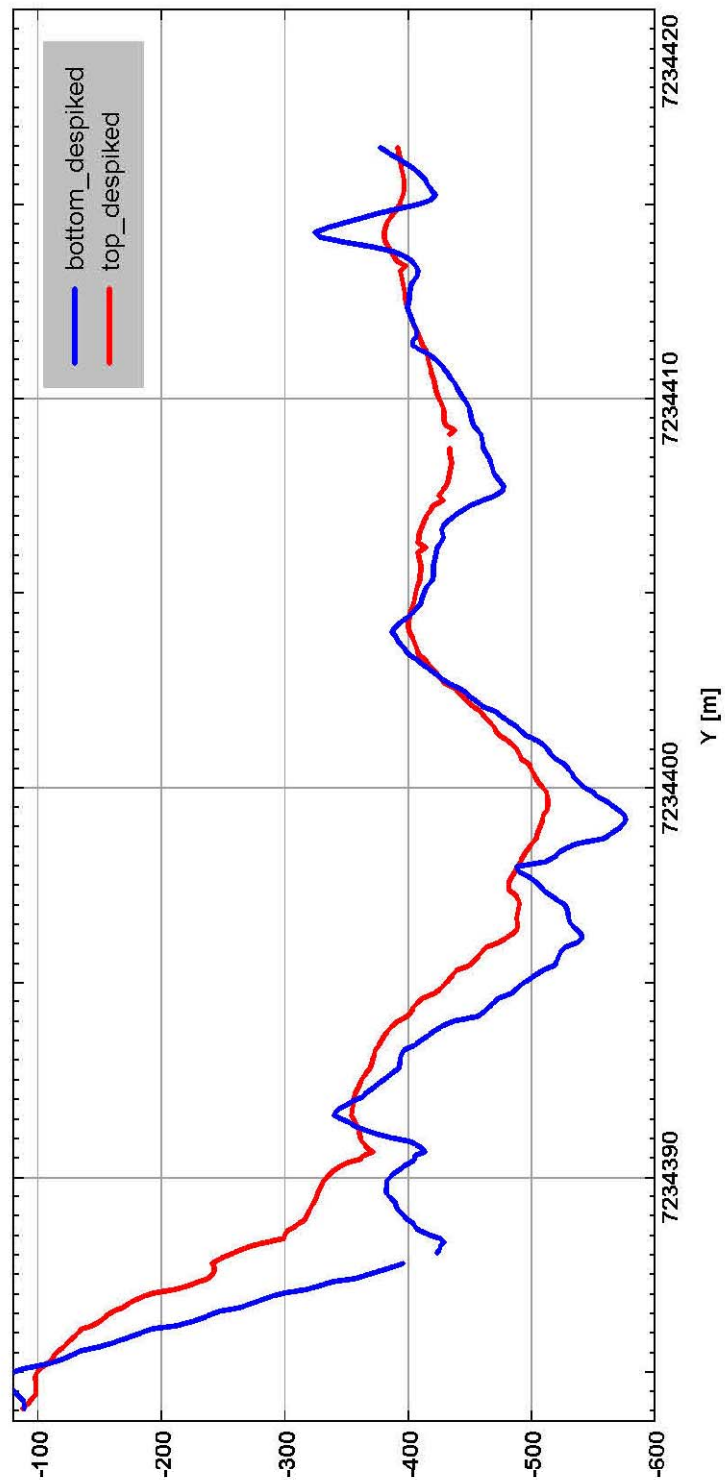
Figure 30. *Magnetic data along profile 3 measured while moving with the magnetometer in South direction. The blue curve shows data measured by the bottom sensor and the red curve shows data measured by the top sensor. The unit of the magnetic field is in nT and abscissa Y is UTM22N North coordinate.*
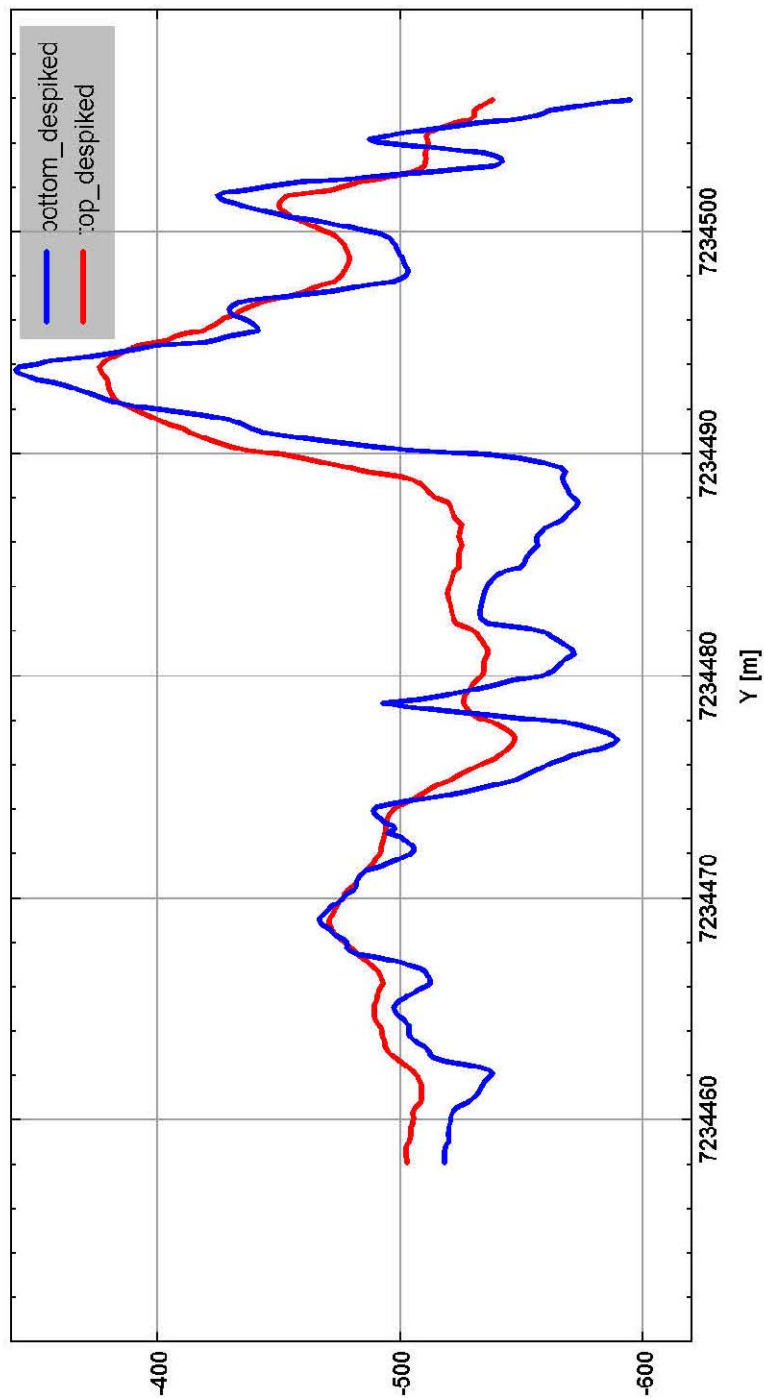
Figure 31. *Magnetic data along profile 4 measured while moving with the magnetometer in North direction. The blue curve shows data measured by the bottom sensor and the red curve shows data measured by the top sensor. The unit of the magnetic field is in nT and abscissa Y is UTM22N North coordinate.*
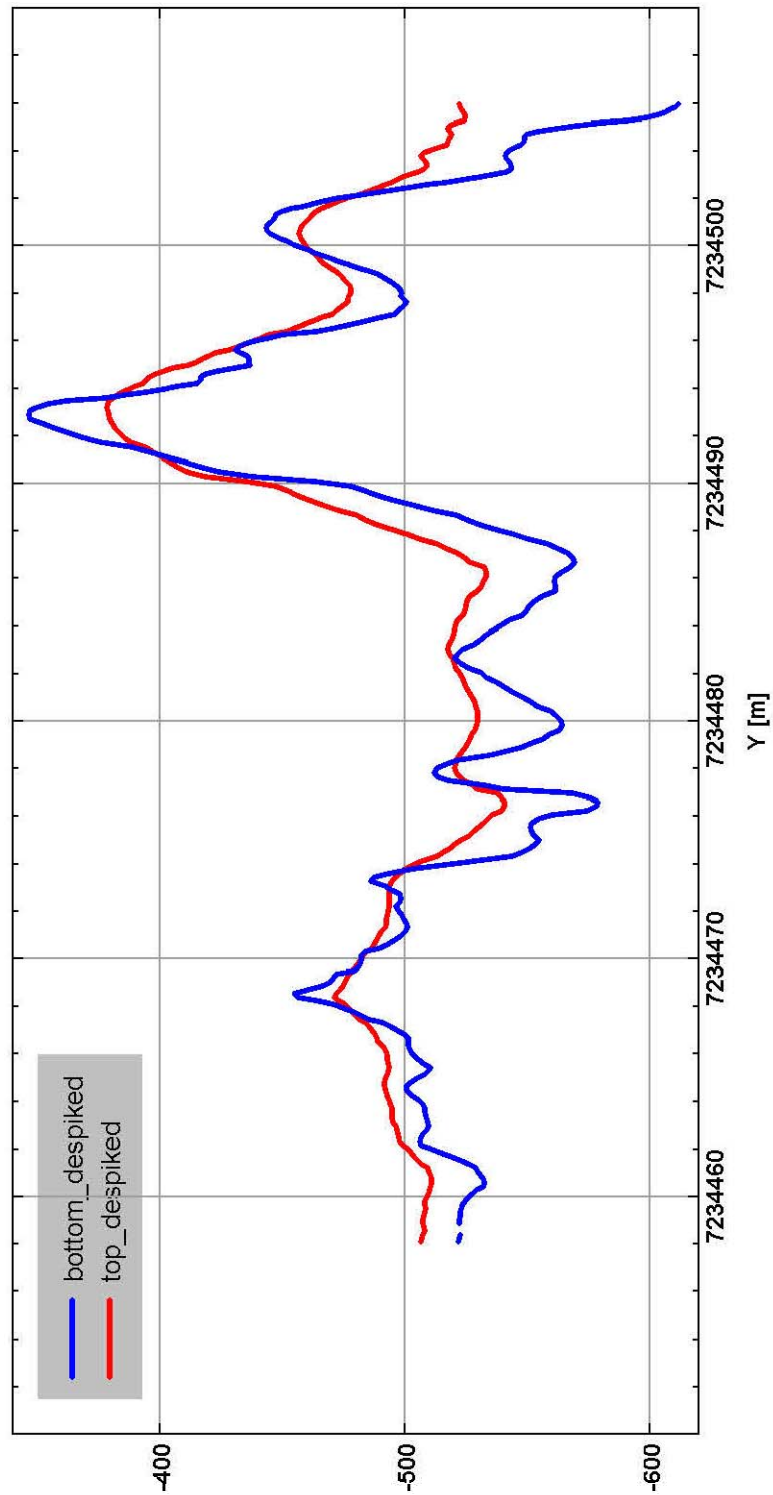
Figure 32. *Magnetic data along profile 4 measured while moving with the magnetometer in South direction. The blue curve shows data measured by the bottom sensor and the red curve shows data measured by the top sensor. The unit of the magnetic field is in nT and abscissa Y is UTM22N North coordinate.*
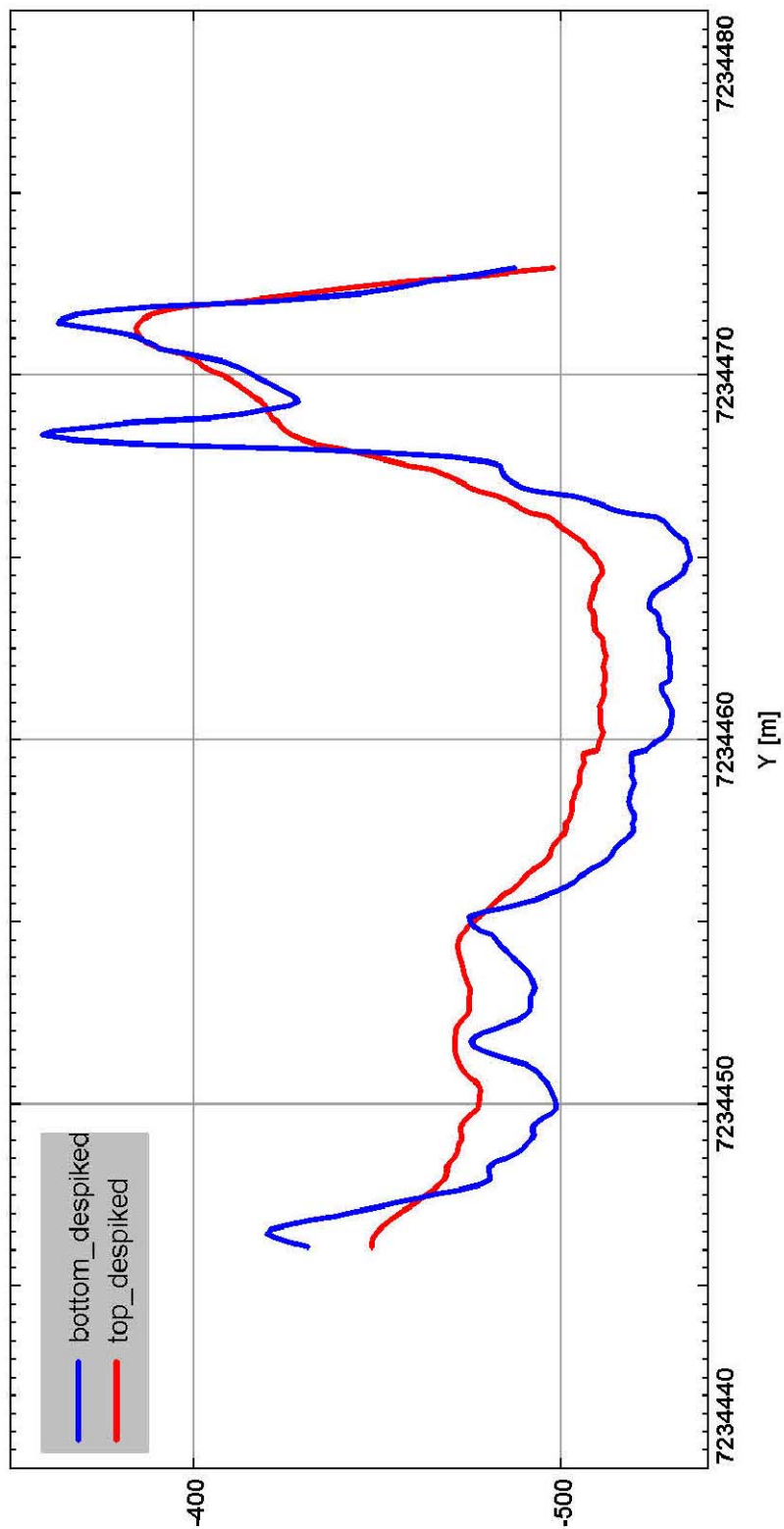
Figure 33. *Magnetic data along profile 5 measured while moving with the magnetometer in Northeast direction. The blue curve shows data measured by the bottom sensor and the red curve shows data measured by the top sensor. The unit of the magnetic field is in nT and abscissa Y is UTM22N North coordinate.*
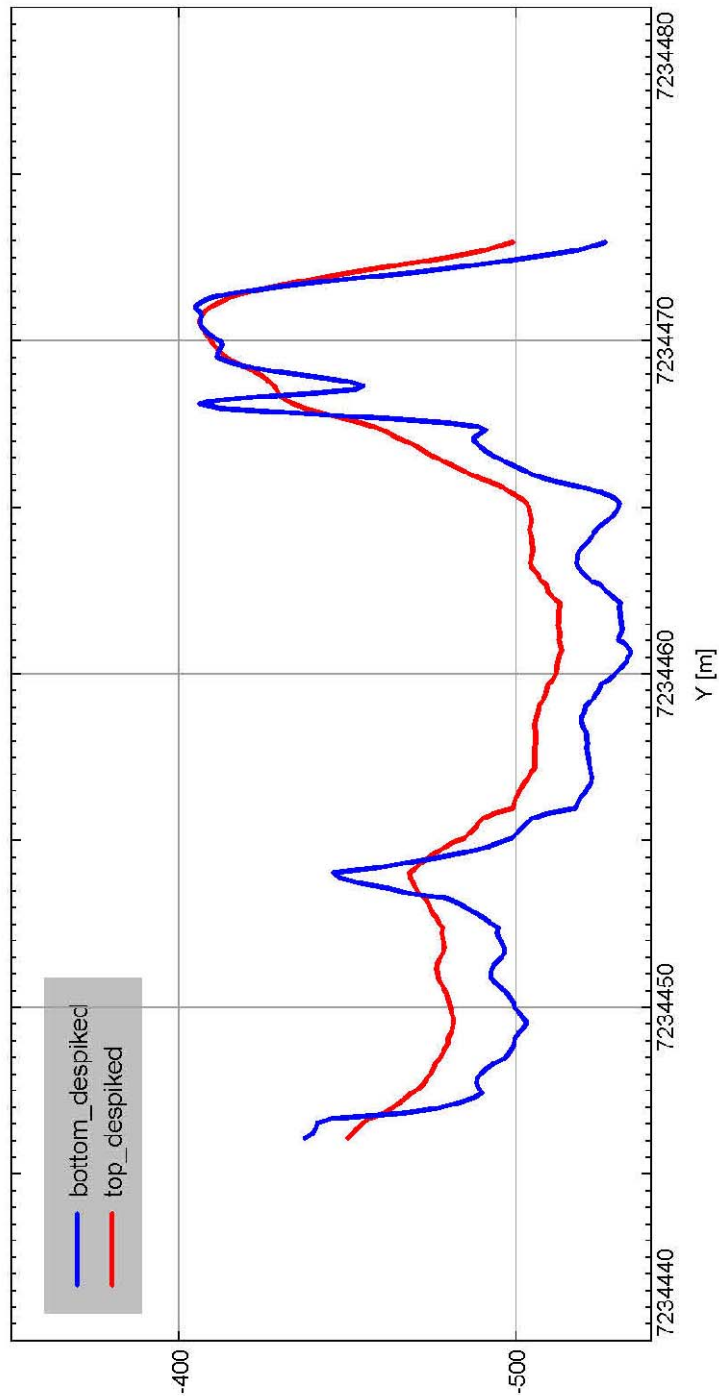
Figure 34. *Magnetic data along profile 5 measured while moving with the magnetometer in Southwest direction. The blue curve shows data measured by the bottom sensor and the red curve shows data measured by the top sensor. The unit of the magnetic field is in nT and abscissa Y is UTM22N North coordinate*
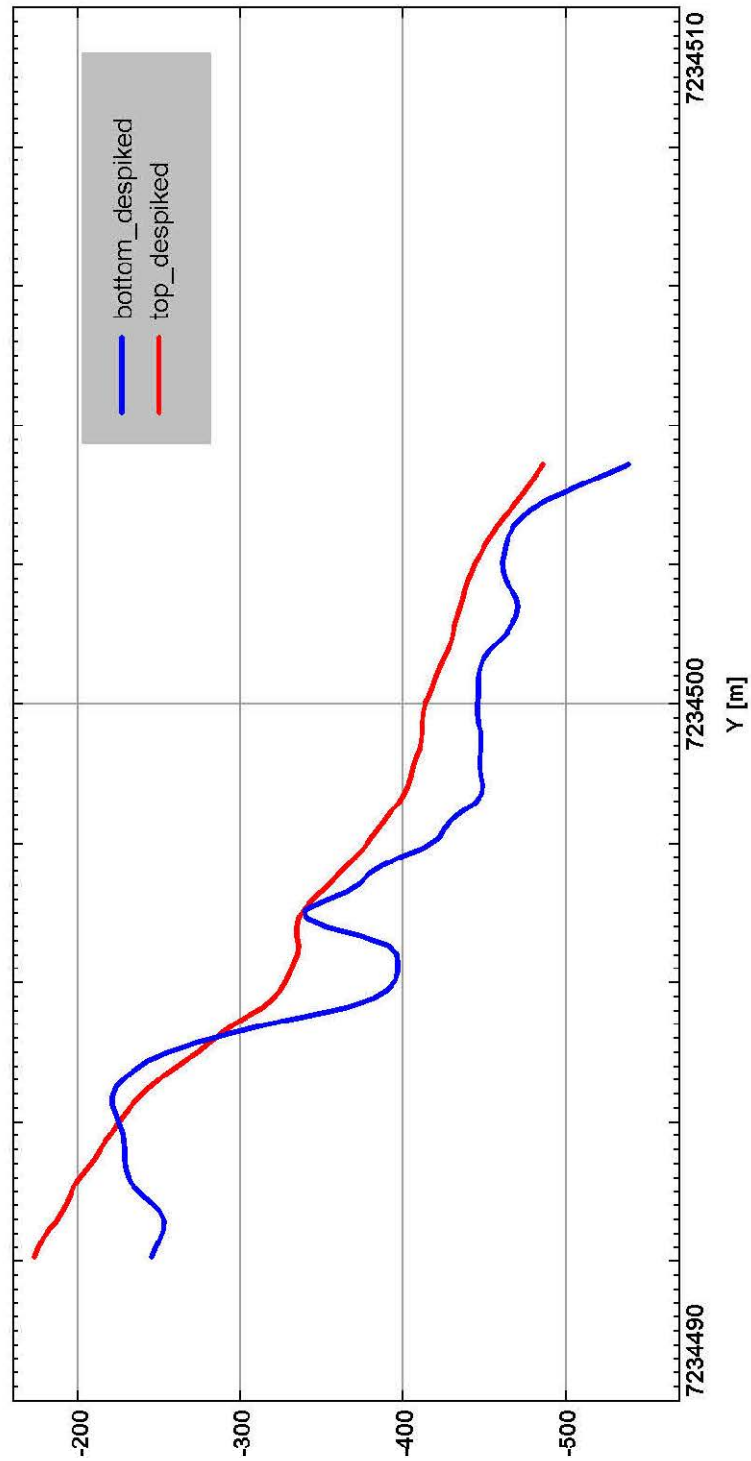
Figure 35. *Magnetic data along profile 6 measured while moving with the magnetometer in Northeast direction. The blue curve shows data measured by the bottom sensor and the red curve shows data measured by the top sensor. The unit of the magnetic field is in nT and abscissa Y is UTM22N North coordinate.*
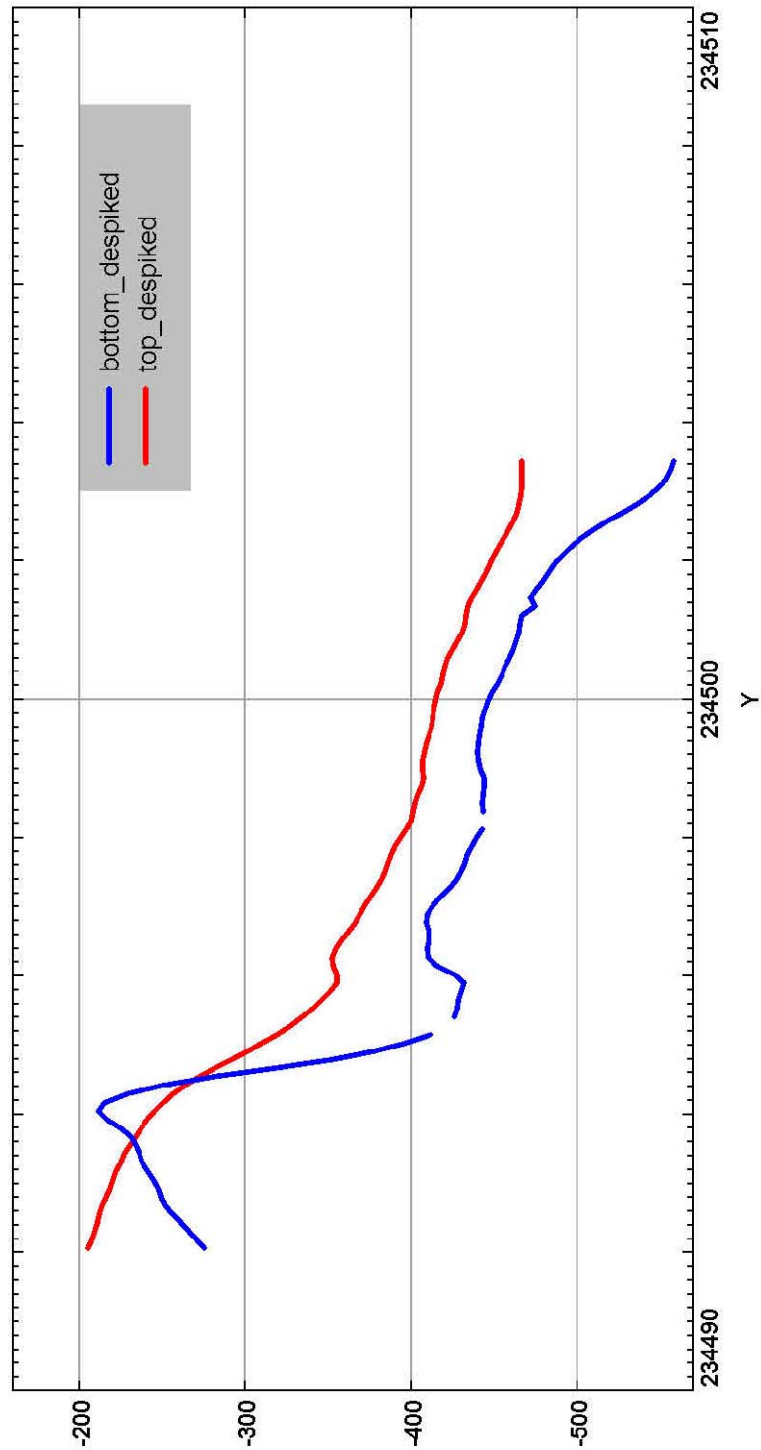
Figure 36. *Magnetic data along profile 6 measured while moving with the magnetometer in Southwest direction. The blue curve shows data measured by the bottom sensor and the red curve shows data measured by the top sensor. The unit of the magnetic field is in nT and abscissa Y is UTM22N North coordinate.*
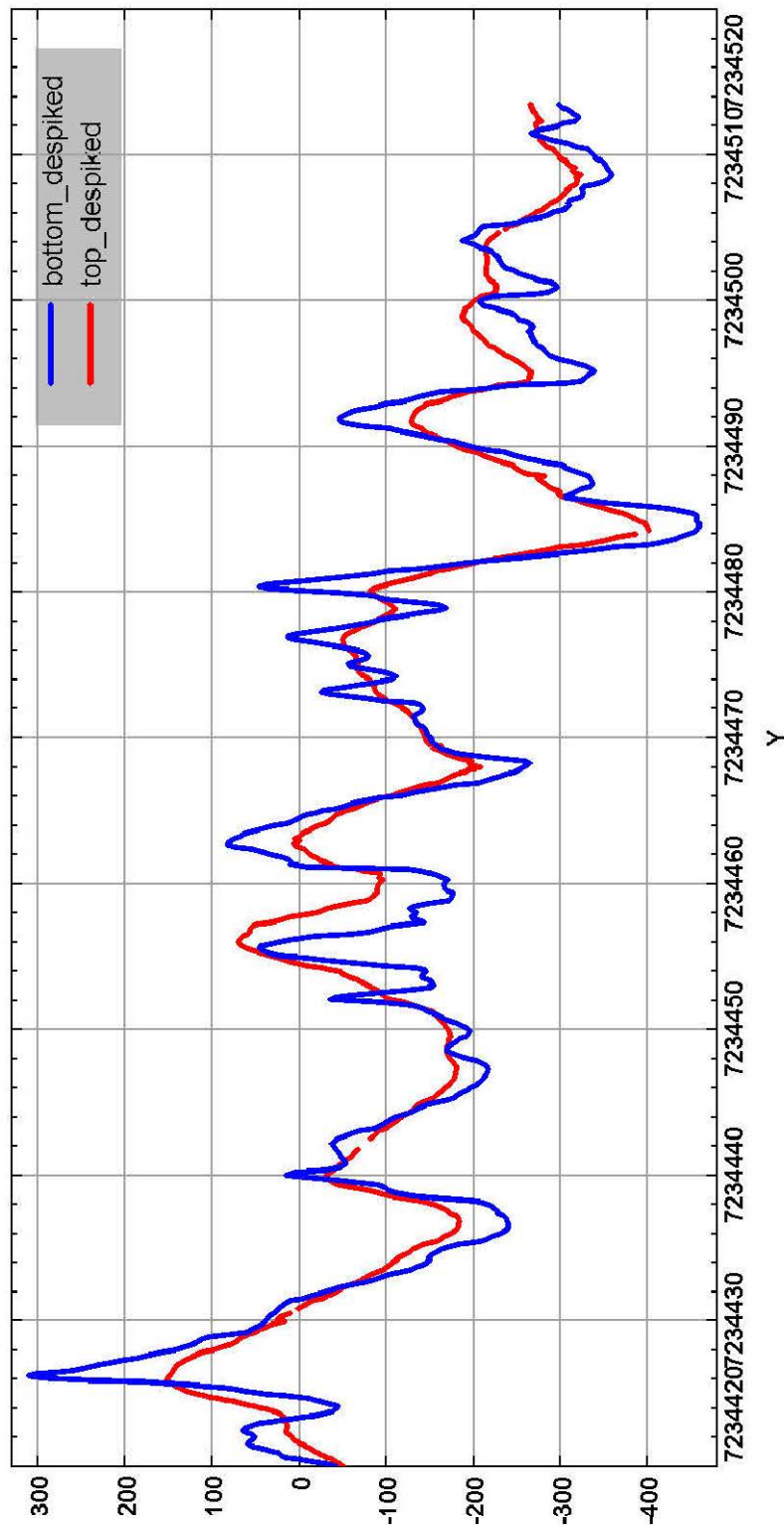
Figure 37. *Magnetic data along profile 7 measured while moving with the magnetometer in North direction. The blue curve shows data measured by the bottom sensor and the red curve shows data measured by the top sensor. The unit of the magnetic field is in nT and abscissa Y is UTM22N North coordinate.*
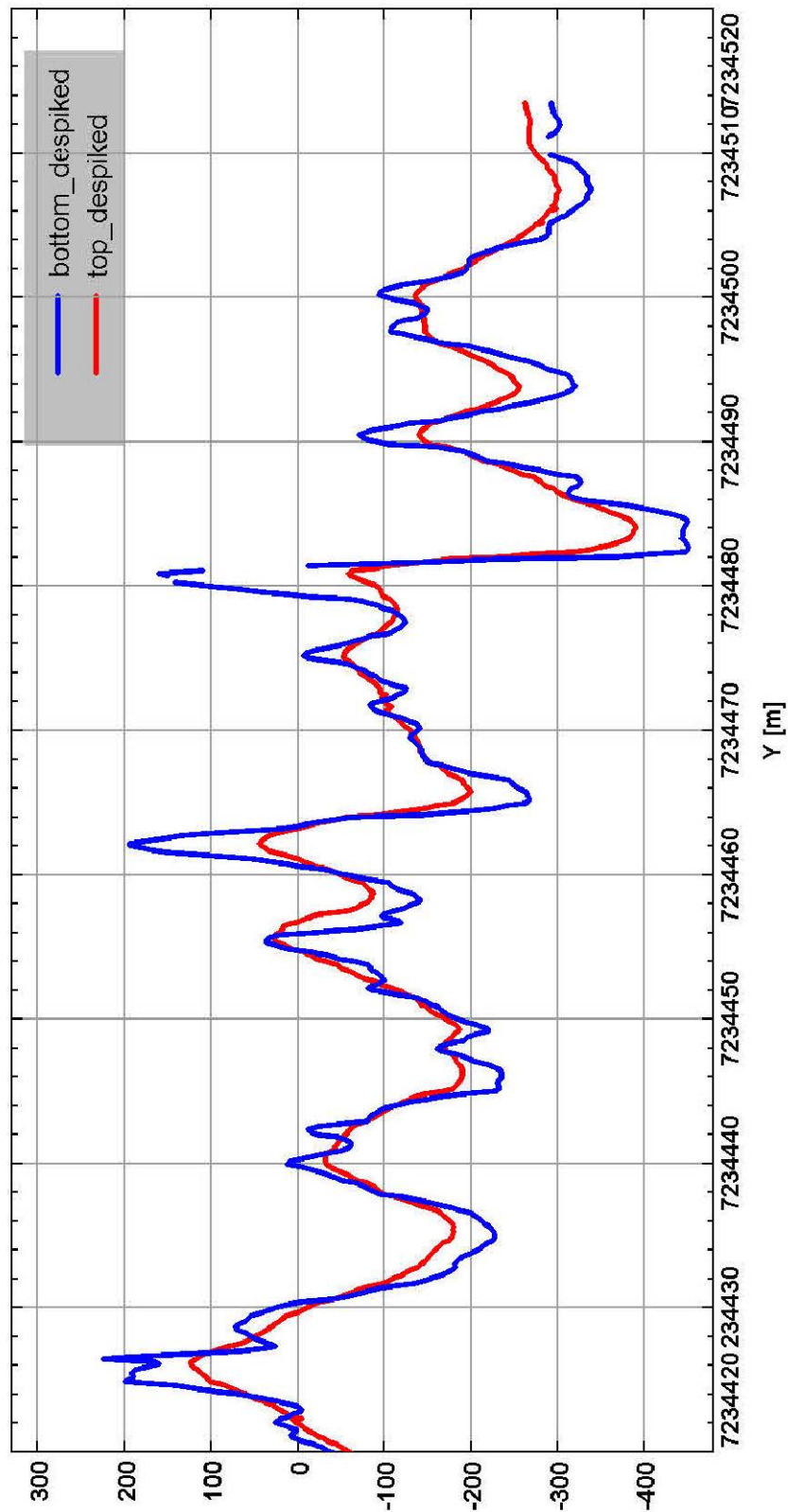
Figure 38. *Magnetic data along profile 7 measured while moving with the magnetometer in South direction. The blue curve shows data measured by the bottom sensor and the red curve shows data measured by the top sensor. The unit of the magnetic field is in nT and abscissa Y is UTM22N North coordinate.*
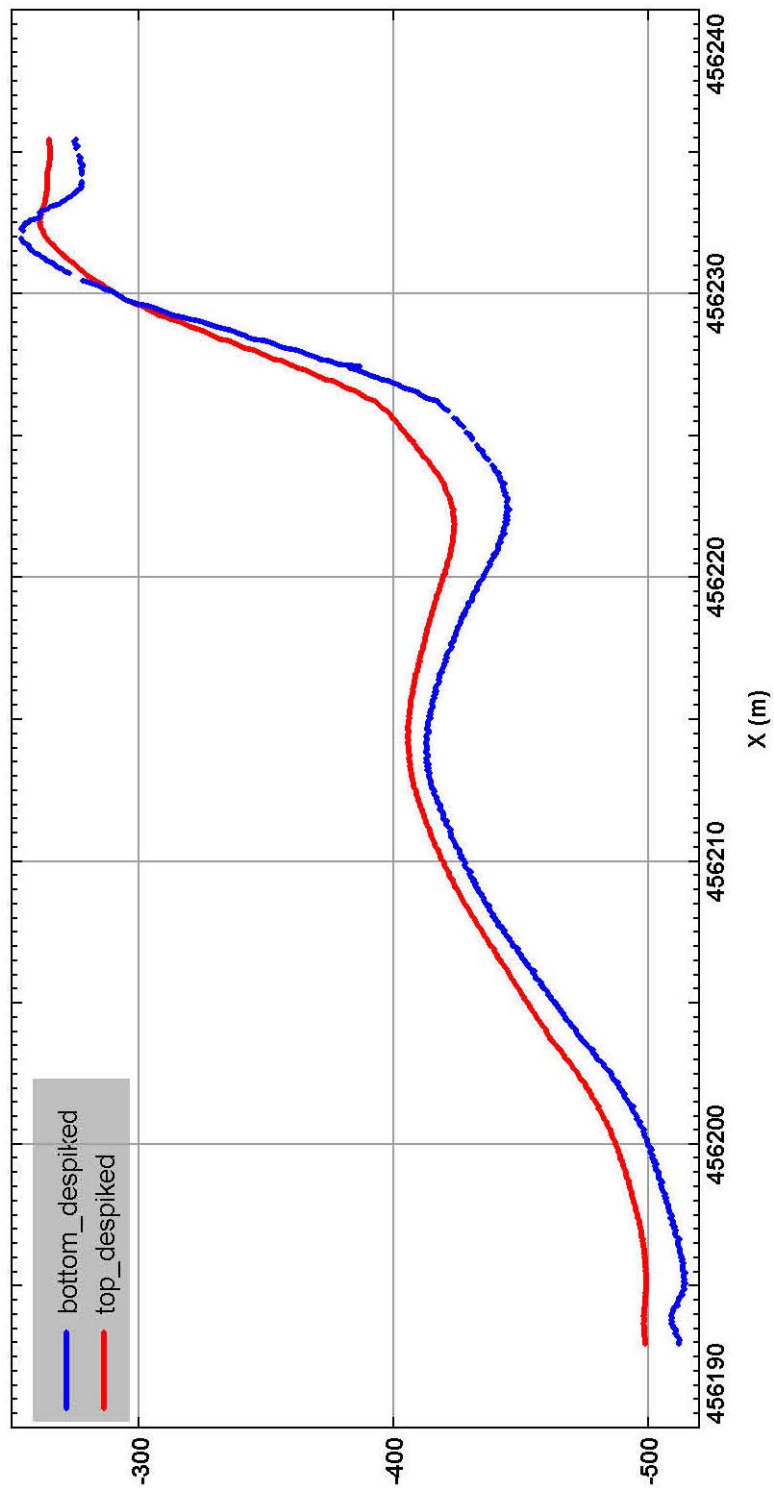
Figure 39. *Magnetic data along profile 8 measured while moving with the magnetometer in Northwest direction. The blue curve shows data measured by the bottom sensor and the red curve shows data measured by the top sensor. The unit of the magnetic field is in nT and abscissa X is UTM22N East coordinate.*
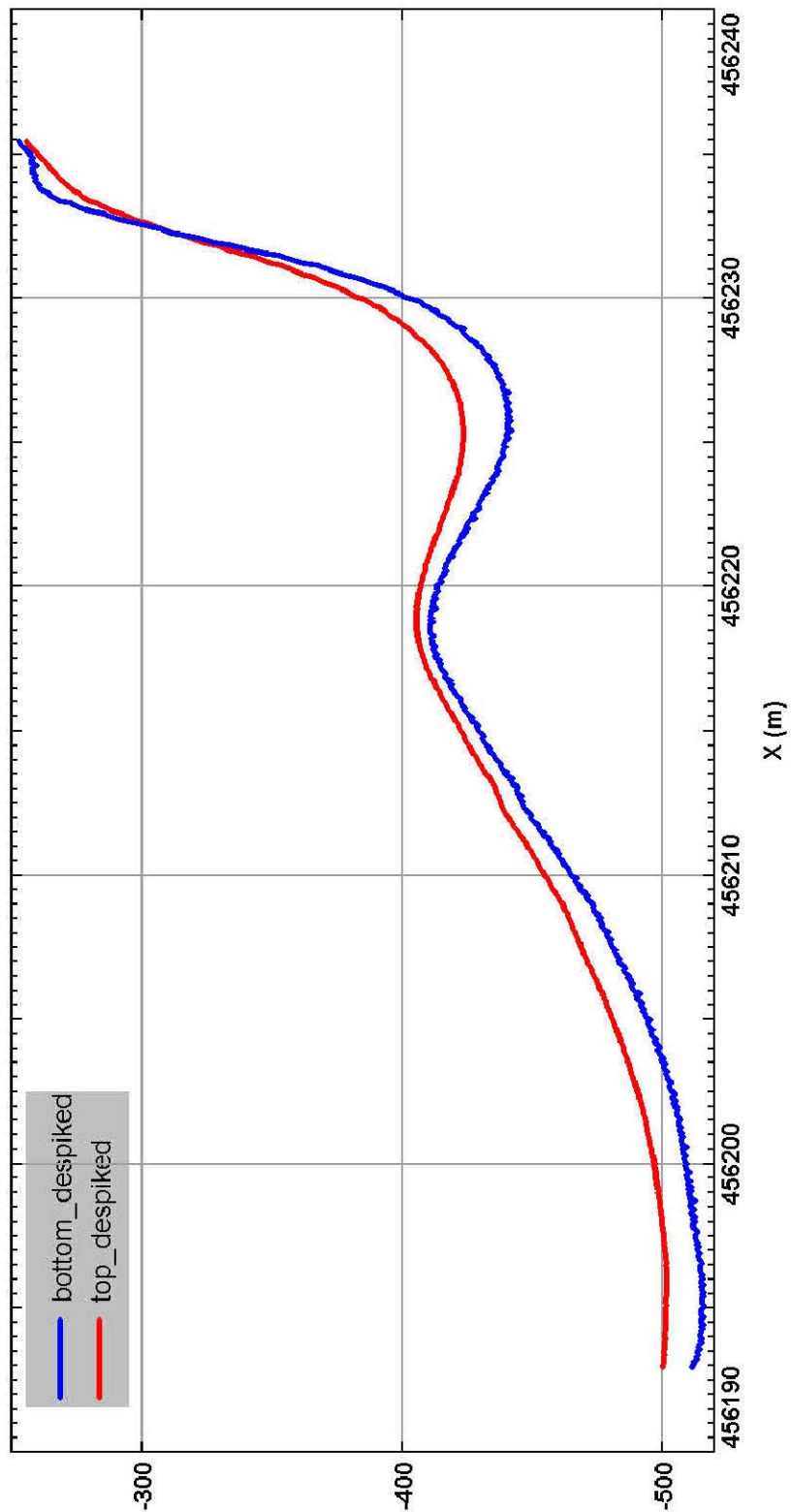
Figure 40. *Magnetic data along profile 8 measured while moving with the magnetometer in Southeast direction. The blue curve shows data measured by the bottom sensor and the red curve shows data measured by the top sensor. The unit of the magnetic field is in nT and abscissa X is UTM22N East coordinate.*
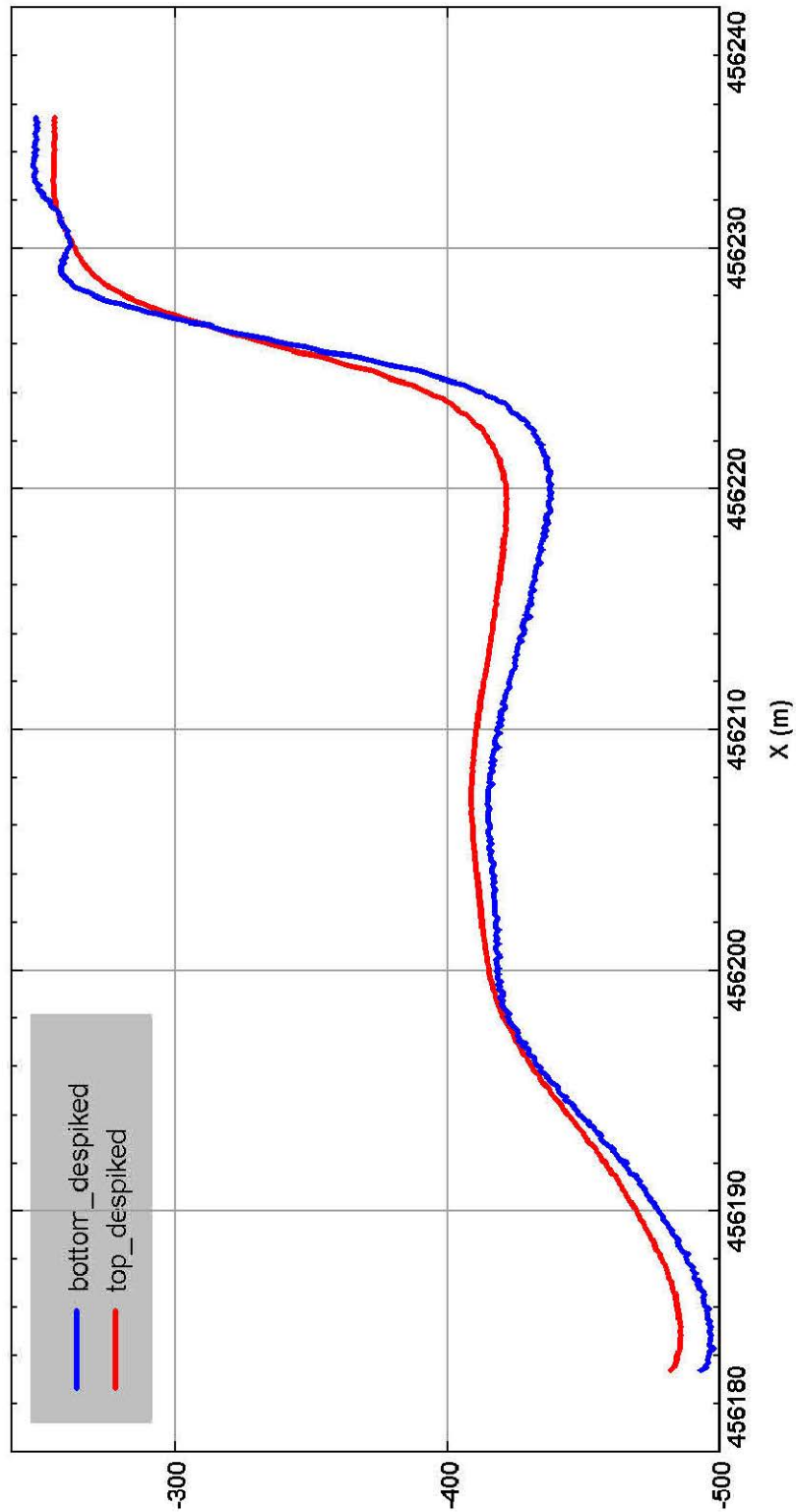
Figure 41. *Magnetic data along profile 9 measured while moving with the magnetometer in West direction. The blue curve shows data measured by the bottom sensor and the red curve shows data measured by the top sensor. The unit of the magnetic field is in nT and abscissa X is UTM22N East coordinate.*
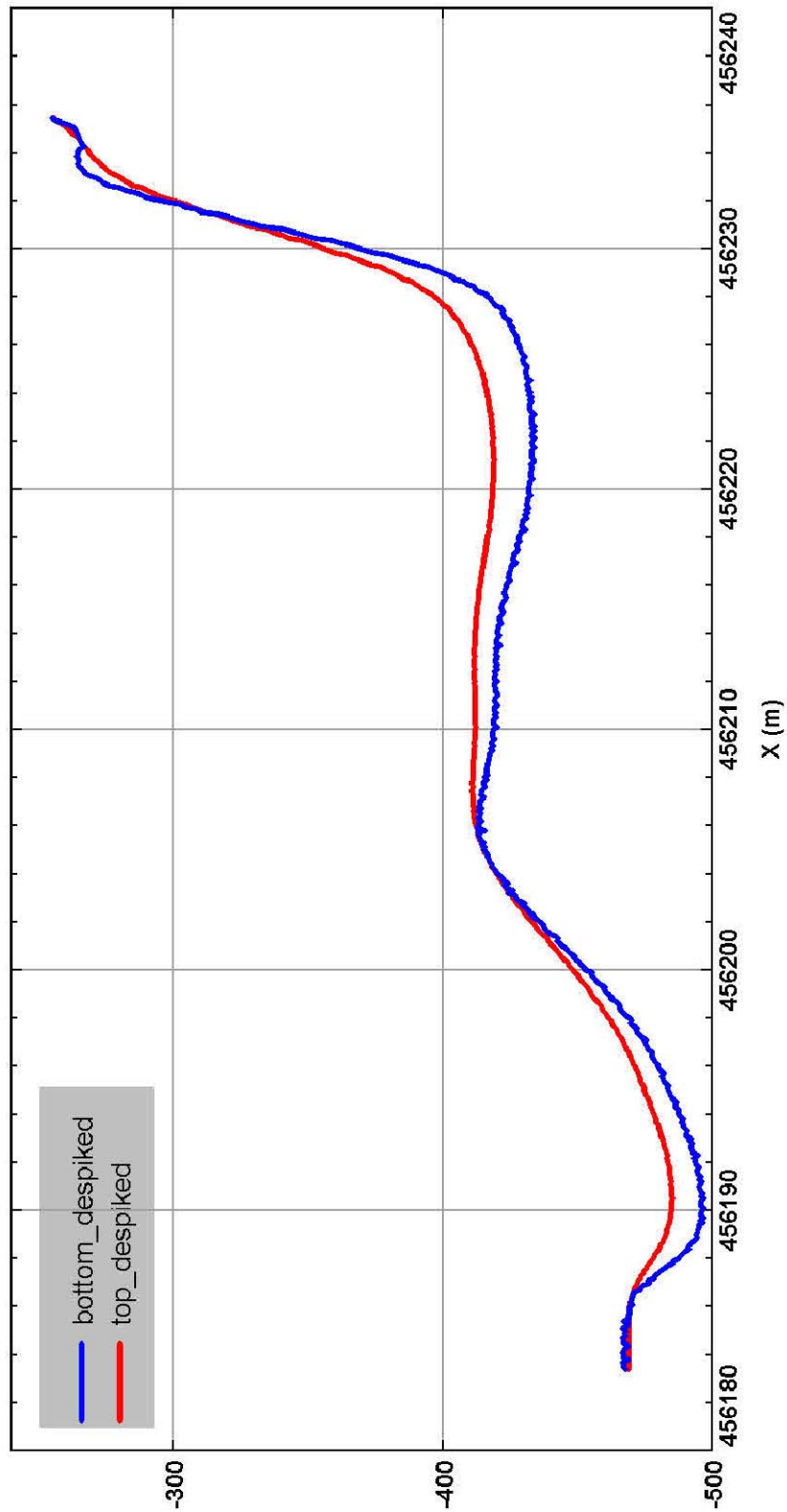
Figure 42. *Magnetic data along profile 9 measured while moving with the magnetometer in East direction. The blue curve shows data measured by the bottom sensor and the red curve shows data measured by the top sensor. The unit of the magnetic field is in nT and abscissa X is UTM22N East coordinate.*
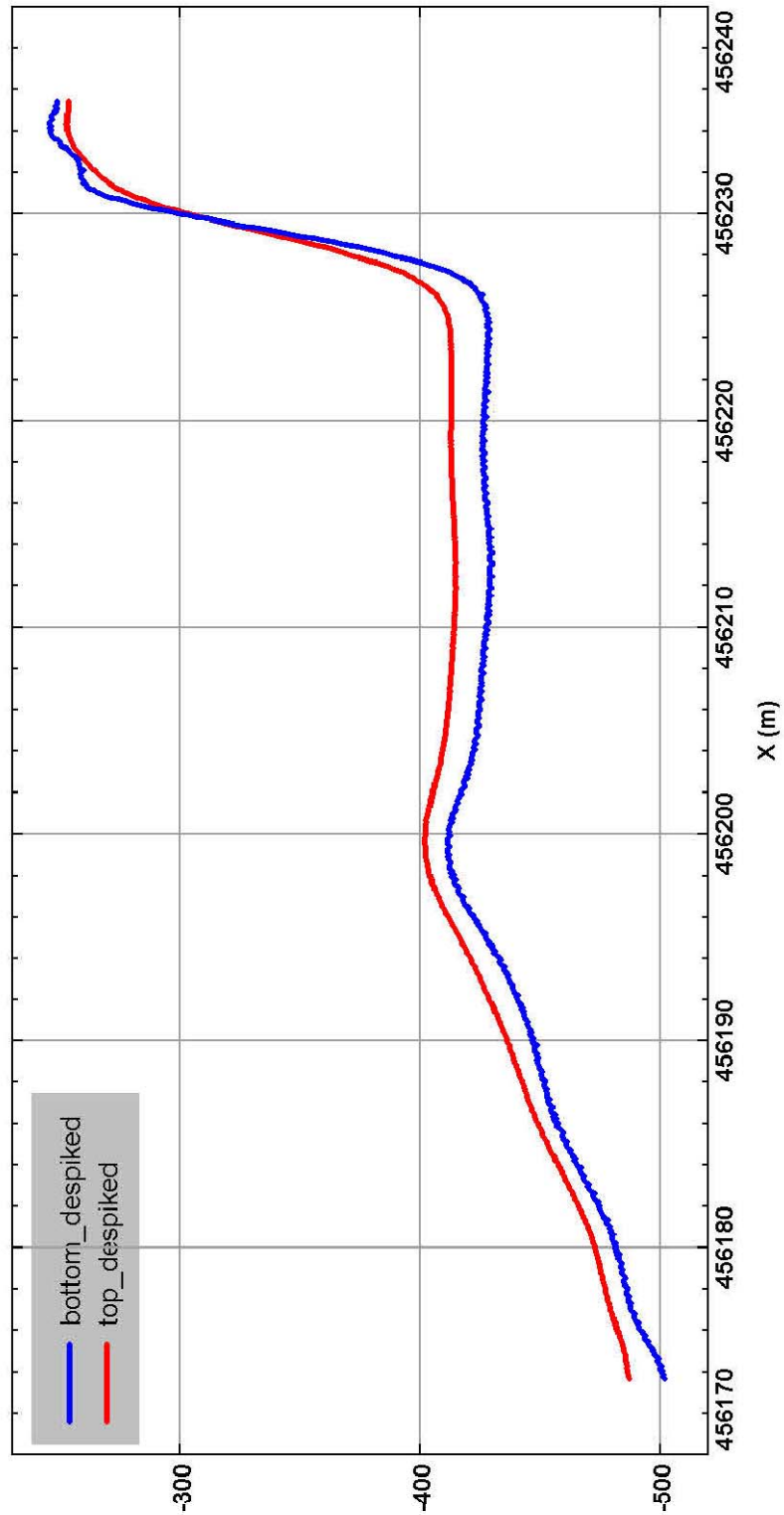
Figure 43. *Magnetic data along profile 10 measured while moving with the magnetometer in West direction. The blue curve shows data measured by the bottom sensor and the red curve shows data measured by the top sensor. The unit of the magnetic field is in nT and abscissa X is UTM22N East coordinate.*
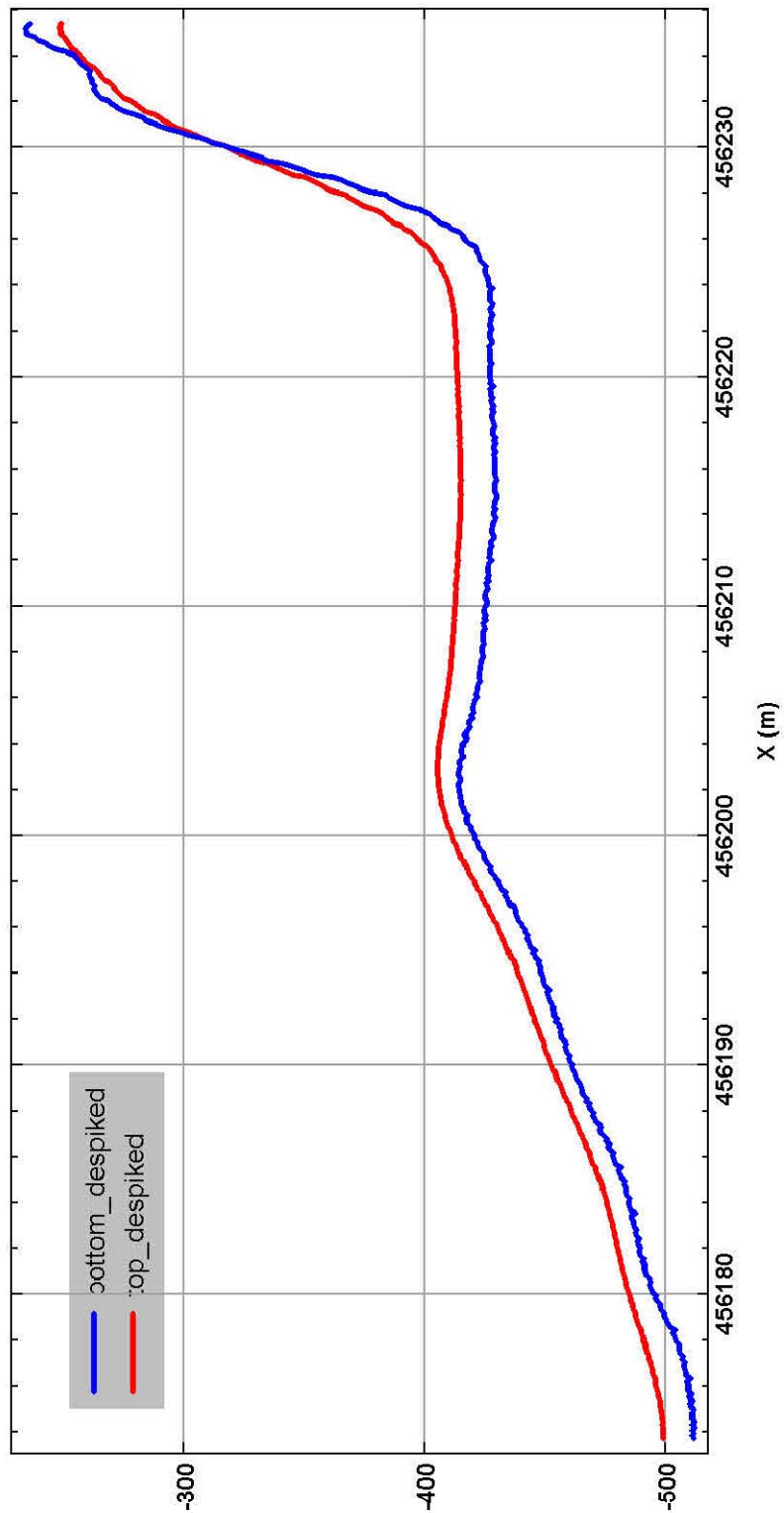
Figure 44. *Magnetic data along profile 10 measured while moving with the magnetometer in East direction. The blue curve shows data measured by the bottom sensor and the red curve shows data measured by the top sensor. The unit of the magnetic field is in nT and abscissa X is UTM22N East coordinate.*
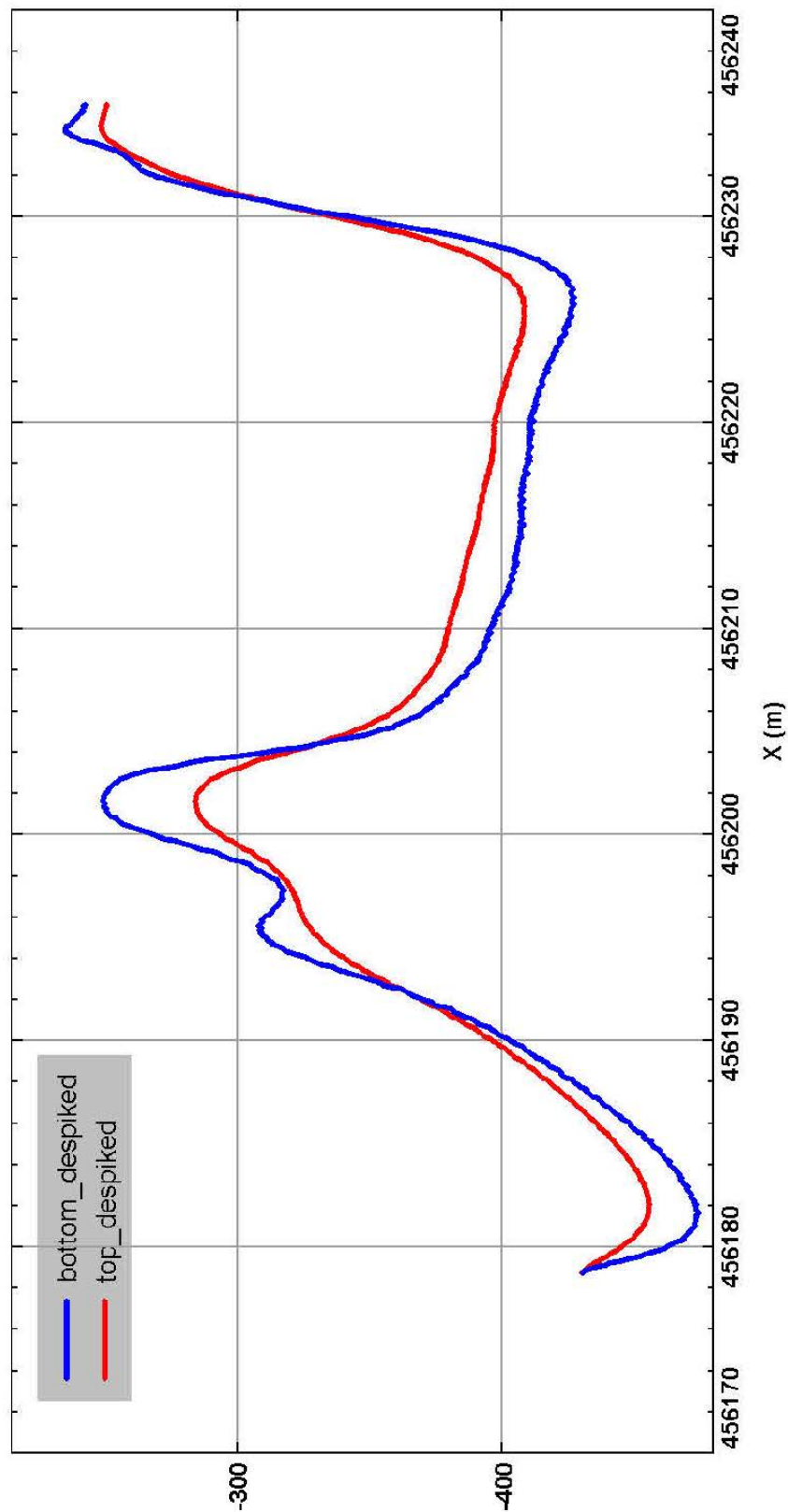
Figure 45. *Magnetic data along profile 11 measured while moving with the magnetometer in West direction. The blue curve shows data measured by the bottom sensor and the red curve shows data measured by the top sensor. The unit of the magnetic field is in nT and abscissa X is UTM22N East coordinate.*
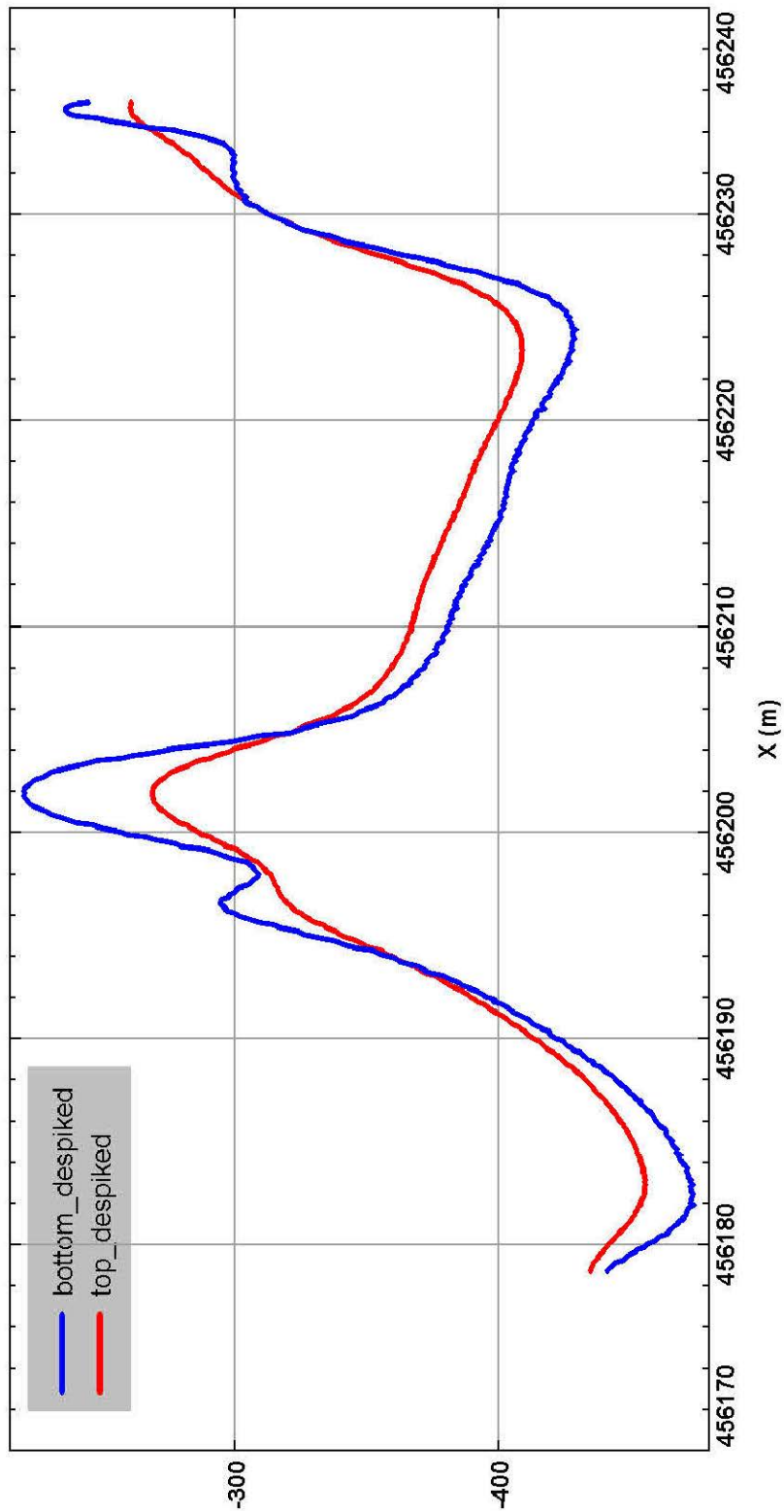
Figure 46. *Magnetic data along profile 11 measured while moving with the magnetometer in East direction. The blue curve shows data measured by the bottom sensor and the red curve shows data measured by the top sensor. The unit of the magnetic field is in nT and abscissa X is UTM22N East coordinate*
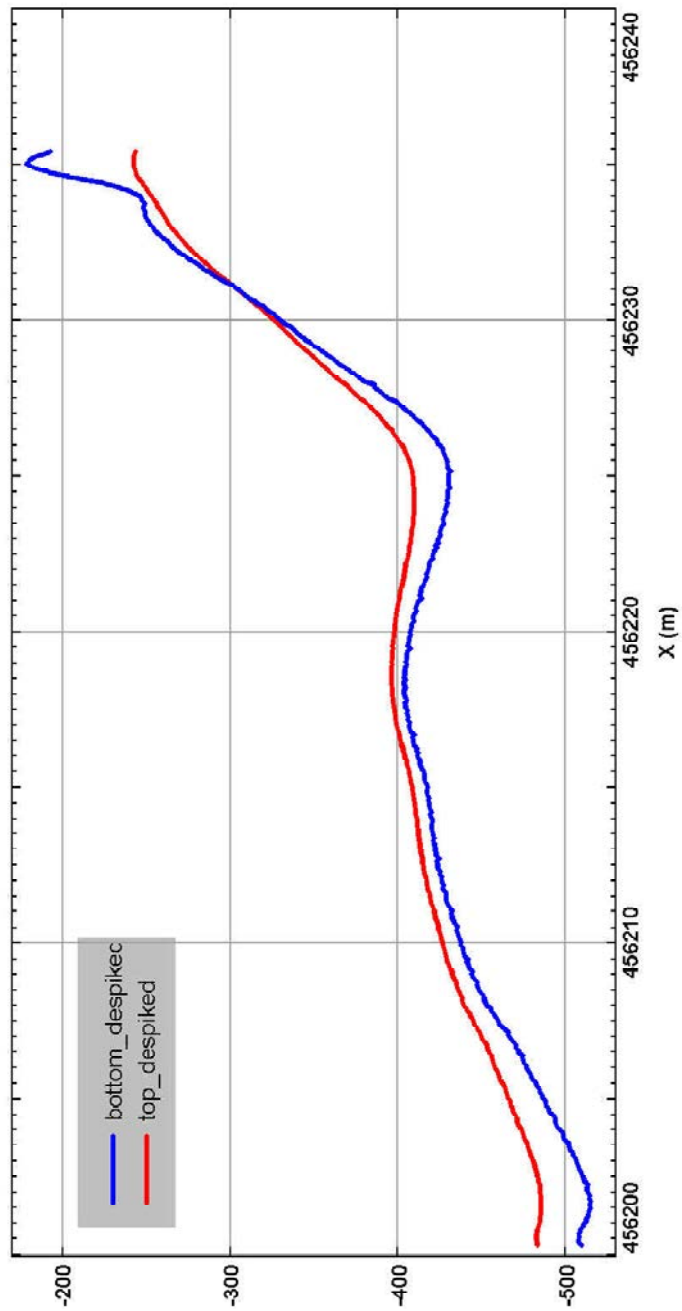
Figure 47. *Magnetic data along profile 12 measured while moving with the magnetometer in Northwest direction. The blue curve shows data measured by the bottom sensor and the red curve shows data measured by the top sensor. The unit of the magnetic field is in nT and abscissa X is UTM22N East coordinate.*
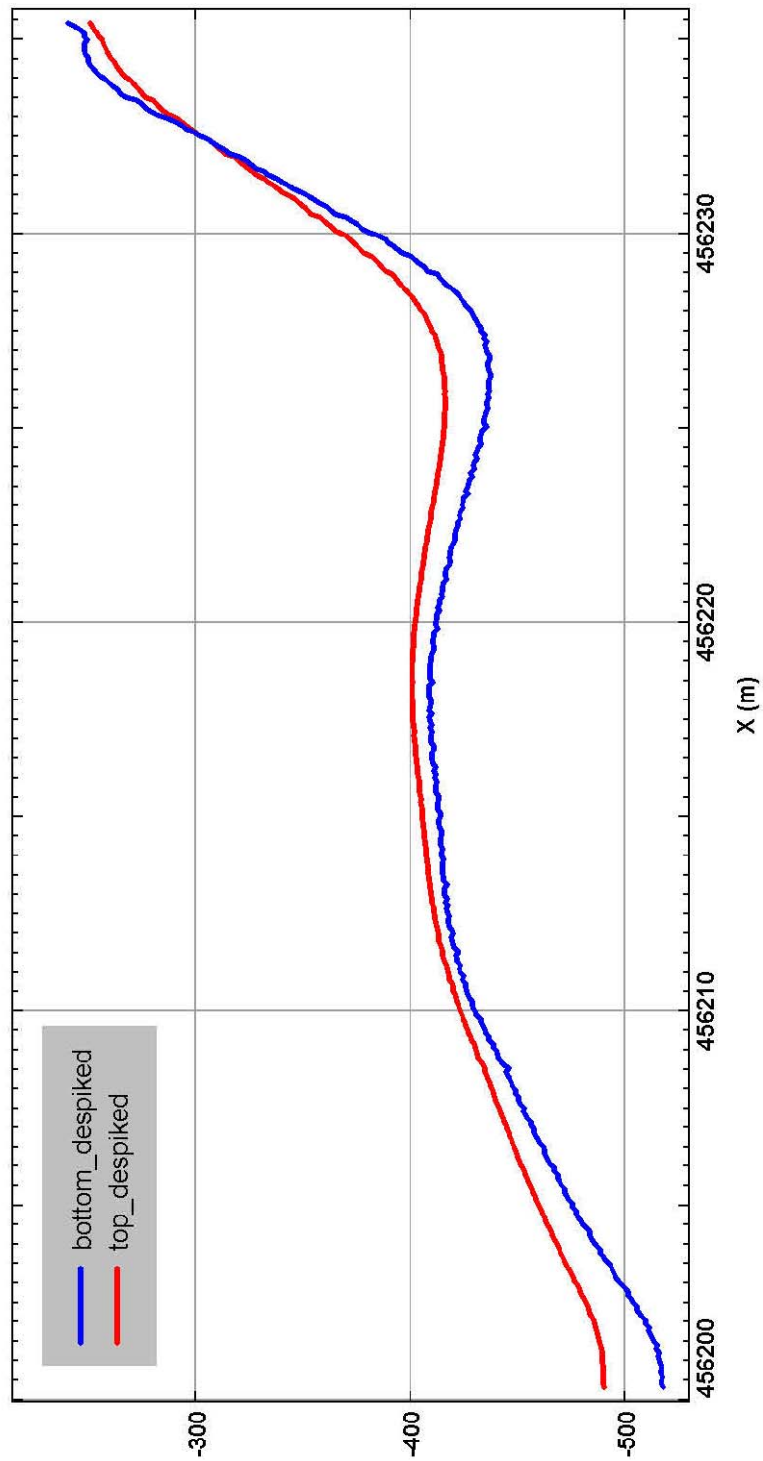
Figure 48. *Magnetic data along profile 12 measured while moving with the magnetometer in Southeast direction. The blue curve shows data measured by the bottom sensor and the red curve shows data measured by the top sensor. The unit of the magnetic field is in nT and abscissa X is UTM22N East coordinate.*
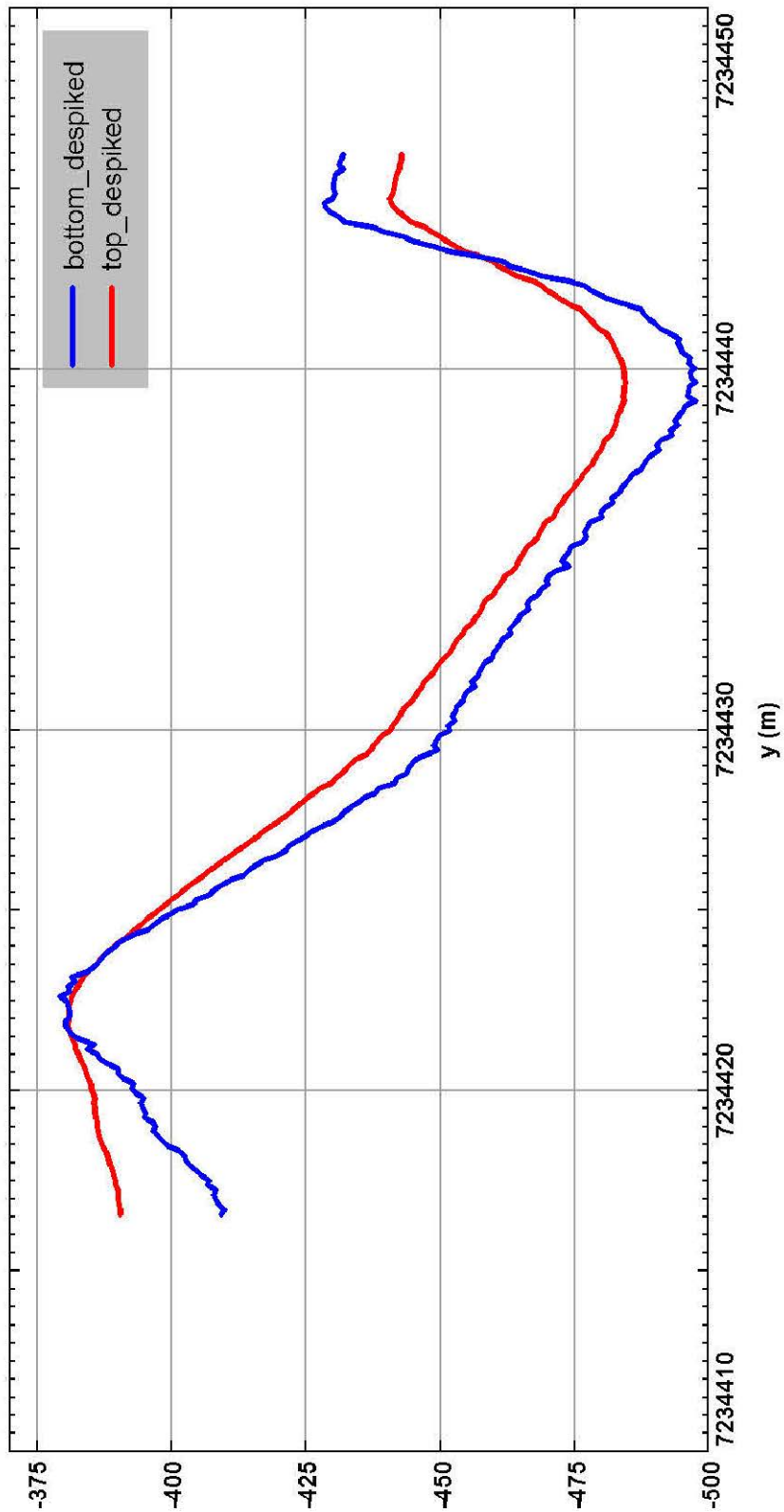
Figure 49. *Magnetic data along profile 13 measured while moving with the magnetometer in North direction. The blue curve shows data measured by the bottom sensor and the red curve shows data measured by the top sensor. The unit of the magnetic field is in nT and abscissa Y is UTM22N North coordinate.*
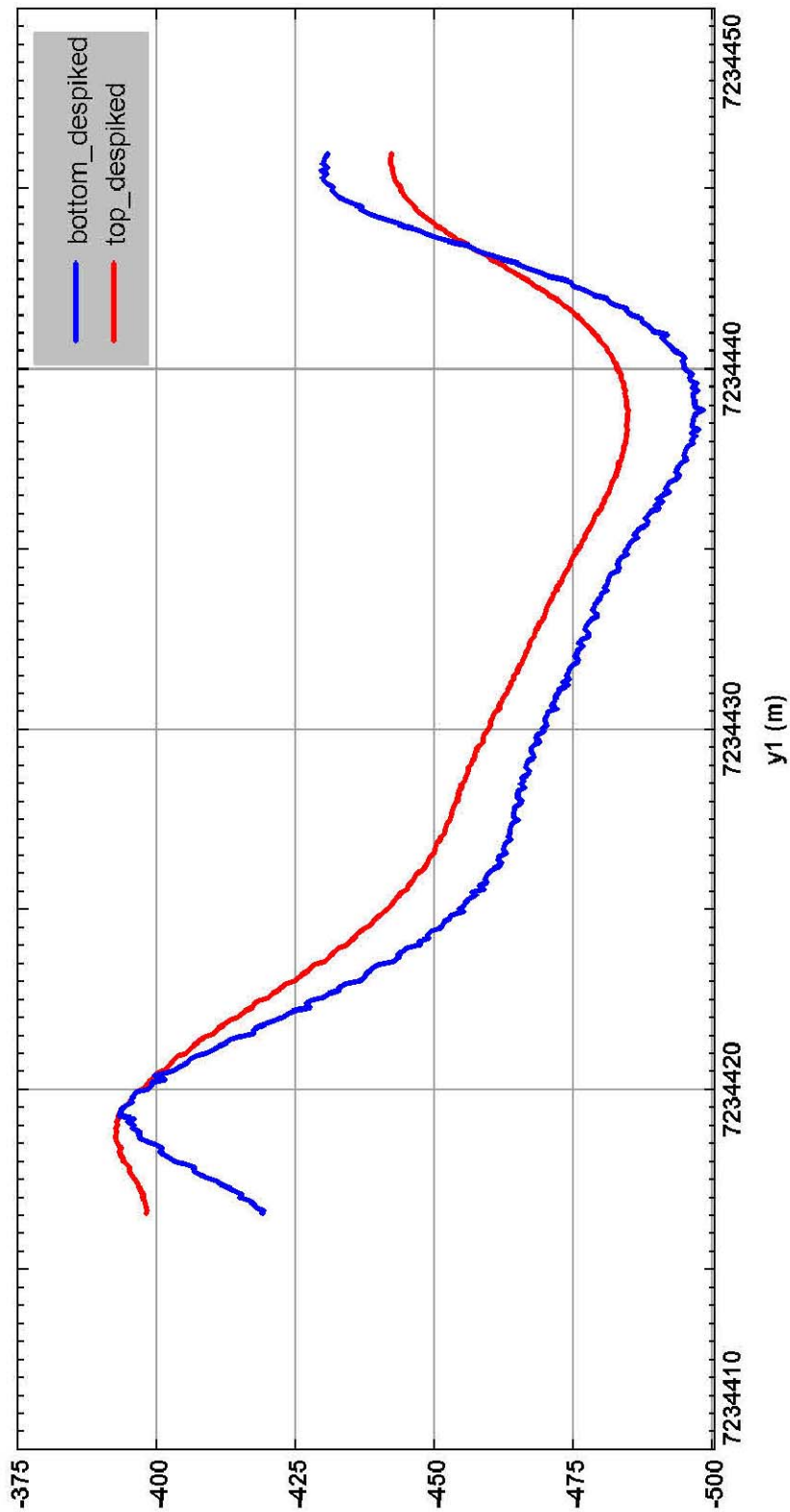
Figure 50. *Magnetic data along profile 13 measured while moving with the magnetometer in South direction. The blue curve shows data measured by the bottom sensor and the red curve shows data measured by the top sensor. The unit of the magnetic field is in nT and abscissa Y is UTM22N North coordinate.*
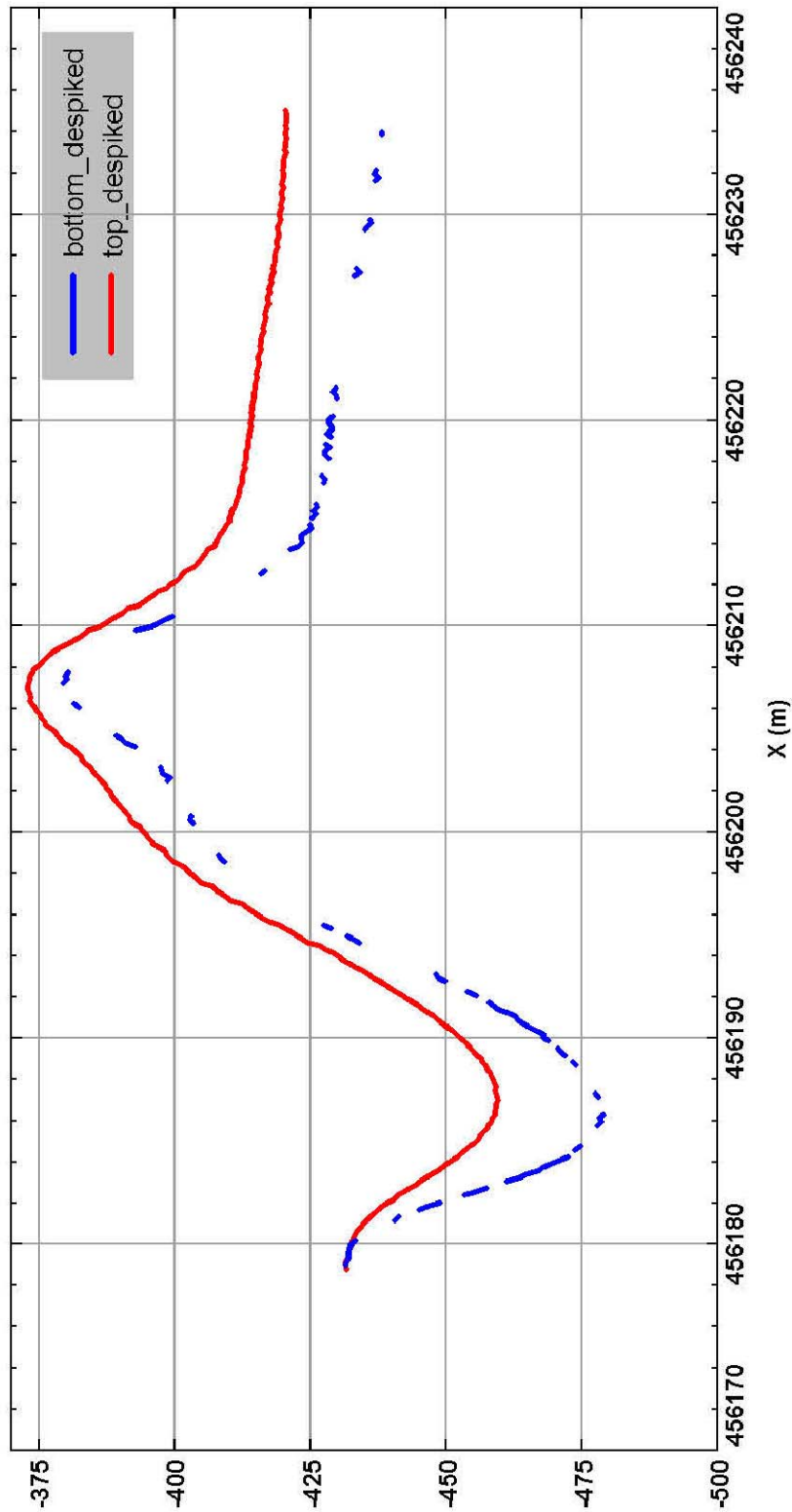
Figure 51. *Magnetic data along profile 14 measured while moving with the magnetometer in Northeast direction. The blue curve shows data measured by the bottom sensor and the red curve shows data measured by the top sensor. The unit of the magnetic field is in nT and abscissa X is UTM22N East coordinate.*
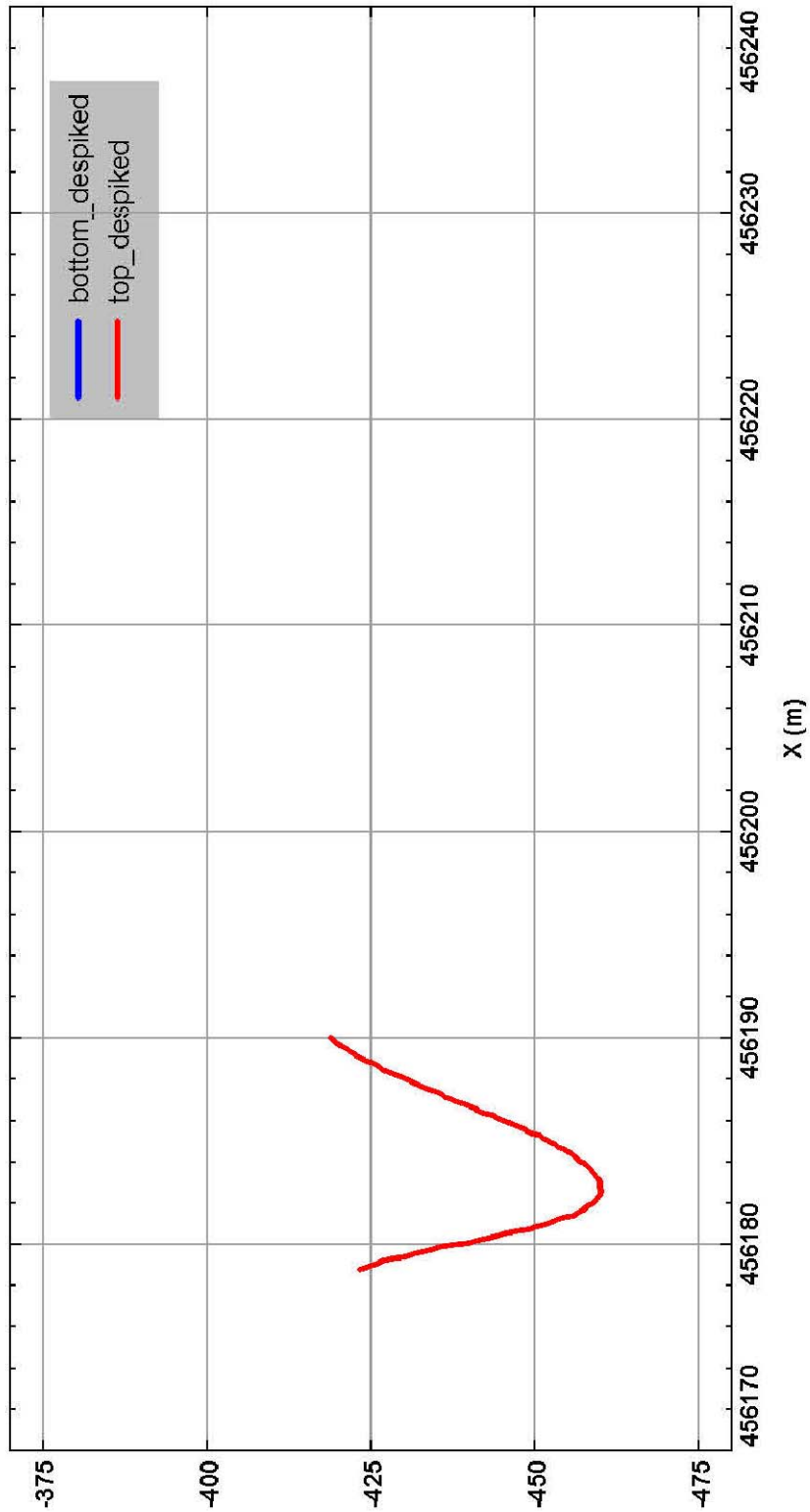
Figure 52. *Magnetic data along profile 14 (partly) measured while moving with the magnetometer in Southwest direction. The red curve shows data measured by the top sensor. No data useful from bottom sensor. The unit of the magnetic field is in nT and abscissa X is UTM22N East coordinate.*
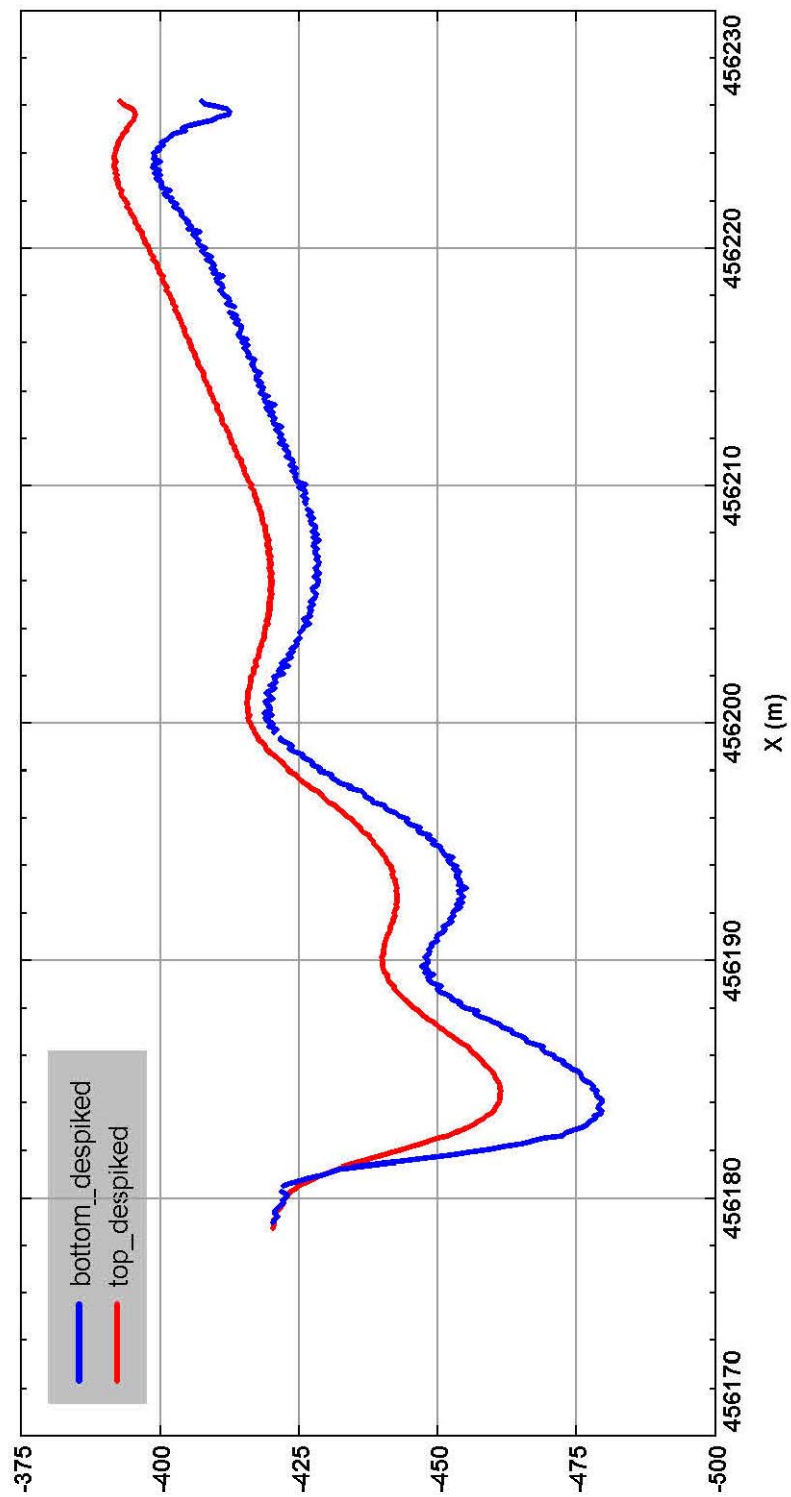
Figure 53. *Magnetic data along profile 15 measured while moving with the magnetometer in Northeast direction. The blue curve shows data measured by the bottom sensor and the red curve shows data measured by the top sensor. The unit of the magnetic field is in nT and abscissa X is UTM22N East coordinate.*
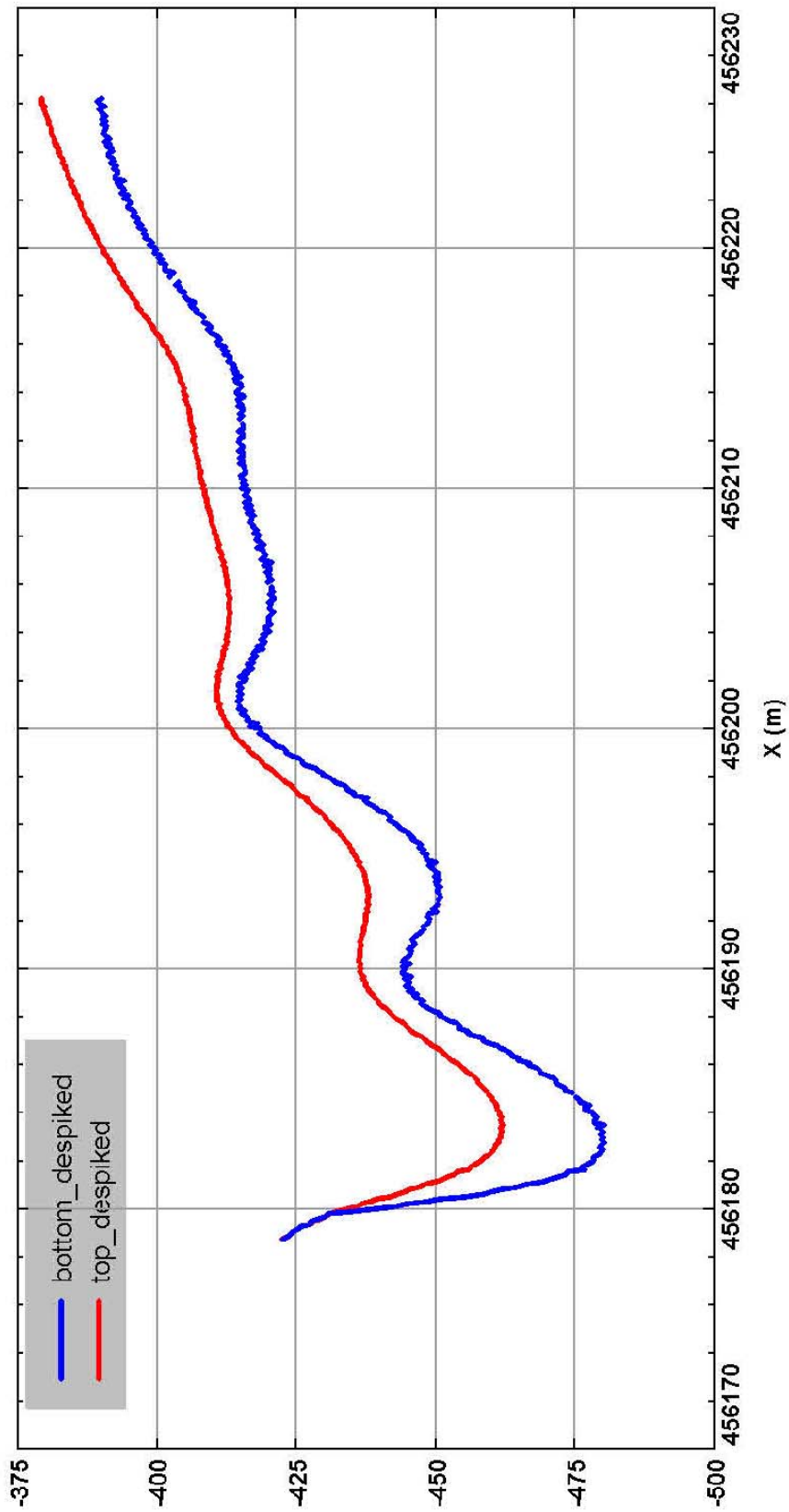
Figure 54. *Magnetic data along profile 15 measured while moving with the magnetometer in Southwest direction. The blue curve shows data measured by the bottom sensor and the red curve shows data measured by the top sensor. The unit of the magnetic field is in nT and abscissa X is UTM22N East coordinate.*
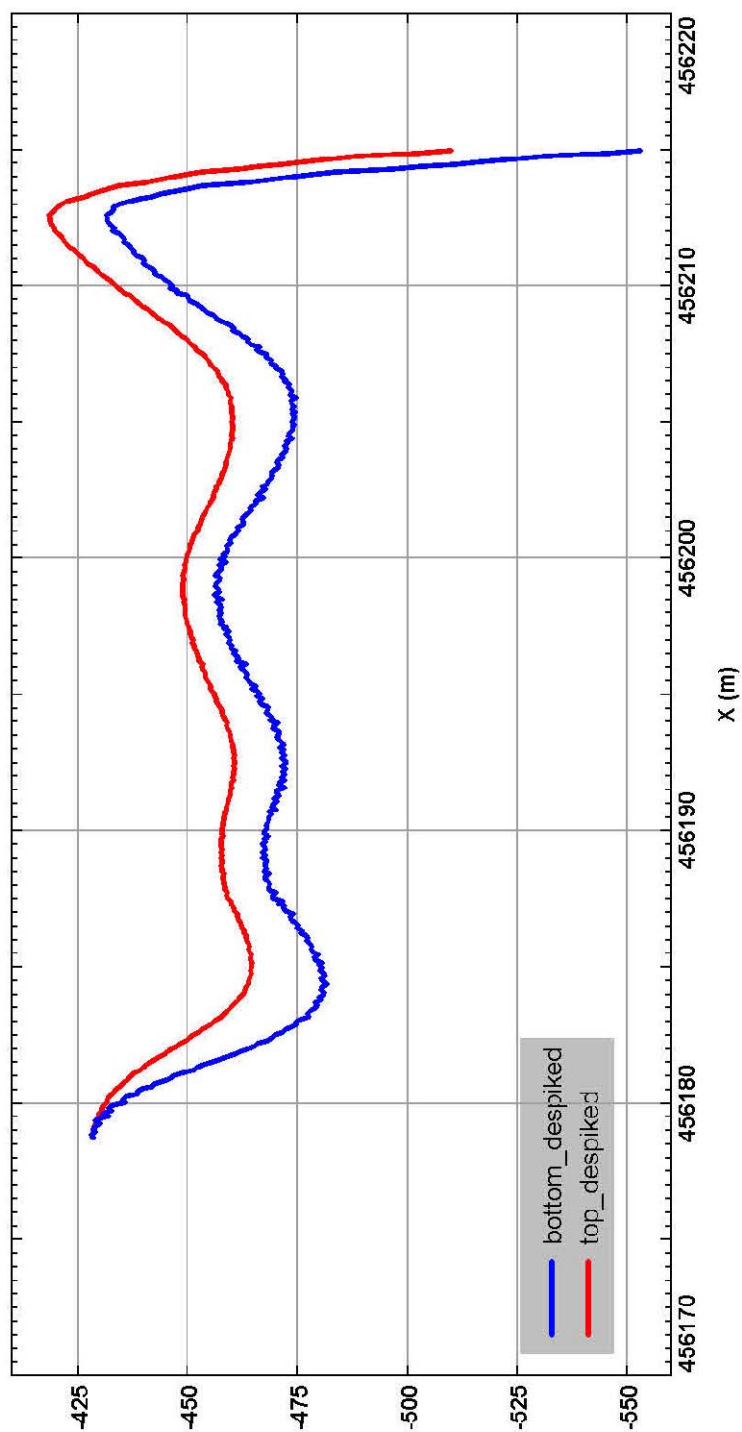
Figure 55. *Magnetic data along profile 16 measured while moving with the magnetometer in Northeast direction. The blue curve shows data measured by the bottom sensor and the red curve shows data measured by the top sensor. The unit of the magnetic field is in nT and ab-scissa X is UTM22N East coordinate.*
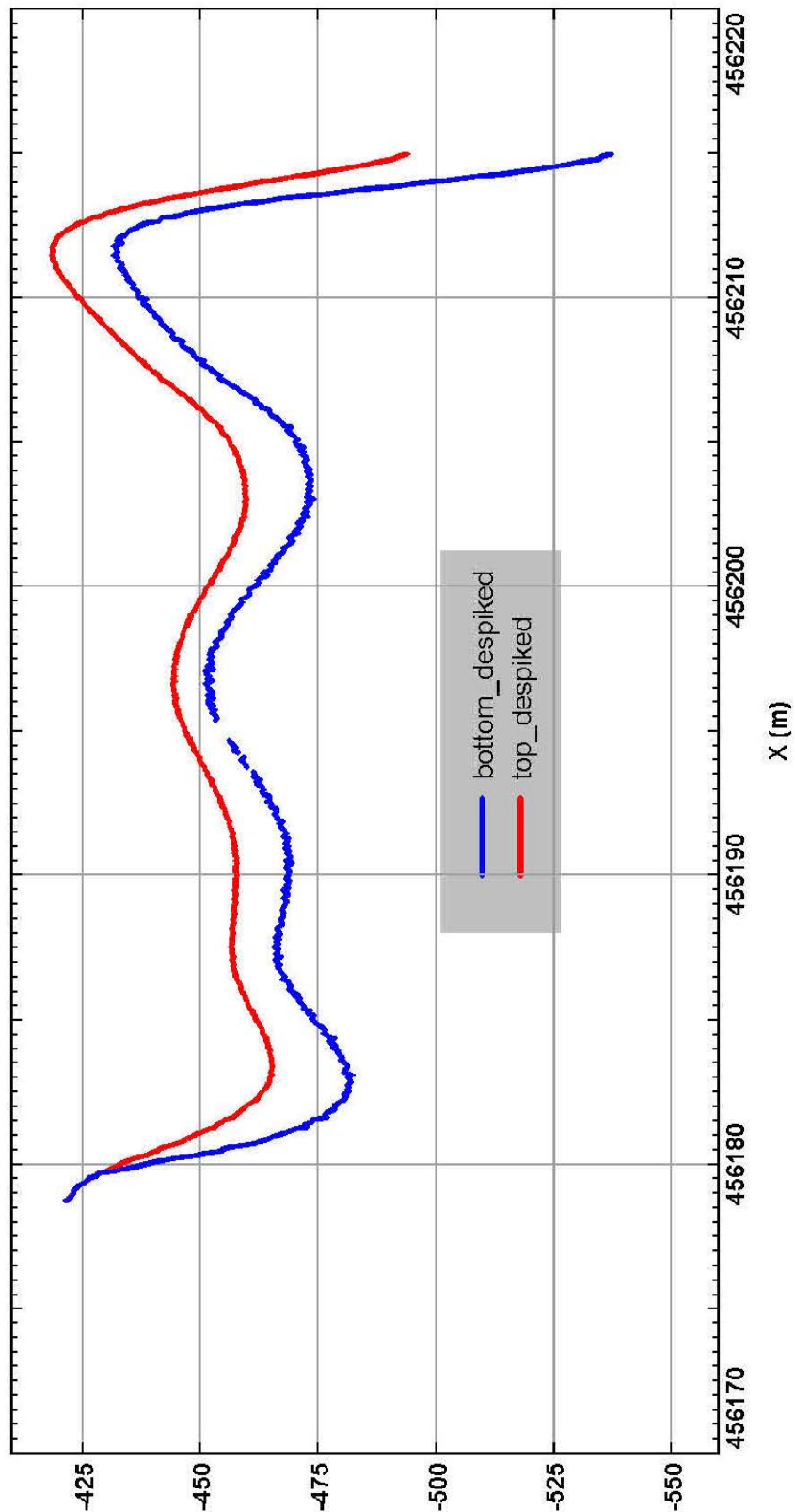
Figure 56. *Magnetic data along profile 16 measured while moving with the magnetometer in Southwest direction. The blue curve shows data measured by the bottom sensor and the red curve shows data measured by the top sensor. The unit of the magnetic field is in nT and abscissa X is UTM22N East coordinate.*
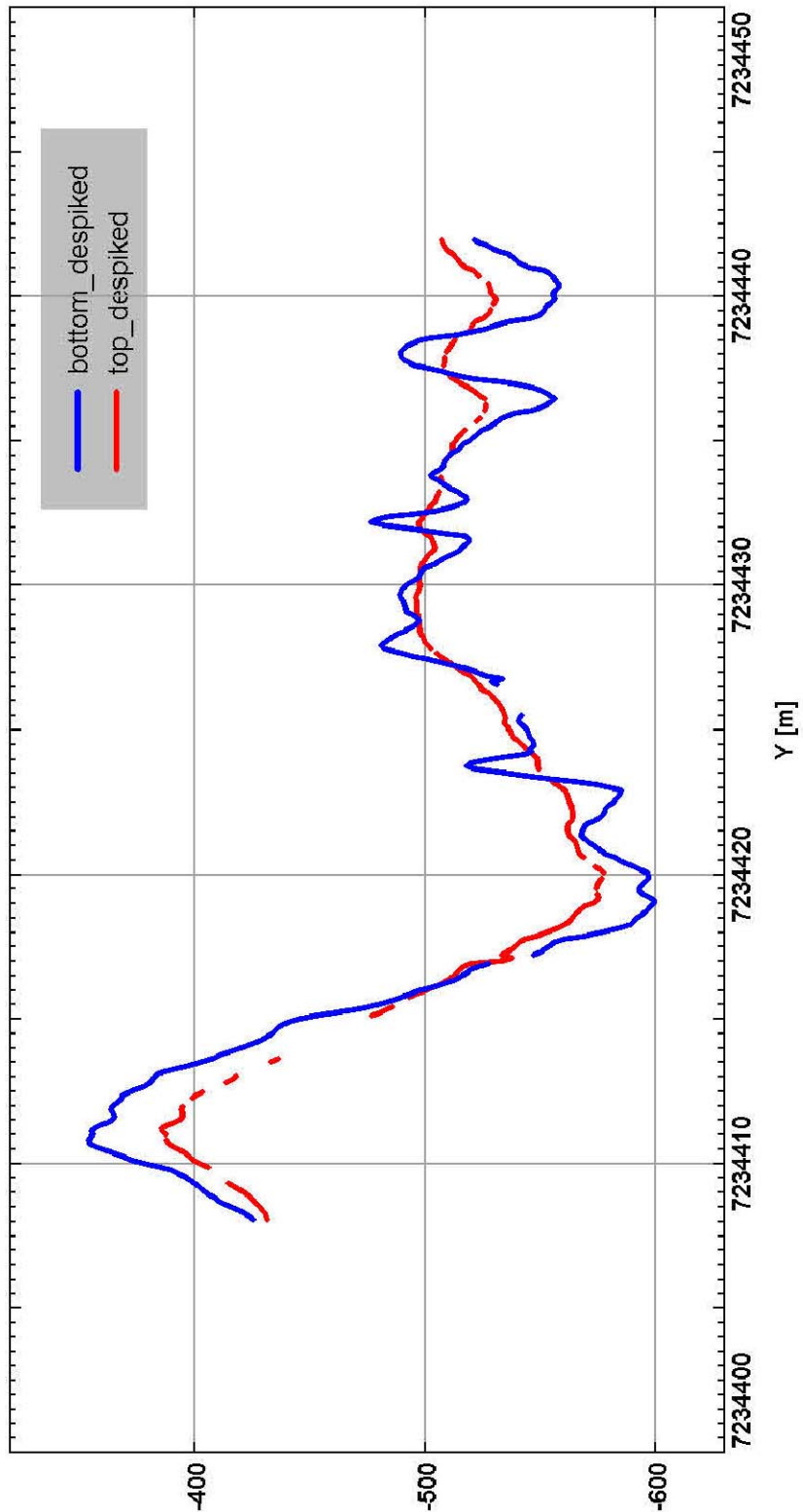
Figure 57. *Magnetic data along profile 17 measured while moving with the magnetometer in North direction. The blue curve shows data measured by the bottom sensor and the red curve shows data measured by the top sensor. The unit of the magnetic field is in nT and abscissa U is UTM22N North coordinate.*
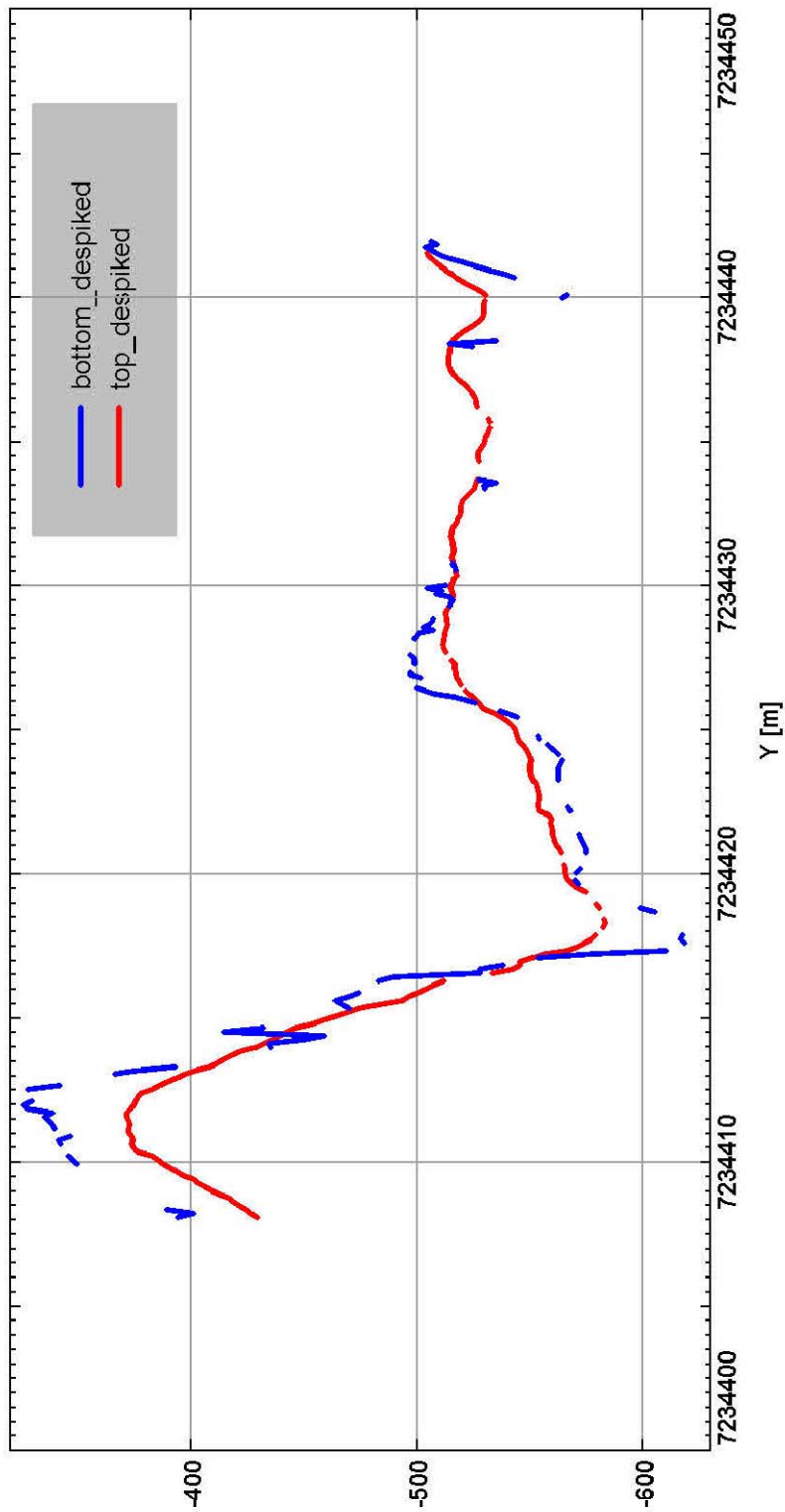
Figure 58. *Magnetic data along profile 17 measured while moving with the magnetometer in South direction. The blue curve shows data measured by the bottom sensor and the red curve shows data measured by the top sensor. The unit of the magnetic field is in nT and abscissa Y is UTM22N North coordinate.*
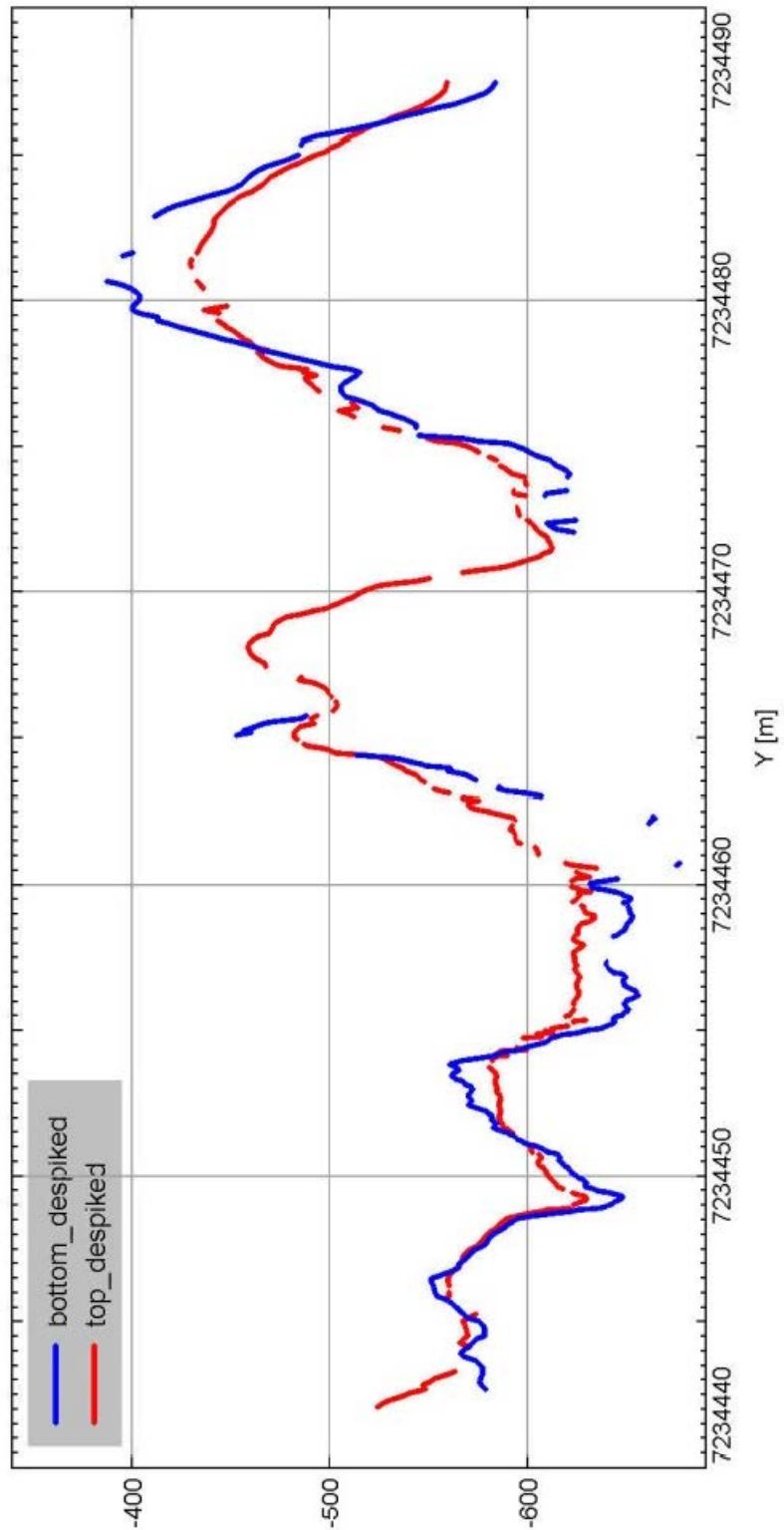
Figure 59. *Magnetic data along profile 18 measured while moving with the magnetometer in South direction. The blue curve shows data measured by the bottom sensor and the red curve shows data measured by the top sensor. The unit of the magnetic field is in nT and abscissa Y is UTM22N North coordinate.*
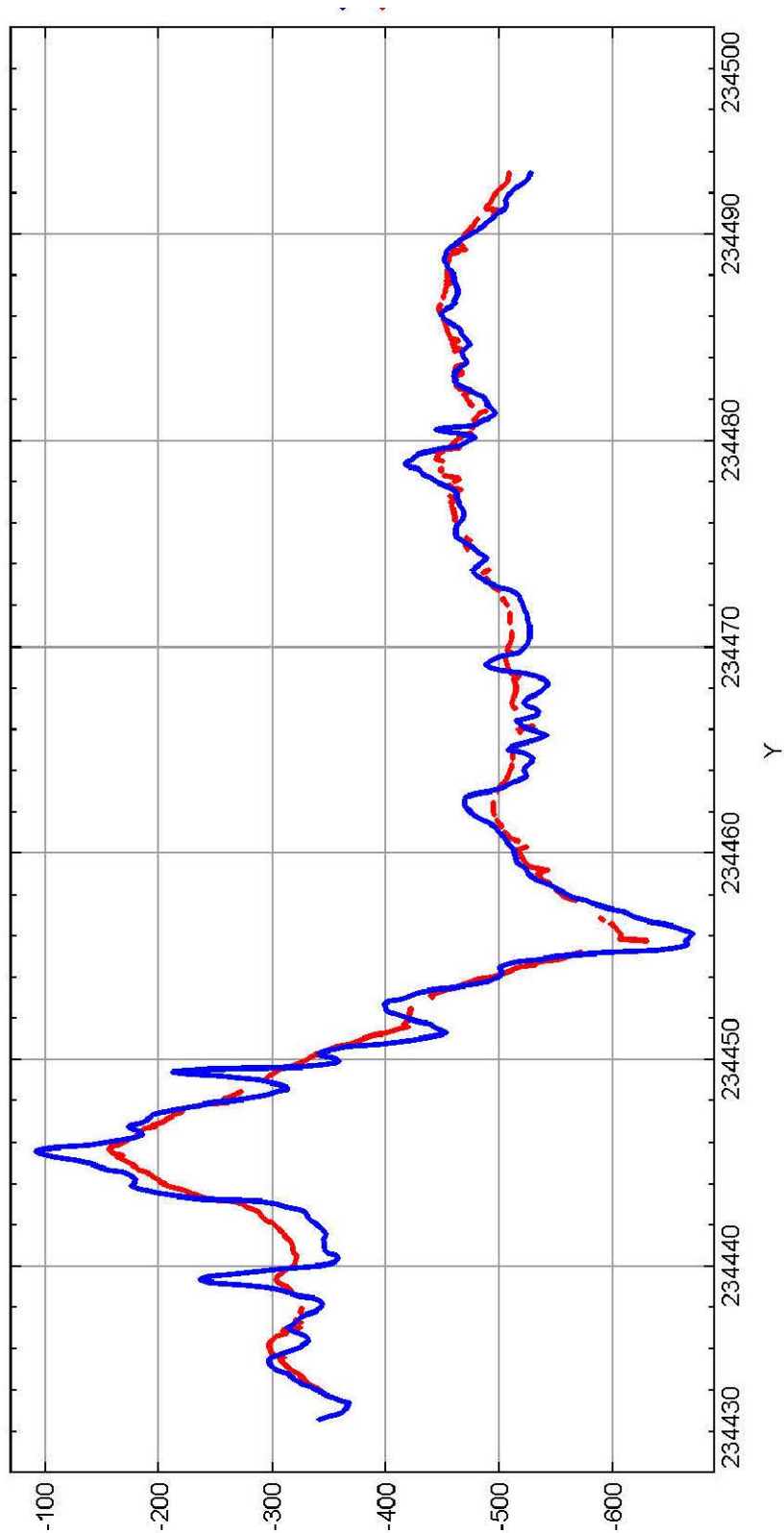
Figure 60. *Magnetic data along profile 19 measured while moving with the magnetometer in Southeast direction. The blue curve shows data measured by the bottom sensor and the red curve shows data measured by the top sensor. The unit of the magnetic field is in nT and ab-scissa Y is UTM22N North coordinate.*
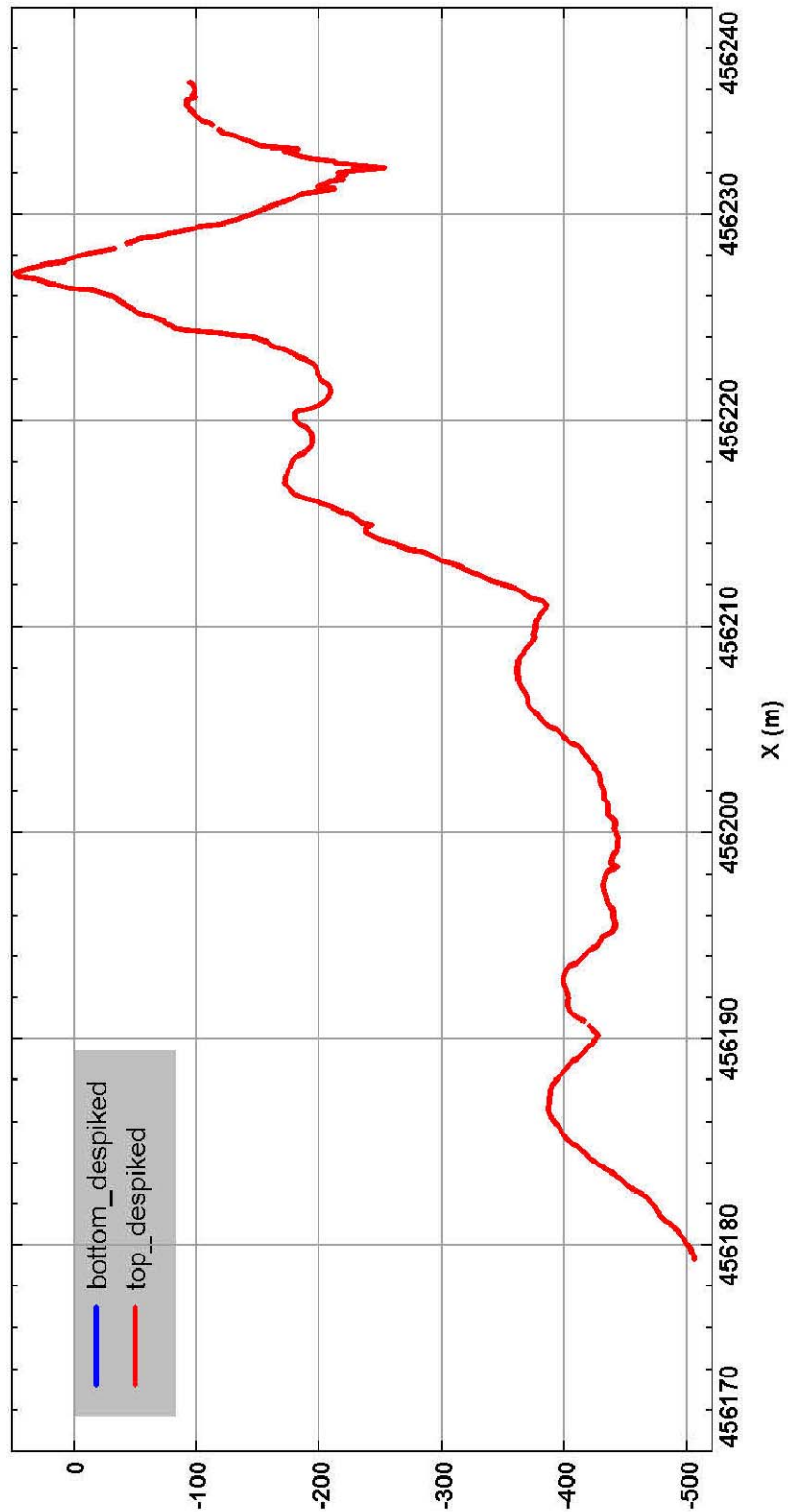
Figure 61. *Magnetic data along profile 20 measured while moving with the magnetometer in Northeast direction. The red curve shows data measured by the top sensor. The unit of the magnetic field is in nT and abscissa X is UTM22N East coordinate.*

GEUS 80
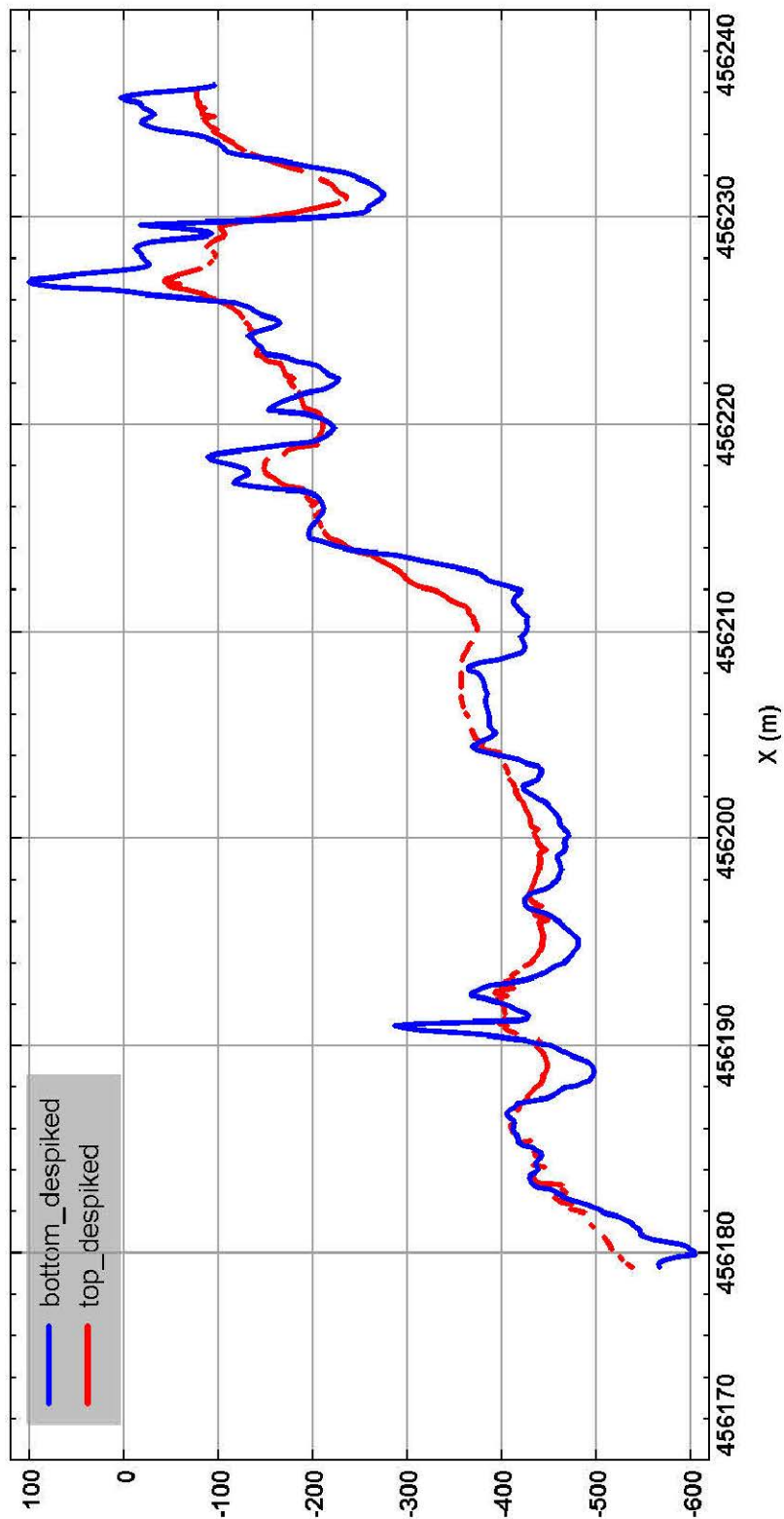
Figure 62. *Magnetic data along profile 20 measured while moving with the magnetometer in Southwest direction. The blue curve shows data measured by the bottom sensor and the red curve shows data measured by the top sensor. The unit of the magnetic field is in nT and ab-scissa X is UTM22N East coordinate.*
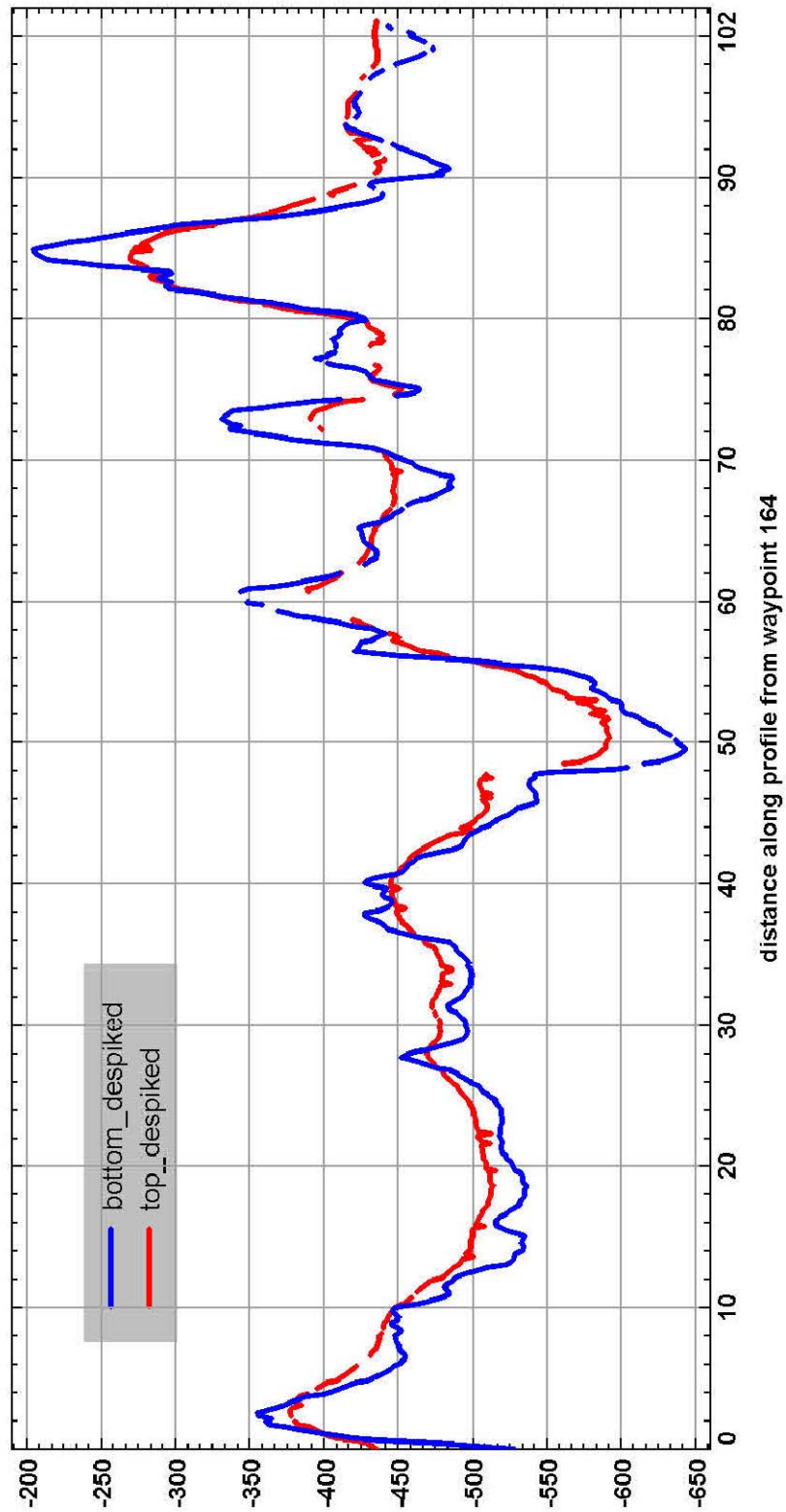
Figure 63. *Magnetic data along profile 21 measured while moving with the magnetometer along the lake shore in a counter-clockwise direction. The blue curve shows data measured by the bottom sensor and the red curve shows data measured by the top sensor. The unit of the magnetic field is in nT and abscissa is distance from waypoint 164.*
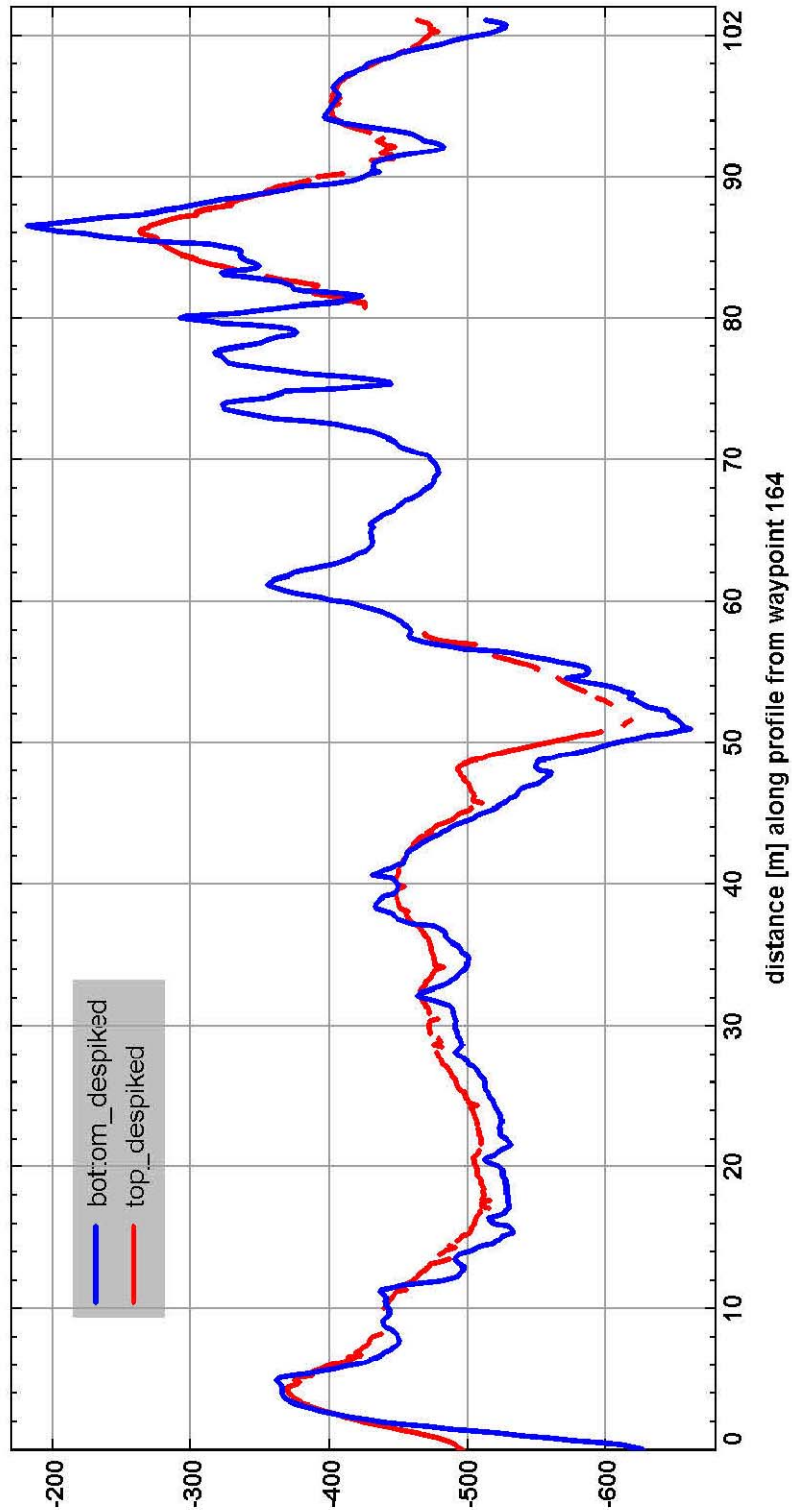
Figure 64. *Magnetic data along profile 21 measured while moving with the magnetometer along the lake shore in a clockwise direction. The blue curve shows data measured by the bottom sensor and the red curve shows data measured by the top sensor. The unit of the magnetic field is in nT and abscissa is distance from waypoint 164.*
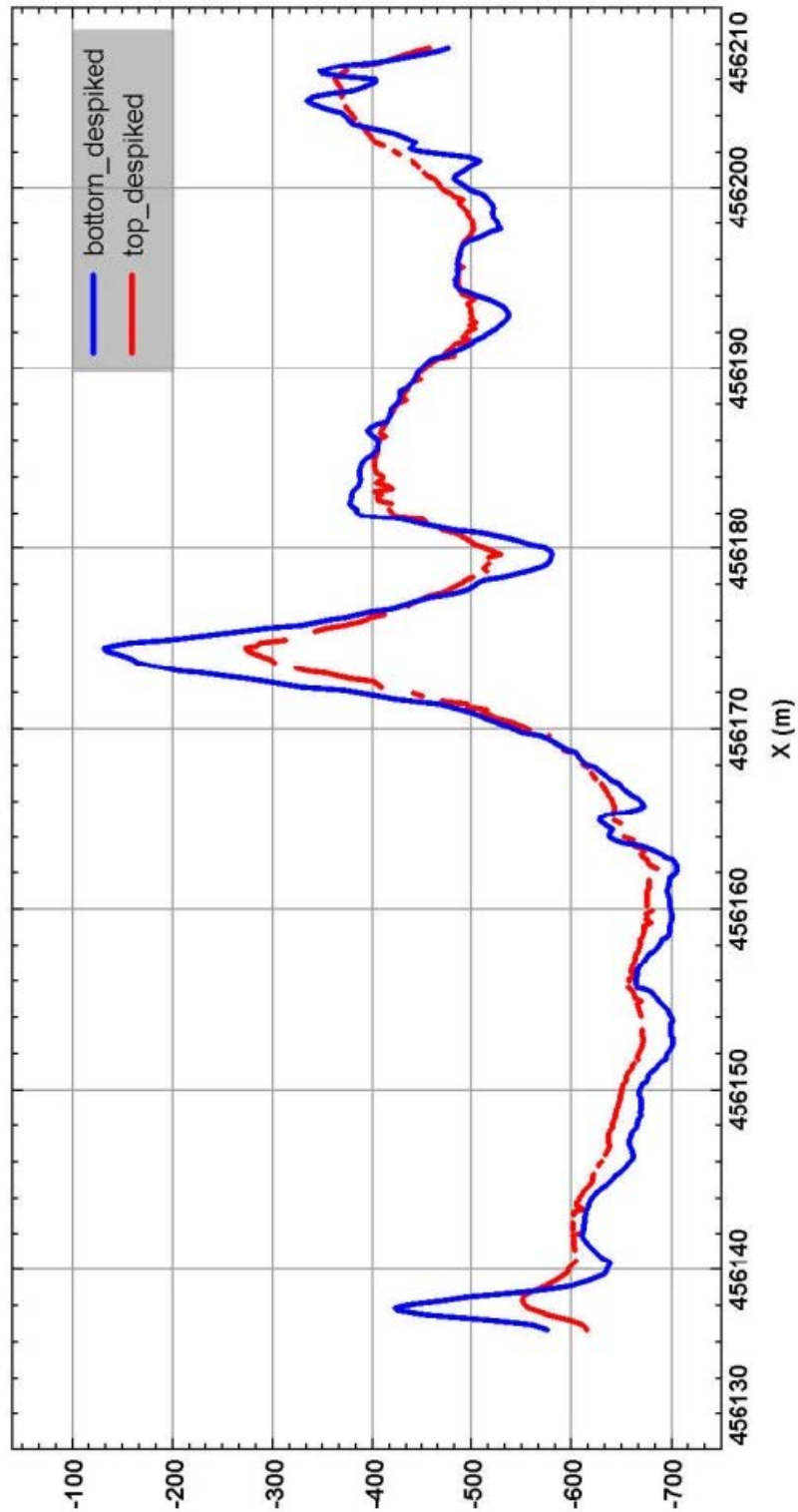
Figure 65. *Magnetic data along profile 22 measured while moving with the magnetometer in East direction. The blue curve shows data measured by the bottom sensor and the red curve shows data measured by the top sensor. The unit of the magnetic field is in nT and abscissa X is UTM22N East coordinate.*
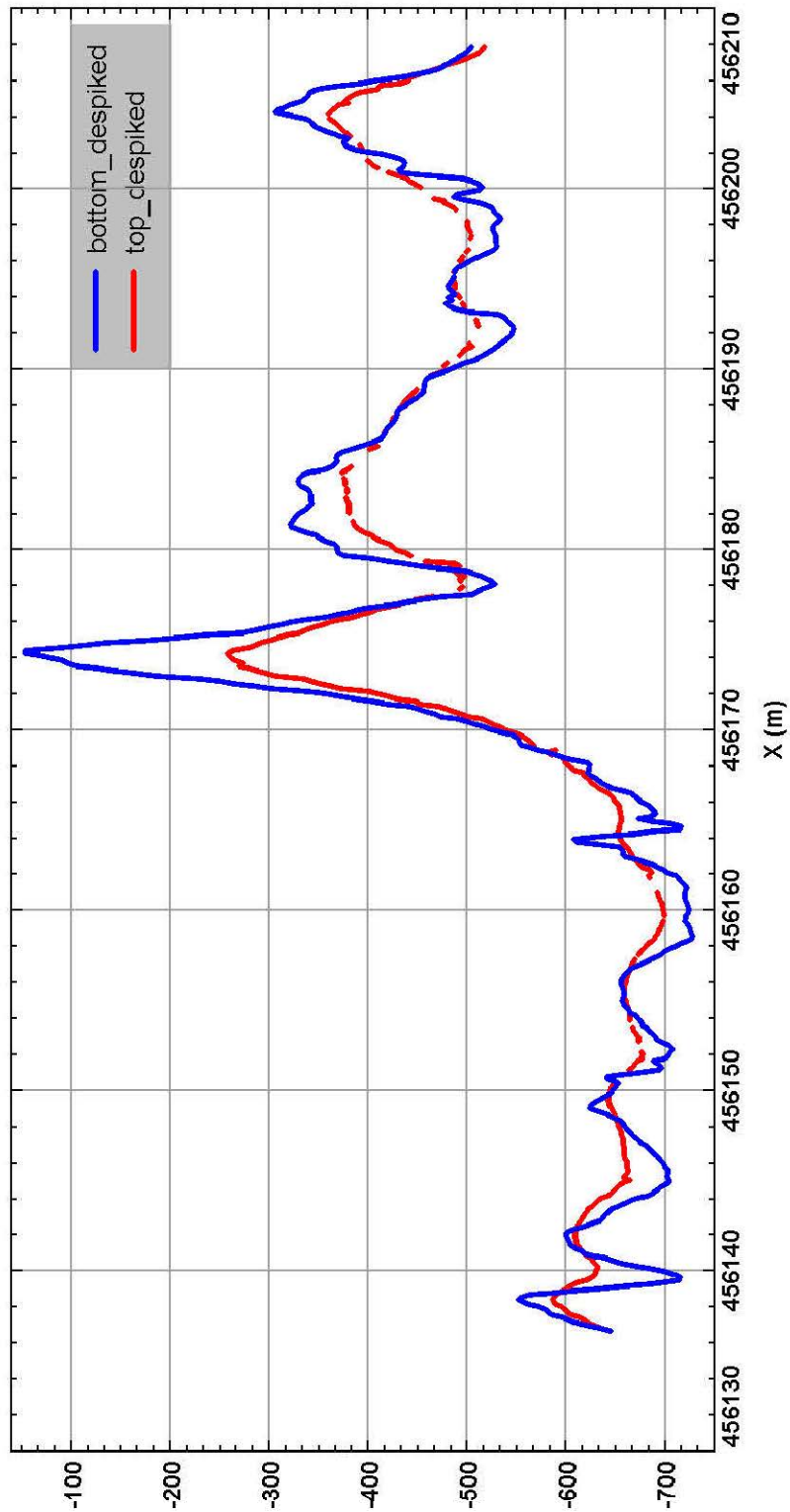
Figure 66. *Magnetic data along profile 22 measured while moving with the magnetometer in West direction. The blue curve shows data measured by the bottom sensor and the red curve shows data measured by the top sensor. The unit of the magnetic field is in nT and abscissa X is UTM22N East coordinate.*
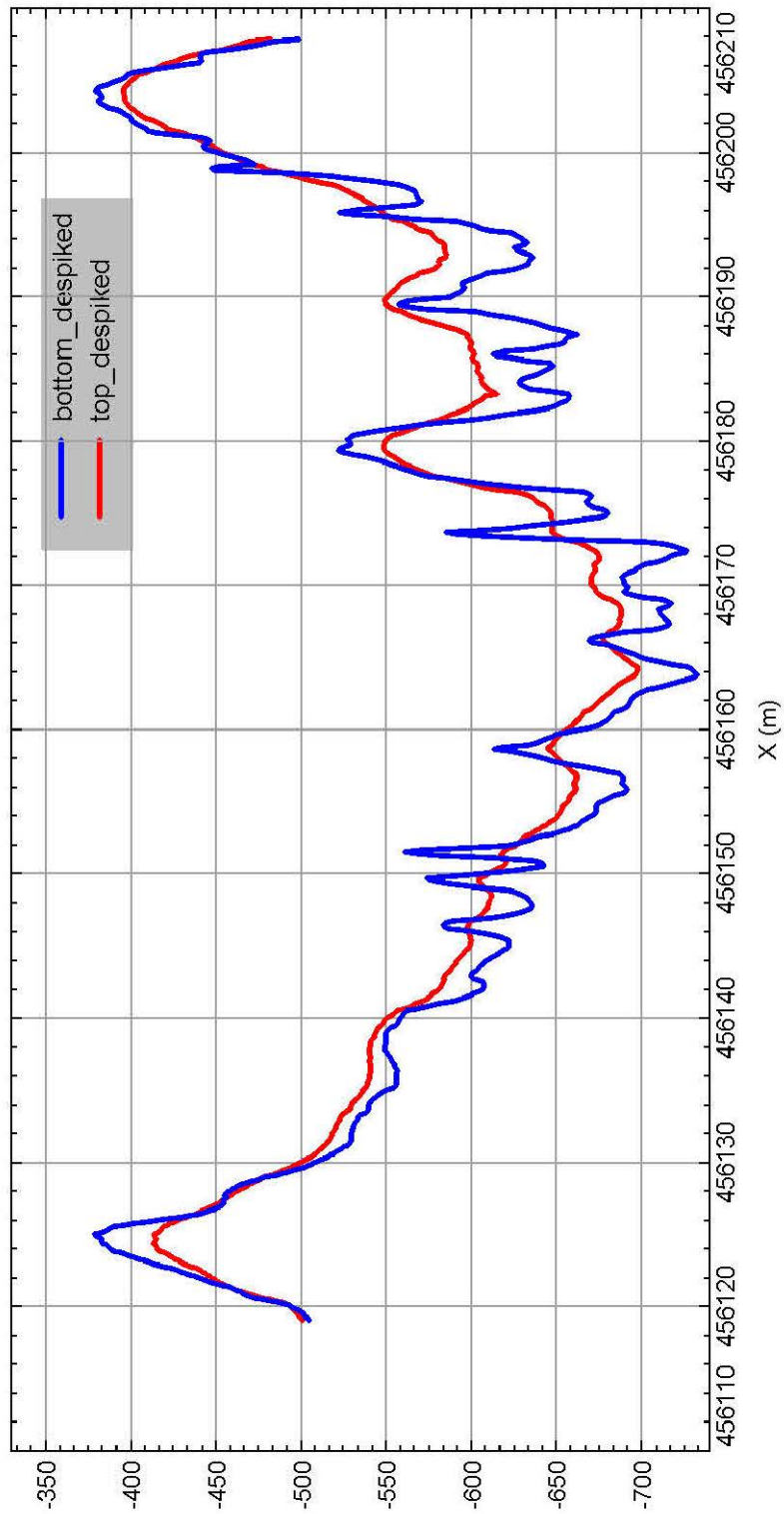
Figure 67. *Magnetic data along profile 23 measured while moving with the magnetometer in Northwest direction. The blue curve shows data measured by the bottom sensor and the red curve shows data measured by the top sensor. The unit of the magnetic field is in nT and abscissa X is UTM22N East coordinate.*
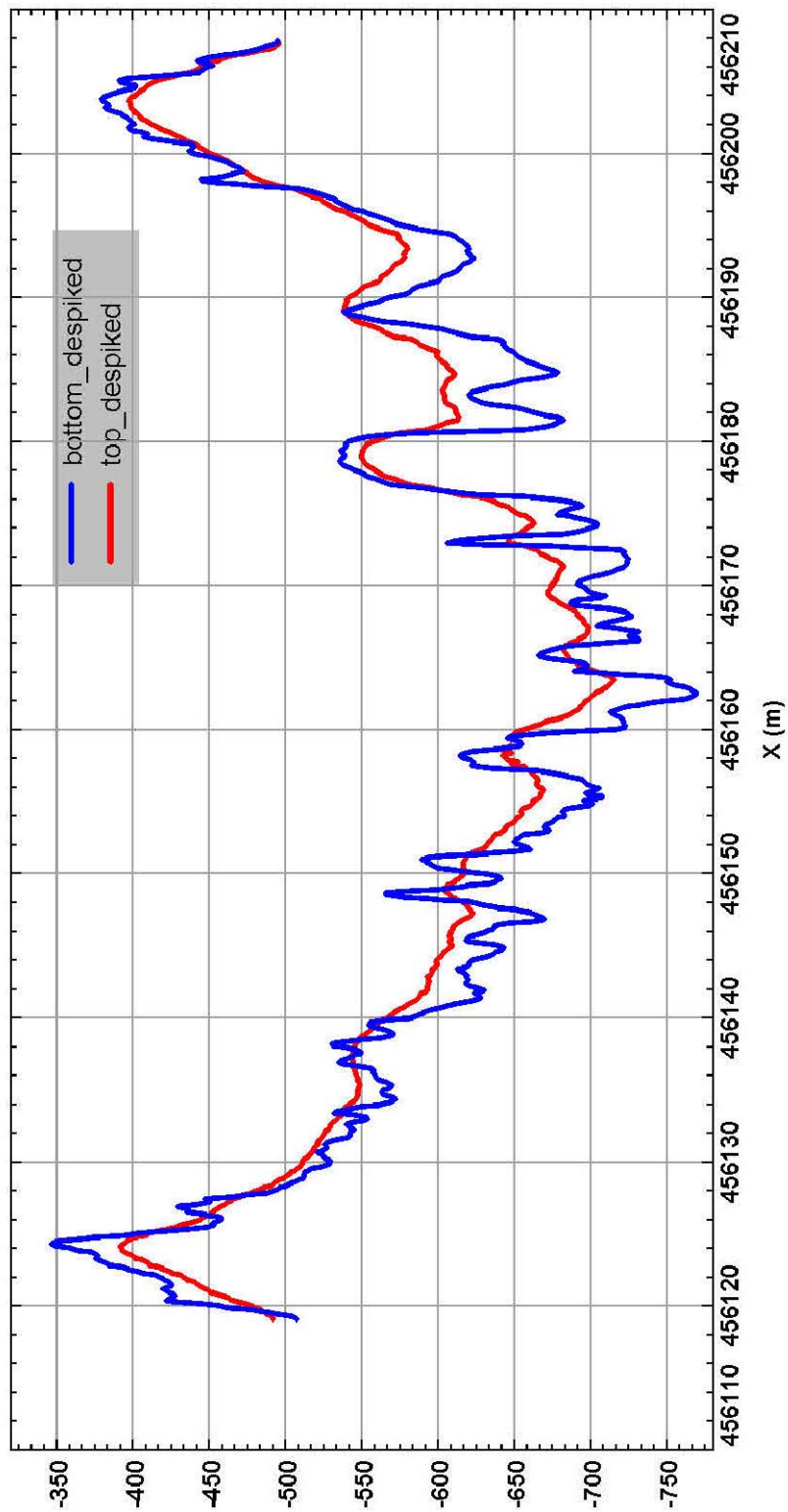
Figure 68. *Magnetic data along profile 23 measured while moving with the magnetometer in Southeast direction. The blue curve shows data measured by the bottom sensor and the red curve shows data measured by the top sensor. The unit of the magnetic field is in nT and abscissa X is UTM22N East coordinate.*
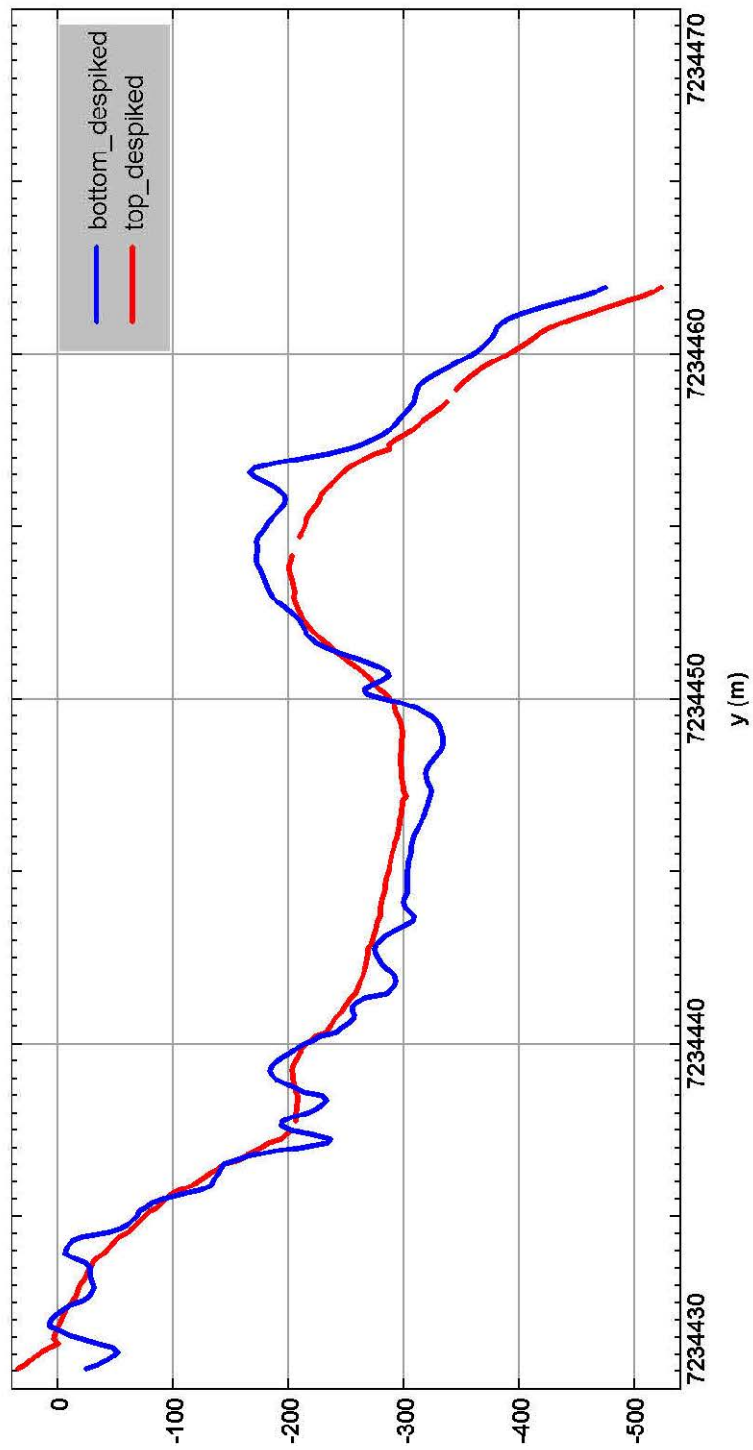
Figure 69. *Magnetic data along profile 24 measured while moving with the magnetometer in South direction. The blue curve shows data measured by the bottom sensor and the red curve shows data measured by the top sensor. The unit of the magnetic field is in nT and abscissa Y is UTM22N North coordinate.*
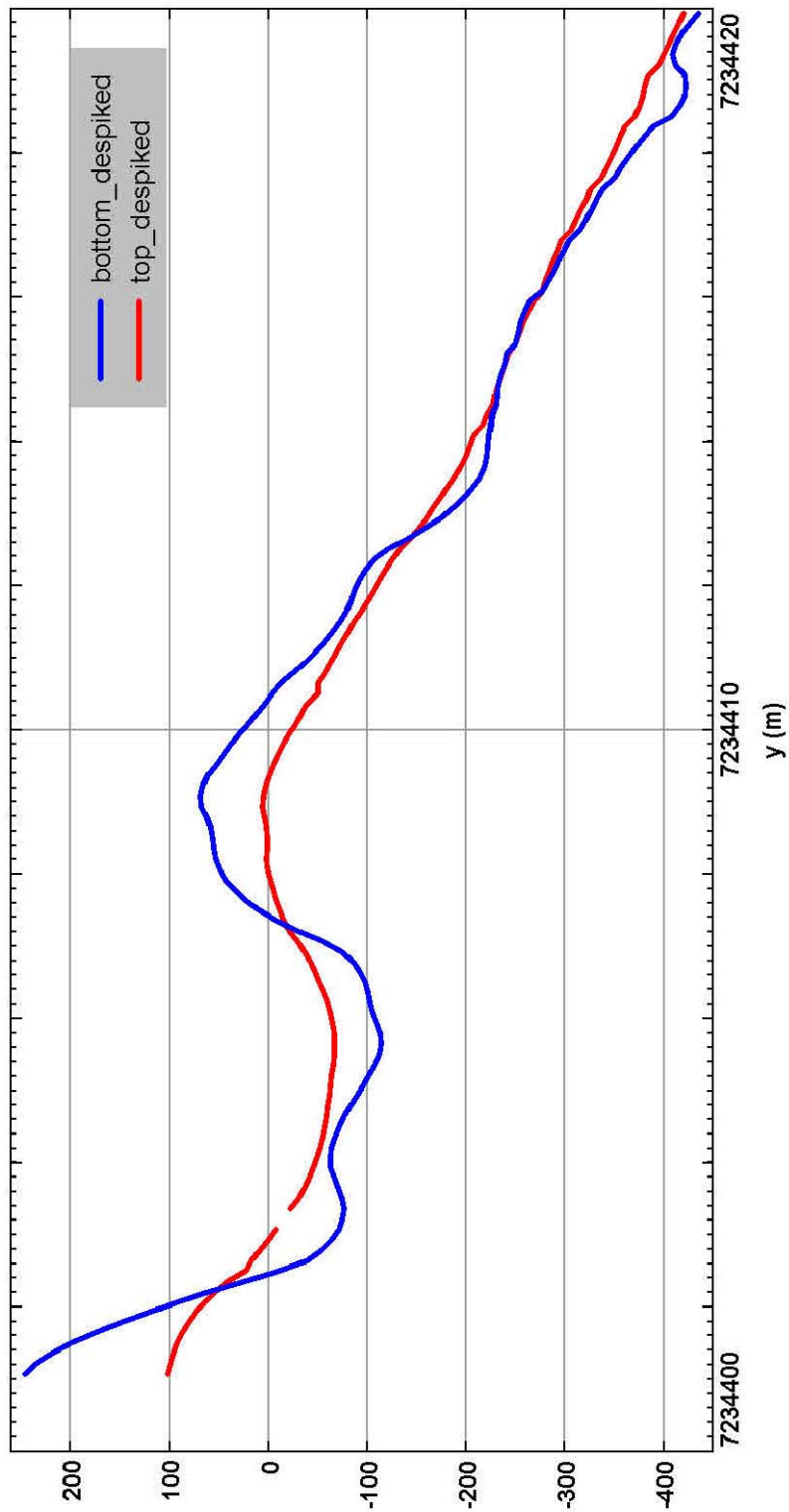
Figure 70. *Magnetic data along profile 25 measured while moving with the magnetometer in North direction. The blue curve shows data measured by the bottom sensor and the red curve shows data measured by the top sensor. The unit of the magnetic field is in nT and abscissa Y is UTM22N North coordinate.*
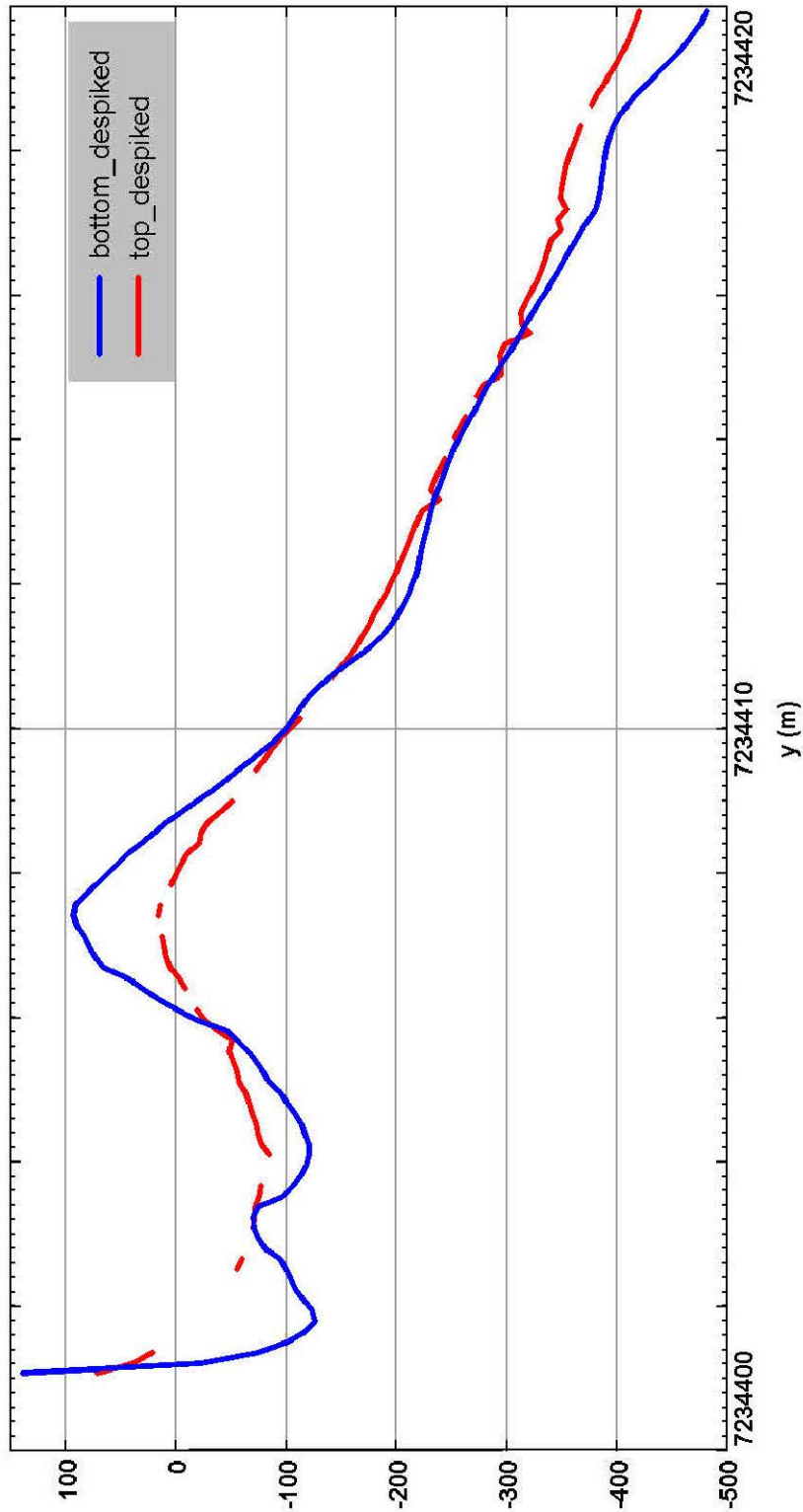
Figure 71. *Magnetic data along profile 25 measured while moving with the magnetometer in South direction. The blue curve shows data measured by the bottom sensor and the red curve shows data measured by the top sensor. The unit of the magnetic field is in nT and abscissa Y is UTM22N North coordinate.*